

7-31-2018

## Investigation of Stereotactic Body Radiation Therapy Delivery Accuracy on an Elekta Linear Accelerator

Addie Barron

*Louisiana State University and Agricultural and Mechanical College*

Follow this and additional works at: [https://digitalcommons.lsu.edu/gradschool\\_theses](https://digitalcommons.lsu.edu/gradschool_theses)



Part of the [Biological and Chemical Physics Commons](#), [Oncology Commons](#), and the [Other Medical Sciences Commons](#)

---

### Recommended Citation

Barron, Addie, "Investigation of Stereotactic Body Radiation Therapy Delivery Accuracy on an Elekta Linear Accelerator" (2018). *LSU Master's Theses*. 4780.

[https://digitalcommons.lsu.edu/gradschool\\_theses/4780](https://digitalcommons.lsu.edu/gradschool_theses/4780)

This Thesis is brought to you for free and open access by the Graduate School at LSU Digital Commons. It has been accepted for inclusion in LSU Master's Theses by an authorized graduate school editor of LSU Digital Commons. For more information, please contact [gradetd@lsu.edu](mailto:gradetd@lsu.edu).

# INVESTIGATION OF STEREOTACTIC BODY RADIATION THERAPY DELIVERY ACCURACY ON AN ELEKTA LINEAR ACCELERATOR

A Thesis

Submitted to the Graduate Faculty of the  
Louisiana State University  
and Agricultural and Mechanical College  
in partial fulfillment of the  
requirements for the degree of  
Master of Science

in

The Department of Physics and Astronomy

by

Addie Jane Barron  
B.S., Centenary College of Louisiana, 2015  
December 2018

## Acknowledgements

I take this opportunity to express my sincerest gratitude to my committee members: Dr. Matthews, David Perrin, and Dr. Moreno. Their guidance and dedication were essential in the development and completion of this project. I express special thanks to my major thesis advisor, Dr. Fontenot, for his commitment to teaching. He has imparted knowledge that will benefit me as I continue in the field of medical physics.

Special thanks to Frank Apollo and the dosimetry team for their attentiveness and counseling during this project. Additional thanks to my fellow classmates Elizabeth Hilliard, Suman Shrestha, Michelle Lis, and Jingzhu Xu for aiding in my academic success. I also take this opportunity to thank my officemates, Phillip Wall and Cam Sprowls, for their support throughout the duration of this project.

I recognize the staff at Mary Bird Perkins Cancer Center for their dedication and patience. Their help and encouragement were often sought during my time as a graduate student. Moreover, I sincerely thank the administrative staff of the Physics Department, including Megan Jarrell, Katherine Pevey, and Susan Hammond, for their friendship and kindness at times when they were needed the most.

Lastly, I thank my friends and family for their unfailing love and support, without which this project would not have been possible. To my friends: your loyalty and compassion were constant reminders of the reason I started my journey in this field. To my family: you have always offered wisdom and perspective that inspired me to persevere, especially my sister, my brother and their families. Finally, I thank my parents, Charles and Cathey Barron, for their support during the peaks and valleys of my life. They have set an unprecedented example of love and devotion that guides me daily and serves as my primary motivation.

# Table of Contents

|  |     |
|--|-----|
| Acknowledgements.....  | ii  |
| List of Tables .....   | iv  |
| List of Figures .....  | vi  |
| Abstract.....  | xii |
| Chapter 1. Introduction .....  | 1   |
| 1.1 Background and Significance.....   | 1   |
| 1.2 Motivation for Research .....  | 5   |
| 1.3 Hypothesis and Specific Aims.....  | 6   |
| Chapter 2. Methods and Materials.....  | 7   |
| 2.1 Aim 1 .....  | 7   |
| 2.2 Aim 2 .....  | 12  |
| 2.3 Aim 3 .....  | 20  |
| Chapter 3. Results.....  | 27  |
| 3.1 Results of Treatment Planning.....                                       | 27  |
| 3.2 MV Isocenter Accuracy Test Results .....                                 | 29  |
| 3.3 Results of Treatment Deliveries .....                                    | 30  |
| 3.4 Individual Gantry Beam Measurement Results.....                          | 41  |
| 3.5 Ion Chamber Measurements.....  | 43  |
| Chapter 4. Discussion.....   | 46  |
| 4.1 Summary of Results.....  | 46  |
| 4.2 Limitations of Work.....   | 48  |
| 4.3 Evaluation of Hypothesis.....  | 48  |
| 4.4 Future Work.....   | 48  |
| References .....   | 49  |
| Appendix A. Profiles Comparing Measured and Calculated Treatment Plans ..... | 52  |
| Appendix B. MV Isocenter Accuracy Test Data .....                            | 97  |
| Appendix C. Data from kV-CBCT Translations.....                              | 100 |
| Vita.....  | 102 |



## List of Tables

|   |    |
|---|----|
| Table 3.1: RTOG 0813 Protocol Requirements .....  | 27 |
| Table 3.2: RTOG 0631 Protocol Requirements and MBPCC Constraints .....  | 28 |
| Table 3.3: Results of the MV Isocenter Accuracy Test for three linear accelerators. ....  | 29 |
| Table 3.4: Average positional alignment comparison between two measured treatment delivery trials demonstrating reproducibility of setup for treatment deliveries on the Elekta Infinity linear accelerator with Agility head. Positive values of $\Delta c$ indicate a left or inferior shift of trial 2 relative to trial 1. Conversely, negative values of $\Delta c$ indicate a right or superior shift of trial 2 relative to trial 1. ....  | 31 |
| Table 3.5: Average shift in 75% isodose level comparison between two measured treatment delivery trials demonstrating reproducibility of setup for treatment deliveries on the Elekta Infinity linear accelerator with Agility head. Values are for profiles of 1-mm resolution along the patient left-right axis, where a positive $\Delta 75_{\text{Left}}$ or $\Delta 75_{\text{Right}}$ indicates the trial 2 isodose level fell within the trial 1 profile. Conversely, a negative $\Delta 75_{\text{Left}}$ or $\Delta 75_{\text{Right}}$ indicates the trial 2 isodose level fell outside the trial 1 profile. ....                        | 31 |
| Table 3.6: Average shift in 75% isodose level comparison between two measured treatment delivery trials demonstrating reproducibility of setup for treatment deliveries on the Elekta Infinity linear accelerator with Agility head. Values are for profiles of 1-mm resolution along the patient superior-inferior axis, where a positive $\Delta 75_{\text{Inferior}}$ or $\Delta 75_{\text{Superior}}$ indicates the trial 2 isodose level fell within the trial 1 profile. Conversely, a negative $\Delta 75_{\text{Inferior}}$ or $\Delta 75_{\text{Superior}}$ indicates the trial 2 isodose level fell outside the trial 1 profile. ....   | 31 |
| Table 3.7: Average shift in 60% isodose level comparison between two measured treatment delivery trials with posterior offsets demonstrating reproducibility of setup for treatment deliveries on the Elekta Infinity linear accelerator with Agility head. Values are for profiles of 1-mm resolution along the patient left-right axis, where a positive $\Delta 60_{\text{Left}}$ or $\Delta 60_{\text{Right}}$ indicates the trial 2 isodose level fell within the trial 1 profile. Conversely, a negative $\Delta 60_{\text{Left}}$ or $\Delta 60_{\text{Right}}$ indicates the trial 2 isodose level fell outside the trial 1 profile. .... | 31 |
| Table 3.8: Percent Difference between TPS calculated dose and delivery of the treatment plan measured dose at the central point of the MapCHECK2 diode array. All measurements were taken in the coronal plane along the right-left direction. ....   | 38 |
| Table 3.9: Summary of $\Delta c$ analysis metric for the delivery of the lung SBRT and SSRS treatment plans delivered on three linear accelerators. Positive values of $\Delta c$ indicate a shift of the measured profile in the left or inferior direction relative to the planned profile. Negative values of $\Delta c$ indicate a shift in the right or superior direction relative to the planned profile.....  | 39 |
| Table 3.10: $\Delta 75_{\text{Left}}$ and $\Delta 75_{\text{Right}}$ for lung SBRT and spine SRS profiles on three linear accelerators. Positive values of $\Delta 75_{\text{Left}}$ and $\Delta 75_{\text{Right}}$ indicated that the position of the measured 75% isodose line fell inside the planned 75% isodose line. Negative values of $\Delta 75_{\text{Left}}$ and $\Delta 75_{\text{Right}}$ indicated that the measured 75% isodose line fell outside the planned 75% isodose line. ....   | 40 |
| Table 3.11: $\Delta 75_{\text{Superior}}$ and $\Delta 75_{\text{Inferior}}$ for lung SBRT and spine SRS profiles on an Elekta Infinity linear accelerator. Positive values of $\Delta 75_{\text{Superior}}$ and $\Delta 75_{\text{Inferior}}$ indicated that the position of the measured 75% isodose line fell inside the planned 75% isodose line. Negative values of $\Delta 75_{\text{Superior}}$ and $\Delta 75_{\text{Inferior}}$ indicated that the measured 75% isodose line fell outside the planned 75% isodose line.....   | 40 |

|  |     |
|--|-----|
| Table 3.12. $\Delta 60_{\text{Left}}$ and $\Delta 60_{\text{Right}}$ for posteriorly offset spine SRS profiles on three linear accelerators. Positive values of $\Delta 60_{\text{Left}}$ and $\Delta 60_{\text{Right}}$ indicated that the position of the measured 60% isodose line fell inside the planned 60% isodose line. Negative values of $\Delta 60_{\text{Left}}$ and $\Delta 60_{\text{Right}}$ indicated that the measured 60% isodose line fell outside the planned 60% isodose line. .... | 40  |
| Table 3.13. SSRS beams at planned gantry angles delivered to a diode array shifted posteriorly by 2 cm on Versa HD linear accelerator. ....  | 41  |
| Table 3.14. SSRS beams at planned gantry angles delivered to a diode array shifted posteriorly by 2.7 cm on Versa HD linear accelerator. ....  | 42  |
| Table 3.15. SSRS beams delivered at gantry angle 0 and collimator angle 0 to a diode array on Versa HD linear accelerator. ....  | 42  |
| Table 3.16. SSRS beams delivered at gantry angle 0 and collimator angle 0 to a diode array on Versa HD linear accelerator. TPS Data was shifted by 1 mm along the Y-axis using SNC Patient™ Software, resulting in smaller percent differences. ....   | 43  |
| Table 3.17. Ion chamber measurements for an active detector volume representing the approximate region where the spinal cord ROI is adjacent to the vertebral body (2 cm from the CTV isocenter). Beams were delivered at their planned gantry and collimator angles. ....   | 44  |
| Table 3.18. Ion chamber measurements for an active detector volume representing the approximate center of the spinal cord (2.7 cm from the CTV isocenter). Beams were delivered at their planned gantry and collimator angles. ....  | 44  |
| Table 3.19. Ion chamber measurements for an active detector volume representing the approximate center of the spinal cord (2.7 cm from the CTV isocenter). Beams were overridden to be delivered at gantry and collimator angles of 0°. ....   | 45  |
| Table C.1. Data acquired from the XVI kV-CBCT image registration used for assessing the positioning of the diode array before measurement sessions. ....   | 100 |

## List of Figures

|  |    |
|--|----|
| Figure 1.1. 2018 Estimates for Leading Sites of New Cancer Cases and Deaths in the United States (American Cancer Society, 2018). .....  | 3  |
| Figure 1.2. Axial, sagittal, and coronal computed tomographic view of a patient with spinal metastasis. The diseased T12 vertebra is contoured in red. ....  | 4  |
| Figure 1.3. Mary Bird Perkins Cancer Center Elekta Infinity linear accelerator with Agility head. MV-CBCT and orthogonal kV-CBCT onboard imaging pictured. ....  | 6  |
| Figure 2.1. Transaxial view of the 7-coplanar and 2-noncoplanar-beam (not pictured) treatment plan for the lung SBRT patient. The PTV is contoured pink in this image plane. ....  | 8  |
| Figure 2.2. Isodose plot of the lung SBRT treatment plan in all three planes. The PTV is highlighted in red. ....  | 9  |
| Figure 2.3. Transaxial view of the 9-beam treatment plan for the vertebral CTV contoured in pink and the spinal cord (OAR) is highlighted in yellow. ....  | 10 |
| Figure 2.4. Isodose plot of the spine SRS treatment plan in all three planes. The PTV is highlighted in pink and the spinal cord (OAR) is highlighted in yellow. ....  | 11 |
| Figure 2.5. Comparison of the longitudinal (1) or lateral (2) edge of EPID images of the collimator aperture collected at collimator angles of 0° and 180° with the gantry placed at 0°. Adjustments to the collimator micrometers were made until the pixel value for the edge of the field were the same. ....                                     | 13 |
| Figure 2.6. Patient left lateral view of x-axis (coronal right/left) shifting mechanism. ....  | 15 |
| Figure 2.7. Patient right lateral view of x-axis (coronal right/left) shifting mechanism. ....   | 15 |
| Figure 2.8. Patient right lateral view of the setup for y-axis (coronal inferior/superior) shifting mechanism. ....  | 16 |
| Figure 2.9. Beam's eye view for the setup for y-axis (coronal inferior/superior) shifting mechanism. ....  | 16 |
| Figure 2.10. SSRS plan with 2cm and 2.7cm distance measured from CTV isocenter displayed in the axial plane with corresponding sagittal (bottom left) and coronal (bottom right) planes displayed. The CTV is outlined in red and the OAR (spinal cord) is contoured in yellow. ....   | 17 |
| Figure 2.11. SSRS coronal plane of 2 cm posterior shift from CTV isocenter. The OAR (spinal cord) is contoured in yellow with the 16 Gy isodose line targeting the CTV outlined in blue and the 24 Gy isodose line targeting the GTV in green. ....  | 17 |
| Figure 2.12. SSRS coronal plane of 2.7 cm posterior shift from CTV isocenter. The OAR (spinal cord) is contoured in yellow with the 16 Gy isodose line targeting the CTV outlined in blue and the 24 Gy isodose line targeting the GTV in green. ....  | 18 |
| Figure 2.13. Screenshot of XVI 3D-kVCBCT registration window. The kVCBCT was aligned to the planning CT at isocenter in this figure. (Cross sections represent the overlaid intersection of the acquired CBCT, shown here as the lighter contrasted image, and the Pinnacle Export reference image, shown here as the darker contrasted image). .... | 19 |

|   |    |
|---|----|
| Figure 2.14. Screenshot of XVI 3D-kVCBCT registration window. The kVCBCT was aligned to the planning CT at isocenter in this figure after a 2cm posterior shift. (Cross sections represent the overlaid intersection of the acquired CBCT, shown here as the lighter contrasted image, and the Pinnacle Export reference image, shown here as the darker contrasted image). ..... | 19 |
| Figure 2.15. Sample profile illustrating the positional alignment error and difference in 75% isodose level metrics on a profile of the delivered and calculated lung SBRT treatment. ....  | 23 |
| Figure 2.16. Solid water “cheese” phantom with ion chamber placed in 2cm patient posterior insert. ....   | 26 |
| Figure 3.1. Scorecard containing objectives for the lung SBRT plan. ....  | 28 |
| Figure 3.2. Scorecard containing objectives for the spine SRS plan. ....  | 29 |
| Figure 3.3. Profiles of repeated measurements for the lung SBRT plan in the coronal plane taken at 0 cm along the superior-inferior axis; used for determining reproducibility of the experimental setup. .   | 32 |
| Figure 3.4. Profiles of repeated measurements for the lung SBRT plan in the coronal plane taken at 0 cm along the left-right axis; used for determining reproducibility of the experimental setup. ....   | 32 |
| Figure 3.5. Profiles of repeated measurements for the spine SRS plan in the coronal plane taken at 0 cm along the superior-inferior axis; used for determining reproducibility of the experimental setup. .   | 33 |
| Figure 3.6. Profiles of repeated measurements for the spine SRS plan in the coronal plane taken at 0 cm along the left-right axis; used for determining reproducibility of the experimental setup. ....   | 33 |
| Figure 3.7. Profiles of repeated measurements for the spine SRS plan posteriorly offset by 2 cm in the coronal plane taken at 0 cm along the superior-inferior axis; used for determining reproducibility of the experimental setup.....  | 34 |
| Figure 3.8. Profiles of repeated measurements for the spine SRS plan posteriorly offset by 2.7 cm in the coronal plane taken at 0 cm along the superior-inferior axis; used for determining reproducibility of the experimental setup.....  | 34 |
| Figure 3.9. (A) SNC Patient Software profile of a single delivery of the lung SBRT plan analyzed at the native resolution of the diode array. (B) Sample plotted profile of the aggregate data file for 9 sequential deliveries of the lung SBRT plan, including that of (A). ....  | 35 |
| Figure 3.10. Comparison of profiles the planned and delivered lung SBRT treatment plan on three linear accelerators; profiles were taken through Y = 0cm on superior-inferior axis. ....  | 36 |
| Figure 3.11. Comparison of the center profiles of the planned and delivered spine SRS treatment plan posteriorly shifted by 2 cm on three linear accelerators profiles; were taken through Y = 0 cm on superior-inferior axis. ....   | 37 |
| Figure 3.12. Comparison of the center profiles of the planned and delivered spine SRS treatment plan posteriorly shifted by 2.7 cm on three linear accelerators; profiles were taken through Y = 0 cm on superior-inferior axis. ....   | 38 |
| Figure A.1. Coronal left-right profile plots of Trials 1 and 2 taken through Y = 1 cm of the lung SBRT treatment plan delivered on the Elekta Infinity with Agility head at the MBPCC Baton Rouge facility. ....  | 52 |

|  |    |
|--|----|
| Figure A.2. Coronal left-right profile plots through $Y = 1$ cm of the lung SBRT treatment plan delivered on the Elekta Versa HD at the MBPCC Baton Rouge facility and the Elekta Infinity with Agility head located at the MBPCC Gonzales facility, respectively. ....    | 53 |
| Figure A.3. Coronal left-right profile plots of Trials 1 and 2 taken through $Y = 0.5$ cm of the lung SBRT treatment plan delivered on the Elekta Infinity with Agility head at the MBPCC Baton Rouge facility. ....   | 54 |
| Figure A.4. Coronal left-right profile plots through $Y = 0.5$ cm of the lung SBRT treatment plan delivered on the Elekta Versa HD at the MBPCC Baton Rouge facility and the Elekta Infinity with Agility head located at the MBPCC Gonzales facility, respectively. ....  | 55 |
| Figure A.5. Coronal left-right profile plots of Trials 1 and 2 taken through $Y = 0$ cm of the lung SBRT treatment plan delivered on the Elekta Infinity with Agility head at the MBPCC Baton Rouge facility. ....   | 56 |
| Figure A.6. Coronal left-right profile plots through $Y = 0$ cm of the lung SBRT treatment plan delivered on the Elekta Versa HD at the MBPCC Baton Rouge facility and the Elekta Infinity with Agility head located at the MBPCC Gonzales facility, respectively. ....    | 57 |
| Figure A.7. Coronal left-right profile plots of Trials 1 and 2 taken through $Y = -0.5$ cm of the lung SBRT treatment plan delivered on the Elekta Infinity with Agility head at the MBPCC Baton Rouge facility. ....  | 58 |
| Figure A.8. Coronal left-right profile plots through $Y = -0.5$ cm of the lung SBRT treatment plan delivered on the Elekta Versa HD at the MBPCC Baton Rouge facility and the Elekta Infinity with Agility head located at the MBPCC Gonzales facility, respectively. .... | 59 |
| Figure A.9. Coronal left-right profile plots of Trials 1 and 2 taken through $Y = -1$ cm of the lung SBRT treatment plan delivered on the Elekta Infinity with Agility head at the MBPCC Baton Rouge facility. ....  | 60 |
| Figure A.10. Coronal left-right profile plots through $Y = -1$ cm of the lung SBRT treatment plan delivered on the Elekta Versa HD at the MBPCC Baton Rouge facility and the Elekta Infinity with Agility head located at the MBPCC Gonzales facility, respectively. ....  | 61 |
| Figure A.11. Coronal superior-inferior profile plots of Trials 1 and 2 taken through $X = 1$ cm of the lung SBRT treatment plan delivered on the Elekta Infinity with Agility head at the MBPCC Baton Rouge facility. ....   | 62 |
| Figure A.12. Coronal superior-inferior profile plots of Trials 1 and 2 taken through $X = 0.5$ cm of the lung SBRT treatment plan delivered on the Elekta Infinity with Agility head at the MBPCC Baton Rouge facility. ....   | 63 |
| Figure A.13. Coronal superior-inferior profile plots of Trials 1 and 2 taken through $X = 0$ cm of the lung SBRT treatment plan delivered on the Elekta Infinity with Agility head at the MBPCC Baton Rouge facility. ....   | 64 |
| Figure A.14. Coronal superior-inferior profile plots of Trials 1 and 2 taken through $X = -0.5$ cm of the lung SBRT treatment plan delivered on the Elekta Infinity with Agility head at the MBPCC Baton Rouge facility. ....  | 65 |
| Figure A.15. Coronal superior-inferior profile plots of Trials 1 and 2 taken through $X = -1$ cm of the lung SBRT treatment plan delivered on the Elekta Infinity with Agility head at the MBPCC Baton Rouge facility. ....  | 66 |

|  |    |
|--|----|
| Figure A.16. Coronal left-right profile plots of Trials 1 and 2 taken through Y = 1 cm of the spine SRS treatment plan delivered on the Elekta Infinity with Agility head at the MBPCC Baton Rouge facility. ....  | 67 |
| Figure A.17. Coronal left-right profile plots of Trials 1 and 2 taken through Y = 0.5 cm of the spine SRS treatment plan delivered on the Elekta Infinity with Agility head at the MBPCC Baton Rouge facility. ....  | 68 |
| Figure A.18. Coronal left-right profile plots of Trials 1 and 2 taken through Y = 0 cm of the spine SRS treatment plan delivered on the Elekta Infinity with Agility head at the MBPCC Baton Rouge facility. ....  | 69 |
| Figure A.19. Coronal left-right profile plots of Trials 1 and 2 taken through Y = -0.5 cm of the spine SRS treatment plan delivered on the Elekta Infinity with Agility head at the MBPCC Baton Rouge facility. ....   | 70 |
| Figure A.20. Coronal left-right profile plots of Trials 1 and 2 taken through Y = -1 cm of the spine SRS treatment plan delivered on the Elekta Infinity with Agility head at the MBPCC Baton Rouge facility. ....   | 71 |
| Figure A.21. Coronal superior-inferior profile plots of Trials 1 and 2 taken through X = 1 cm of the spine SRS treatment plan delivered on the Elekta Infinity with Agility head at the MBPCC Baton Rouge facility. ....   | 72 |
| Figure A.22. Coronal superior-inferior profile plots of Trials 1 and 2 taken through X = 0.5 cm of the spine SRS treatment plan delivered on the Elekta Infinity with Agility head at the MBPCC Baton Rouge facility. ....   | 73 |
| Figure A.23. Coronal superior-inferior profile plots of Trials 1 and 2 taken through X = 0 cm of the spine SRS treatment plan delivered on the Elekta Infinity with Agility head at the MBPCC Baton Rouge facility. ....   | 74 |
| Figure A.24. Coronal superior-inferior profile plots of Trials 1 and 2 taken through X = -0.5 cm of the spine SRS treatment plan delivered on the Elekta Infinity with Agility head at the MBPCC Baton Rouge facility. ....  | 75 |
| Figure A.25. Coronal superior-inferior profile plots of Trials 1 and 2 taken through X = -1 cm of the spine SRS treatment plan delivered on the Elekta Infinity with Agility head at the MBPCC Baton Rouge facility. ....  | 76 |
| Figure A.27. Coronal left-right profile plots of Trials 1 and 2 taken through Y = 0 cm of the spine SRS treatment plan shifted posteriorly by 2 cm with kV-CBCT positioning and delivered on the Elekta Infinity with Agility head at the MBPCC Baton Rouge facility. ....                         | 77 |
| Figure A.28. Coronal left-right profile plots through Y = 0 cm of the spine SRS treatment plan shifted posteriorly by 2 cm delivered on the Elekta Versa HD at the MBPCC Baton Rouge facility and the Elekta Infinity with Agility head located at the MBPCC Gonzales facility, respectively. .... | 78 |
| Figure A.29. Coronal left-right profile plots of Trials 1 and 2 taken through Y = 1 cm of the spine SRS treatment plan shifted posteriorly by 2 cm with kV-CBCT positioning and delivered on the Elekta Infinity with Agility head at the MBPCC Baton Rouge facility. ....                         | 79 |
| Figure A.30. Coronal left-right profile plots through Y = 1 cm of the spine SRS treatment plan shifted posteriorly by 2 cm delivered on the Elekta Versa HD at the MBPCC Baton Rouge facility and the Elekta Infinity with Agility head located at the MBPCC Gonzales facility, respectively. .... | 80 |

|  |    |
|--|----|
| Figure A.31. Coronal left-right profile plots of Trials 1 and 2 taken through Y = 0.5 cm of the spine SRS treatment plan shifted posteriorly by 2 cm with kV-CBCT positioning and delivered on the Elekta Infinity with Agility head at the MBPCC Baton Rouge facility.....                            | 81 |
| Figure A.32. Coronal left-right profile plots through Y = 0.5 cm of the spine SRS treatment plan shifted posteriorly by 2 cm delivered on the Elekta Versa HD at the MBPCC Baton Rouge facility and the Elekta Infinity with Agility head located at the MBPCC Gonzales facility, respectively. ....   | 82 |
| Figure A.33. Coronal left-right profile plots of Trials 1 and 2 taken through Y = -0.5 cm of the spine SRS treatment plan shifted posteriorly by 2 cm with kV-CBCT positioning and delivered on the Elekta Infinity with Agility head at the MBPCC Baton Rouge facility.....                           | 83 |
| Figure A.34. Coronal left-right profile plots through Y = -0.5 cm of the spine SRS treatment plan shifted posteriorly by 2 cm delivered on the Elekta Versa HD at the MBPCC Baton Rouge facility and the Elekta Infinity with Agility head located at the MBPCC Gonzales facility, respectively. ....  | 84 |
| Figure A.35. Coronal left-right profile plots of Trials 1 and 2 taken through Y = -1 cm of the spine SRS treatment plan shifted posteriorly by 2 cm with kV-CBCT positioning and delivered on the Elekta Infinity with Agility head at the MBPCC Baton Rouge facility.....                             | 85 |
| Figure A.36. Coronal left-right profile plots through Y = - 1 cm of the spine SRS treatment plan shifted posteriorly by 2 cm delivered on the Elekta Versa HD at the MBPCC Baton Rouge facility and the Elekta Infinity with Agility head located at the MBPCC Gonzales facility, respectively. ....   | 86 |
| Figure A.37. Coronal left-right profile plots of Trials 1 and 2 taken through Y = 0 cm of the spine SRS treatment plan shifted posteriorly by 2.7 cm with kV-CBCT positioning and delivered on the Elekta Infinity with Agility head at the MBPCC Baton Rouge facility.....                            | 87 |
| Figure A.38. Coronal left-right profile plots through Y = 0 cm of the spine SRS treatment plan shifted posteriorly by 2.7cm delivered on the Elekta Versa HD at the MBPCC Baton Rouge facility and the Elekta Infinity with Agility head located at the MBPCC Gonzales facility, respectively. ....    | 88 |
| Figure A.39. Coronal left-right profile plots of Trials 1 and 2 taken through Y = 1 cm of the spine SRS treatment plan shifted posteriorly by 2.7 cm with kV-CBCT positioning and delivered on the Elekta Infinity with Agility head at the MBPCC Baton Rouge facility.....                            | 89 |
| Figure A.40. Coronal left-right profile plots through Y = 1 cm of the spine SRS treatment plan shifted posteriorly by 2.7cm delivered on the Elekta Versa HD at the MBPCC Baton Rouge facility and the Elekta Infinity with Agility head located at the MBPCC Gonzales facility, respectively. ....    | 90 |
| Figure A.41. Coronal left-right profile plots of Trials 1 and 2 taken through Y = 0.5 cm of the spine SRS treatment plan shifted posteriorly by 2.7 cm with kV-CBCT positioning and delivered on the Elekta Infinity with Agility head at the MBPCC Baton Rouge facility.....                          | 91 |
| Figure A.42. Coronal left-right profile plots through Y = 0.5 cm of the spine SRS treatment plan shifted posteriorly by 2.7cm delivered on the Elekta Versa HD at the MBPCC Baton Rouge facility and the Elekta Infinity with Agility head located at the MBPCC Gonzales facility, respectively. ....  | 92 |
| Figure A.43. Coronal left-right profile plots of Trials 1 and 2 taken through Y = -0.5 cm of the spine SRS treatment plan shifted posteriorly by 2.7 cm with kV-CBCT positioning and delivered on the Elekta Infinity with Agility head at the MBPCC Baton Rouge facility.....                         | 93 |
| Figure A.44. Coronal left-right profile plots through Y = -0.5 cm of the spine SRS treatment plan shifted posteriorly by 2.7cm delivered on the Elekta Versa HD at the MBPCC Baton Rouge facility and the Elekta Infinity with Agility head located at the MBPCC Gonzales facility, respectively. .... | 94 |

|   |    |
|---|----|
| Figure A.45. Coronal left-right profile plots of Trials 1 and 2 taken through Y = -1 cm of the spine SRS treatment plan shifted posteriorly by 2.7 cm with kV-CBCT positioning and delivered on the Elekta Infinity with Agility head at the MBPCC Baton Rouge facility.....                              | 95 |
| Figure A.46. Coronal left-right profile plots through Y = -1 cm of the spine SRS treatment plan shifted posteriorly by 2.7cm delivered on the Elekta Versa HD at the MBPCC Baton Rouge facility and the Elekta Infinity with Agility head located at the MBPCC Gonzales facility, respectively.....       | 96 |
| Figure B.1. MV Isocenter analysis of the Elekta Infinity platform with Agility head located at the Baton Rouge MBPCC facility (Infinity 1). EPID mages were analyzed with the RIT Isocenter Analysis Tool for the four cardinal gantry angles with couch at 0° and four couch angles with gantry at 0° .  | 97 |
| Figure B.2. MV Isocenter analysis of the Versa HD™ platform located at the Baton Rouge MBPCC facility (Infinity 1). EPID mages were analyzed with the RIT Isocenter Analysis Tool for the four cardinal gantry angles with couch at 0° and four couch angles with gantry at 0° .....                      | 98 |
| Figure B.3. MV Isocenter analysis of the Elekta Infinity platform with Agility head located at the Gonzales MBPCC facility (Infinity 2). EPID mages were analyzed with the RIT Isocenter Analysis Tool for the four cardinal gantry angles with couch at 0° and four couch angles with gantry at 0° ..... | 99 |



## Abstract

**Purpose:** This work investigated the delivery accuracy of high-dose lung and spine stereotactic treatments delivered with the Elekta Infinity and Versa HD platforms. The accuracy of these platforms will be used for consideration in implementing a spine stereotactic radiosurgery (SSRS) program at Mary Bird Perkins Cancer Center.

**Methods:** A geometric phantom was used to perform Winston-Lutz type tests that assessed the relevant degrees of freedom (gantry, collimator, and couch) of the delivery system. A lung stereotactic body radiation therapy (SBRT) and spine SRS treatment plan were generated for use in end-to-end testing. Delivery accuracy was tested using a novel diode array design, which achieved a spatial resolution of 1 mm along a single axis. On board imaging aided in setup of the diode array to the desired position before commencing treatment delivery. The delivered dose distribution and calculated planar dose distributions were compared and analyzed. Several metrics were analyzed from the overlaid profiles, including: percent difference between calculated and measured field centers, and comparison of spatial shifts of the 75% and 60% isodose levels. Percent difference between a calculated and measured point dose quantified discrepancies for the approximate region of the spinal cord. Calculated dose profiles and shifts at the 60 and 75% isodose levels indicated distortions in the profiles.

**Results:** All machines demonstrated an MV Isocenter radius for gantry and treatment table rotation less than 0.70 mm as limited by the Elekta customer acceptance protocol. For SSRS plans, percent difference of the point representing the spinal cord produced results that were consistently higher as a result of a higher dose delivery than calculated. All lung SBRT and SSRS deliveries were capable of achieving an average of 1-mm accuracy. Moreover, profiles showed that the measured profile fell within the planned profile, suggesting a systematic distortion in the profiles.

**Conclusion:** Based on the findings of this project, the Elekta Infinity and Versa HD delivery systems were adequate for lung SBRT treatments but require further exploration for the commencement of spine SRS treatments at Mary Bird Perkins Cancer Center.

# Chapter 1. Introduction

## 1.1 Background and Significance

### 1.1.1 Stereotactic Body Radiation Therapy

Stereotactic Body Radiation Therapy (SBRT) is a non-invasive cancer treatment where high doses of external beam radiation are delivered in a limited number of fractions to extra-cranial sites. SBRT derived from stereotactic radiosurgery (SRS), which was originally used to treat intracranial and spinal tumors as well as other disorders of the brain with the use of body frames and three-dimensional imaging to localize lesions (Khan, 2010). Since the advent of on-board imaging, SBRT has become a feasible treatment options since body frames are not required for treatments. Systems now utilize x-ray imaging of bony anatomy and implanted fiducial marker to localize the target (Khan, 2010). Reductions in errors and uncertainties in patient positioning and targeting have been made possible due to image guided radiation therapy (IGRT) (Court *et al.*, 2008). IGRT has provided new capabilities of treatment that have increased dose delivery precision to the target and avoidance of organs at risk (OAR). This is achievable since image guidance can be utilized before, during, or after any radiation therapy treatment. Implementation of beam shaping and image guidance technology have enhanced the performance of SBRT in reducing safety margins and precisely conforming to the tumor outline in all three dimensions (Greco *et al.*, 2015). The additional confidence that IGRT provides for patient positioning has been crucial in implementing innovative treatments to ablate tumors, such as with stereotactic body radiation therapy (Greco *et al.*, 2015).

A typical SBRT plan will vary from a conventional radiotherapy plan in several ways. SBRT plans employ 1 to 5 fractions with doses ranging from 6 to 30 Gy per fraction, whereas conventional treatments use anywhere from 10 to 30 treatments with doses ranging from 1.8 to 3Gy per fraction (Benedict *et al.*, 2010). Typically those treatments with only one treatment fraction are termed stereotactic radiosurgery because of its similar outcome to surgery without invasive means. Target definition also varies for the two treatment plans. Conventional radiotherapy treatments will treat tumors that may not have sharp boundaries, which are accounted for with margins on the order of centimeters, whereas SBRT treatments require tumors to be well defined with any additional margins on the order of millimeters due to the high,

conformal dose of the target volume (Benedict *et al.*, 2010). Targeting and conformity requirements are higher for SBRT and SRS treatments because of the larger doses delivered in fewer fractions, meaning that inaccurate targeting will have a greater effect on normal tissues with stereotactic treatments. Also, SBRT treatments typically employ more beams than conventional treatments in order to achieve this degree of conformality. In addition to the number of beams, delivery techniques such as noncoplanar beam arrangements, inhomogeneous dose distributions, and IMRT are often used for SBRT treatments in order to minimize the dose to surrounding normal tissue (Benedict *et al.*, 2010).

Whereas conventional radiotherapy delivers a prescribed dose to large volumes over many small-dose fractions spanning months, SBRT delivers the prescription dose to smaller target volumes via hypofractionation (Benedict *et al.*, 2010). Hypofractionation utilizes a higher dose per fraction to increase the biologically effective dose (BED), which is used to evaluate the effects of different fractionation schedules because it varies according to dose per fraction, number of fractions, and tissue characteristics. In order for the objective of ablative radiation therapy to be met, as opposed to regional adjuvant therapy for cancers such as rectum, breast, and sarcoma that have been treated by other means such as surgery and chemotherapy, the dose prescription must radically change by increasing the dose and decreasing the number of fractions (Papiez and Timmerman, 2008). The result is an ablative dose per fraction where damage to adjacent critical structures is avoided by maintaining a sharp dose fall-off around the target (Amini *et al.*, 2014). When effects of equivalent total doses with different fractionation regimens are compared, they produce unequal biological effects (Kong *et al.*, 2014). Achieving a high BED has been shown to increase overall survival by improving tumor control rate for non-small cell lung cancer, paraspinal and spinal metastasis, and oligometastatic liver disease (Kong *et al.*, 2014; Zhang *et al.*, 2011; Sheehan and Jagannathan, 2008; Berkovic *et al.*, 2017). Due to the ablative nature of SBRT, this hypofractionated approach more closely follows the model of surgery than conventional radiotherapy. This makes SBRT an attractive option for patients unwilling or incapable of undergoing surgery (Papiez and Timmerman, 2008). Specifically, SBRT has been proven highly effective for controlling specific cancers of the thorax, abdomen, and spine (Benedict *et al.*, 2010; Nalichowski *et al.*, 2017).

## 1.1.2 Lung Cancer

As shown in Figure 1.1, lung cancer is estimated to be the second cancer in terms of incidence and the leading cause of cancer death within the United States, accounting for approximately 25% of estimated deaths for both men and women (American Cancer Society, 2018). In order to treat this prevalent cancer, primary tumor control becomes the essential requirement for the treatment of lung cancer (Timmerman *et al.*, 2010). Long-term follow up of patients treated with conventional fractionation techniques for non-small cell lung cancer showed that only 20-30% of these tumors stopped growth or recessed (Papiez and Timmerman, 2008). Moreover, it has been shown that patients with early stage, medically inoperable lung cancer have low primary tumor control rates of approximately 30-40% (Timmerman *et al.*, 2010). According to Timmerman *et al.*'s findings, SBRT delivered according Radiation Therapy Oncology Group Report 0236 to early stage lung cancer patients provided more than double the rate of primary tumor control than reports describing conventional radiotherapy.

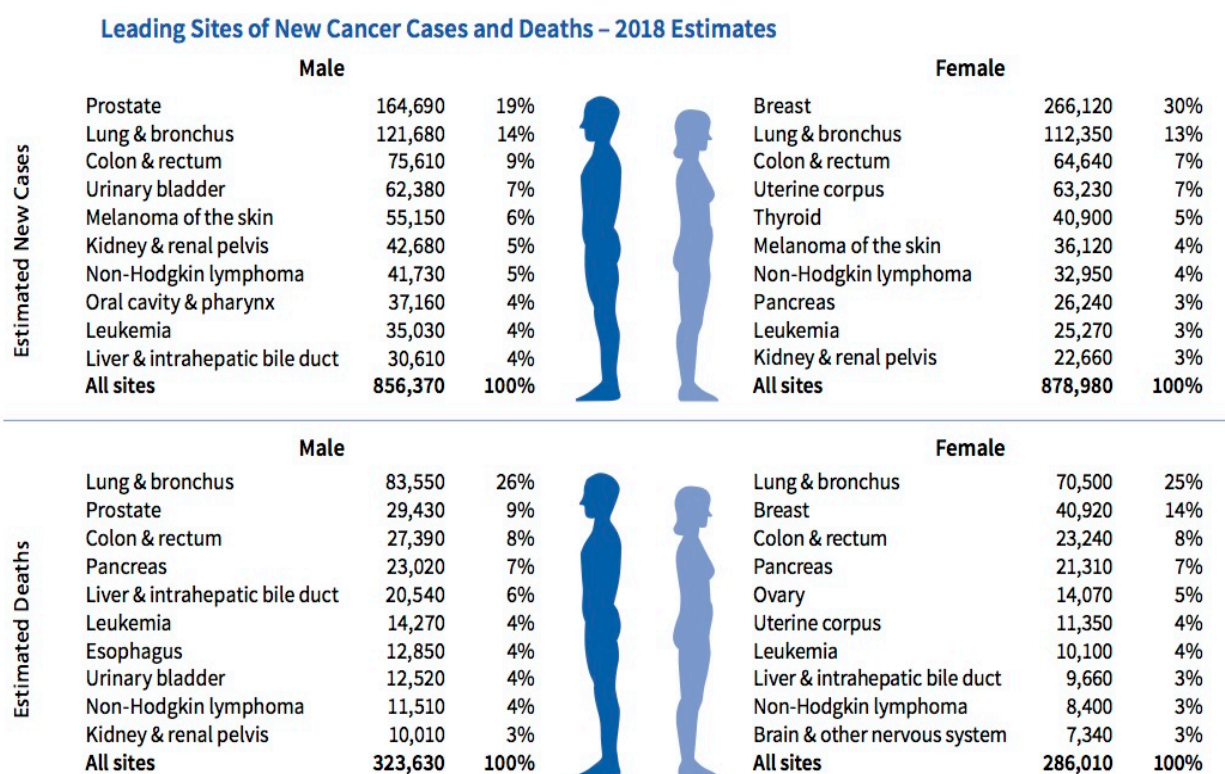


Figure 1.1. 2018 Estimates for Leading Sites of New Cancer Cases and Deaths in the United States (American Cancer Society, 2018).

It is believed that the hypofractionated doses in SBRT contribute to an improved local control via clonogenic cell death from DNA strand breaks, chromosome aberrations, and vascular damage in tumors

that lead to indirect cell death (Song *et al.*, 2013). Since SBRT delivers a much higher BED than conventional therapy, it has been shown to lead to long survival and local tumor control for patients with non-small cell lung cancer (Kong *et al.*, 2014).

### 1.1.3 Spinal Metastases

It is estimated that approximately 10% of cancer patients will develop vertebral or spinal metastases, typically originating from primary breast, lung, prostate, and renal cell carcinomas (Greco *et al.*, 2015). This type of metastasis can affect a patient's stability and neurologic function, therefore the two primary therapeutic targets of single dose SBRT for spinal metastases are pain control and spine stabilization in order to avoid cord compression (Greco *et al.*, 2015). Deterioration of the vertebral column as a result of spinal metastasis is shown in Figure 1.2. SBRT is a non-invasive treatment option for patients unwilling to undergo surgery, with gross residual disease or deemed high risk for recurrence post-surgery, and for those with a poor performance status (Sahgal *et al.*). SBRT allows for escalation of tumor dose while also sparing adjacent organs at risk, particularly the spinal cord, making it an attractive alternative to surgery for patients with spinal metastases. Moreover, it has been reported that 86% of patients experienced long-term pain improvement and excellent local control with SBRT (Nalichowski *et al.*, 2017). Overall, radiation therapy has primarily been used for palliative management of spinal metastases in patients unwilling or unfit for surgery.

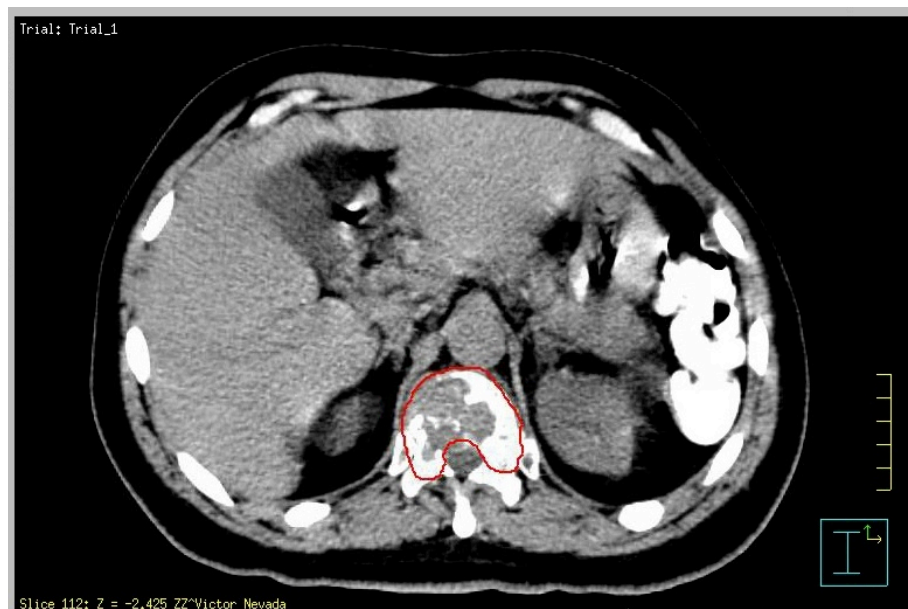


Figure 1.2. Axial computed tomographic view of a patient with spinal metastasis. The diseased T12 vertebra is contoured in red.

## 1.2 Motivation for Research

Due to the numerous people affected by lung cancer and the challenge its location in a non-rigid structure presents, high levels of precision must be obtained in order to achieve a curative treatment. Specifically, 2-mm accuracy falls within the range of achievable setup accuracies for lung SBRT treatments utilizing various immobilization devices (Benedict *et al.*, 2010; Nagata *et al.*, 2002; Hara *et al.*, 2002; Wulf *et al.*, 2000; Hof *et al.*, 2003; Wang *et al.*, 2006) with a 1-mm accuracy proven to be achievable for end-to-end localization accuracy including setup uncertainty but withholding intrafraction errors (Solberg *et al.*, 2008; Verellen *et al.*, 2003; Sharpe *et al.*, 2006). 1-mm accuracy is generally recommended for spine SBRT cases considering the dosimetric effect to the spinal cord of translational errors greater than 1 mm (Guckenberger *et al.*, 2007; Wang *et al.*, 2008). Moreover, 1-mm accuracy has been achieved for setup with the use of stereotactic body frames (Guckenberger *et al.*, 2007; Wang *et al.*, 2008; Chang *et al.*, 2004; Yenice *et al.*, 2003; Lohr *et al.*, 1999) as well as end-to-end localization (Ryu *et al.*, 2001; Yu *et al.*, 2004). Additionally, with the spine as the most common site of bone metastases, their management poses a challenge in clinical oncology due to larger treatment volumes, numerous organs at risk, and lack of rigid, frame-based immobilization (Katagiri *et al.*, 1998; Sheehan and Jagannathan, 2008).

The large doses per fraction in SBRT lead to tumor ablation. However, healthy tissue cells can be critically damaged if they are exposed to these high levels of radiation (Papiez and Timmerman, 2008). Therefore, SBRT requires a high degree of accuracy. This is achieved throughout the treatment process with the use of immobilization devices, simulation, treatment planning, and on-board imaging. Overall, accurate dose delivery is dependent on correct patient positioning and physical delivery of the planned dose. There are uncertainties that one encounters during the treatment process; for example, uncertainties resulting from the imaging system used in simulation and patient positioning verification, mechanical uncertainties in positioning (such as the treatment couch position), and dose delivery uncertainties. The latter are related to the linear accelerator output and its mechanical uncertainties in delivery such as gantry positioning and multi-leaf collimator positioning.

This research focuses on these types of uncertainties as they apply to the Elekta Infinity linear accelerator equipped with an Agility head, as shown in Figure 1.3, as well as the Versa HD™ linear

accelerator (Elekta, Stockholm, Sweden). The evaluation of these linear accelerators for their continued use in lung stereotactic body radiotherapy and their initial use in spinal stereotactic radiosurgery (SSRS) at Mary Bird Perkins Cancer Center (MBPCC) serves as the motivation for this project.



Figure 1.3. Mary Bird Perkins Cancer Center Elekta Infinity linear accelerator with Agility head. MV-CBCT and orthogonal kV-CBCT onboard imaging pictured.

### 1.3 Hypothesis and Specific Aims

The hypothesis of this work is that the Elekta Infinity and Versa HD platforms will be sufficient for lung SBRT and spine SRS treatments as deemed by clinical standards and metrics including percent difference between measured and calculated doses, positional alignment, and shifts in isodose levels that were designed for this project. The specific aims formulated to address the hypothesis of this work are:

Aim 1: Generate a lung SBRT treatment plan following RTOG 0813 protocol and a spine SRS treatment plan following RTOG 0631 protocol.

Aim 2: Measure delivery accuracy through geometric and end-to-end testing.

Sub-Aim 2a: Perform Winston-Lutz type test to assess MV isocenter accuracy.

Sub-Aim 2b: Deliver treatment plans using a diode array phantom with 1-millimeter resolution.

Aim 3: Evaluate delivery accuracy of the Elekta Infinity with Agility Head and Versa HD platforms.

## Chapter 2. Methods and Materials

### 2.1 Aim 1

To assess the delivery accuracy of the Elekta linear accelerators, treatment plans were developed so that their delivery could be evaluated on multiple platforms. In Aim 1, two treatment plans were created using the Pinnacle<sup>3</sup> treatment planning system (Philips Radiation Oncology Systems, Fitchburg, WI). A 3D conformal treatment plan was generated for a lung SBRT case and a static MLC (sMLC) IMRT treatment plan was created for a spine SRS case.

#### 2.1.1 Lung SBRT Treatment Plan

A single patient with a right lung tumor was selected and anonymized for this study. The patient was previously treated with SBRT to a prescription of 50 Gy over 5 fractions using a volumetric modulate arc therapy (VMAT) technique. Since the goal of this study was to assess the delivery accuracy of the system as a whole, highly modulated or dynamically modulated plans increase complexity and introduce additional uncertainties attributable to the MLC model in the TPS. Therefore, a 3D conformal treatment plan was created to reduce TPS model uncertainties (Sutton *et al.*, 2014). The Radiation Therapy Oncology Group (RTOG) Report 0813 protocol was followed to generate the treatment plan. Per the protocol, a 9-field 3D conformal lung stereotactic body radiotherapy plan was created consisting of seven static coplanar beams with the couch at 0 degrees and gantry angles of 0, 40, 135, 180, 220, 265, and 310 degrees; and two noncoplanar beams with the couch placed at 45 degrees and gantry placed at 315 degrees and conversely, with the couch placed at 315 degrees and gantry placed at 45 degrees (Figure 2.1). Seven of the nine beams were planned at 6 megavoltage (MV) photon energy, with the remaining two beams planned at 10 MV photon energy. Two 6 MV beams were changed to 10 MV beams in order to minimize a few small hot spots. Gantry angles were chosen to avoid dose to normal tissue, which is of particular concern in SBRT cases that employ high doses per fraction. The chosen gantry beam formation permitted for tolerable doses to two prominent OARS for this case: the great vessels and the contralateral lung.



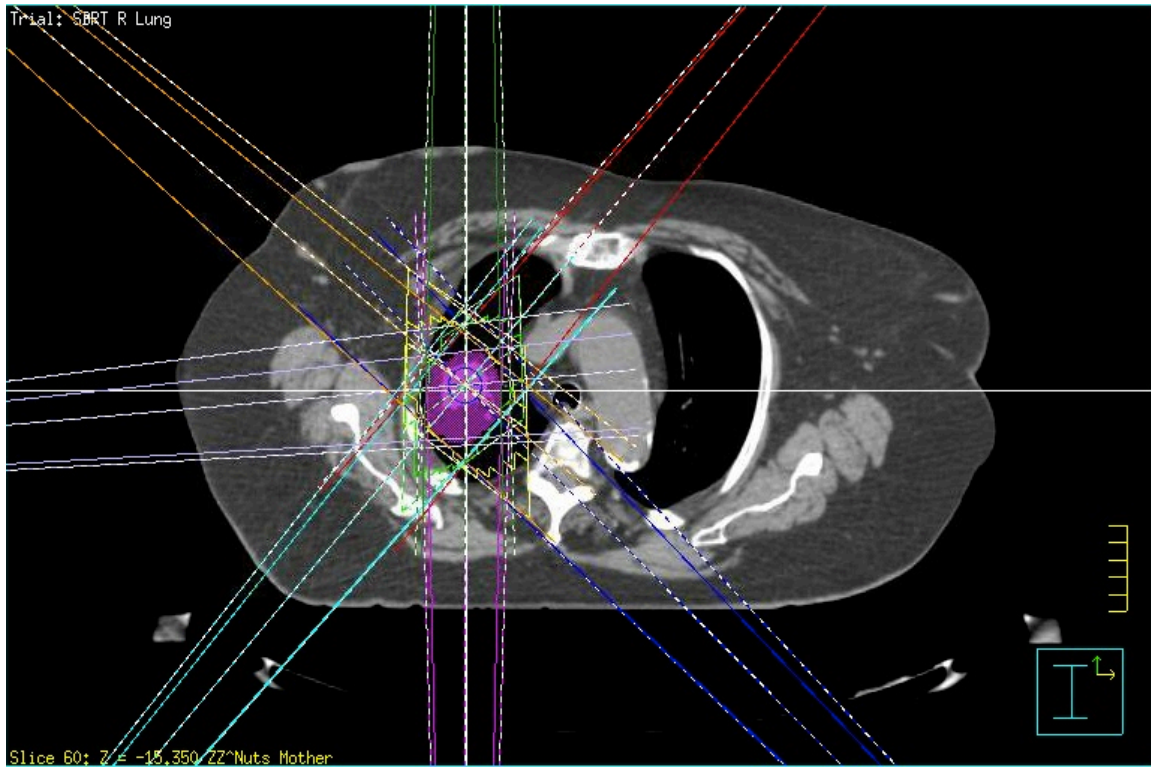


Figure 2.1. Transaxial view of the 7-coplanar and 2-noncoplanar-beam (not pictured) treatment plan for the lung SBRT patient. The PTV is contoured pink in this image plane.

The internal target volume (ITV), which includes the gross tumor volume (GTV) and accounts for respiratory motion, planning target volume (PTV), and additional contours were generated by a radiation oncologist. The PTV is defined by the International Committee on Radiation Units and Measurements (ICRU) Report 62 as the target volume necessary to account for external treatment inaccuracies including those resulting from patient positioning, mechanical uncertainties of the equipment, and dosimetric uncertainties (Wambersie, 1999). Field aperture size and shape conformed to the projection of the PTV along the beam's eye view for each beam, therefore no additional margin was added to the edge of the blocks or MLC jaws beyond the PTV. This approach followed RTOG 0813 protocol. Beams at gantry angles of 40 and 135° with the treatment table at 0° as well as the two non-coplanar beams at gantry angles of 45 and 315° with treatment table angles of 315° and 45°, respectively, were weighted approximately 14% due to the shorter path they traversed through normal tissue. Conversely, the remaining oblique beams were given approximately half this weight. The remaining beam of 265° was weighted approximately 12%, even though it was traversing the most amount of normal tissue, in order to offset those beams approaching from the contralateral side. The isocenter corresponded to the center of

the mass and the plan was normalized to this point by approximately 67% so that the prescription dose would be delivered to the margin of the PTV. In addition to the beam parameters, the dose grid resolution was set to 1mm when calculating the projected dose calculation. Isodose plots for the lung SBRT treatment plan are shown in Figure 2.2.

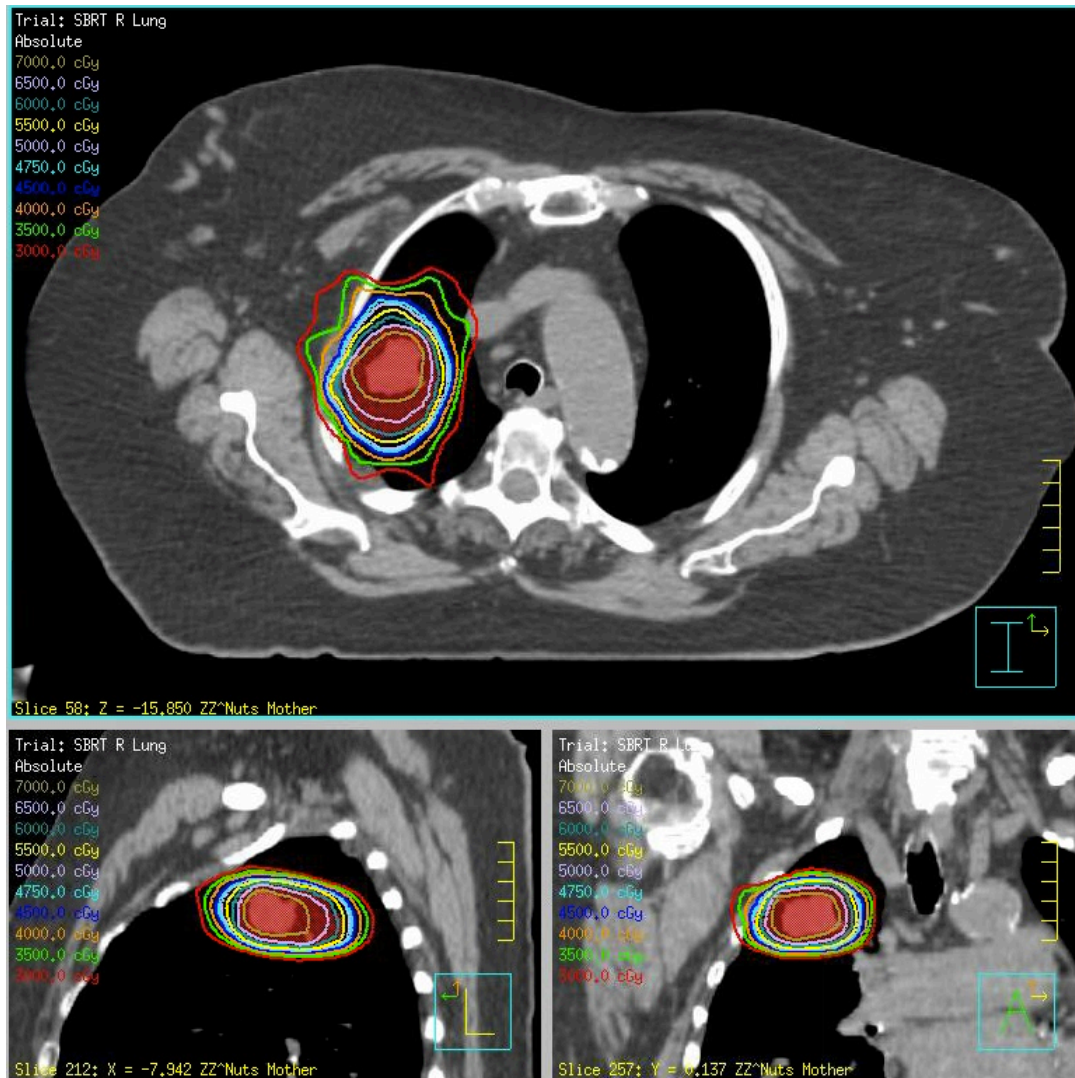


Figure 2.2. Isodose plot of the lung SBRT treatment plan in the axial (top center), sagittal (bottom left) and coronal (bottom right) planes. The PTV is highlighted in red.

## 2.1.2 SSRS Treatment Plan

A patient previously treated for a spine metastasis of the T-12 vertebra was anonymized for this study. The gross tumor volume (GTV) and clinical target volume (CTV) were contoured by a radiation oncologist. Per ICRU Report 62, the gross tumor volume is defined as the visible extent and location of the malignant growth with the CTV containing the GTV as well as an expansion for any subclinical

microscopic disease that is not visible by diagnostic means (Wambersie, 1999). For this treatment plan, the CTV was contoured to include the entire vertebral body. The GTV prescription was set to 24 Gy and the CTV prescription was set to 16 Gy for a single fraction. These doses were specified as objectives in the form of a minimum of 95% coverage in the inverse planning module of the Pinnacle treatment planning system. Per protocol, a treatment plan is acceptable as long as >90% of the target volume receives the prescribed radiosurgery dose. A step and shoot IMRT plan was created according to RTOG Report 0631, since the use of IMRT could not be avoided for a plan with the target volume directly adjacent to the spinal cord. With the patient supine, 9 posterior 6 MV photon beams were generated with 20 degrees of separation spanning from 260 to 100 degrees (Figure 2.3). Other objectives included maximum doses to the stomach, liver, kidneys, and bowel that were not to exceed their tolerance (to be described in Section 3.1.2) as defined by RTOG Report 0631 and MBPCC. The highest weight of the objectives was assigned to those pertaining to the GTV and CTV. The plan was initially optimized to 75 iterations, with 25 iterations for the opening density matrix via pencil beam. A “warm start” of 50 iterations followed, and finally 30 further iterations were used to achieve a composite objective value of 0.11, which is satisfactory for this type of plan. The dose grid resolution was set to 1mm. The isodose plot of the treatment plan is shown in Figure 2.4. Per RTOG Report 0631, the clinical target volume included the involved vertebral body as well as both left and right pedicles.

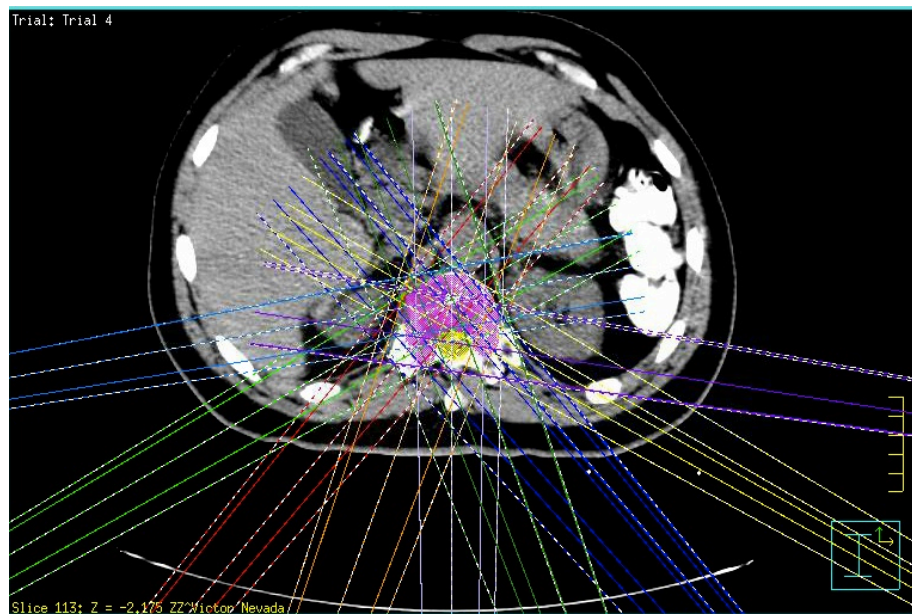


Figure 2.3. Transaxial view of the 9-beam treatment plan for the vertebral CTV contoured in pink and the spinal cord (OAR) is highlighted in yellow.



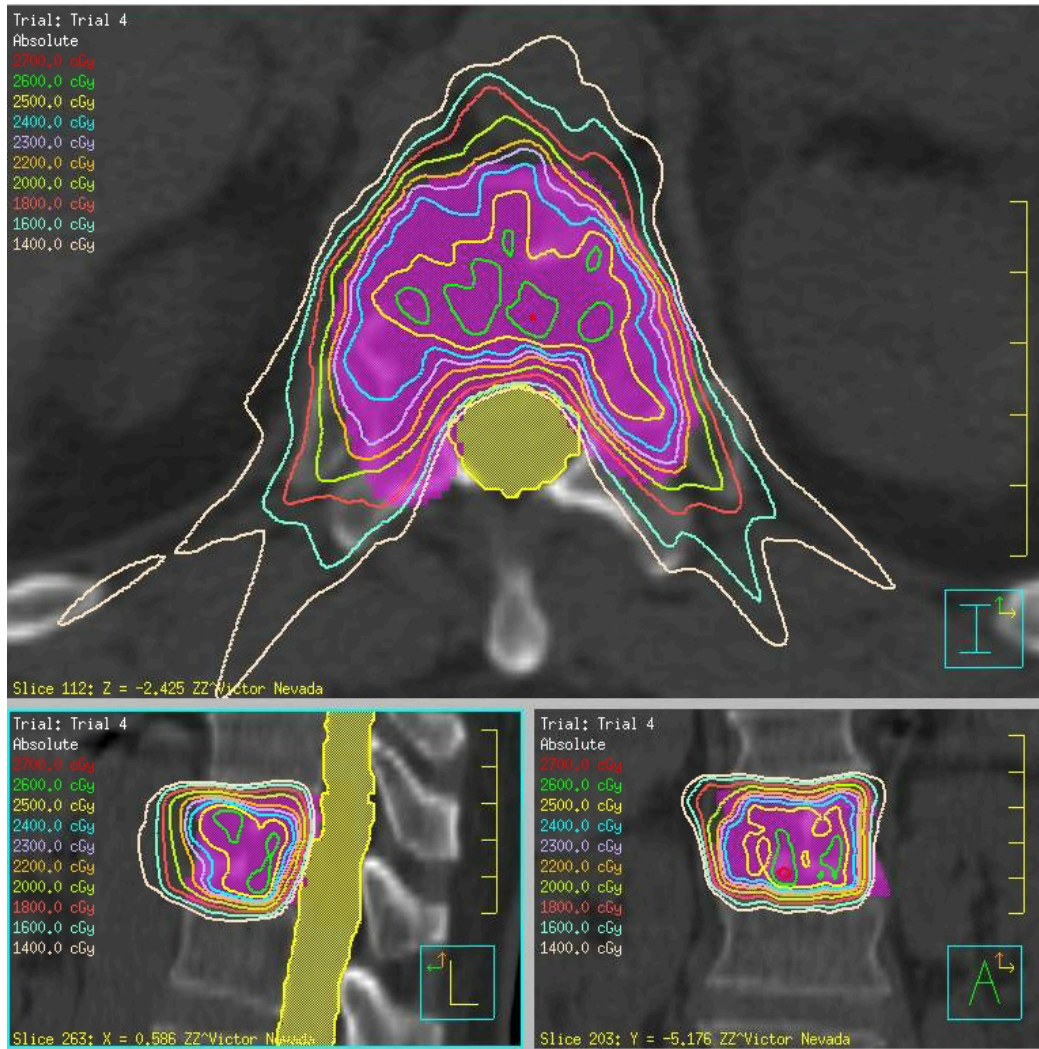


Figure 2.4. Isodose plot of the spine SRS treatment plan in all three planes. The PTV is highlighted in pink and the spinal cord (OAR) is highlighted in yellow.

### 2.1.3 Planar Dose Export

Plans were copied to an image set of the MapCHECK2 phantom with MapPHAN in order to generate planar dose files which were used for comparison to delivered treatment plans. Density overrides of  $1.05 \text{ g/cm}^3$ ,  $1.5027 \text{ g/cm}^3$ , and  $1.6667 \text{ g/cm}^3$  were performed to account for the MapPHAN, bottom section, and top section of the MapCHECK2, respectively. The planar dose tool in Pinnacle<sup>3</sup> v9.10 was used to generate and export an ASCII planar dose file for each plan. The 2D coronal dose plane through isocenter of the spine SRS and lung SBRT plans, as well as the posterior points of 2.0 cm and 2.7 cm for the SSRS plan (see Section 2.2.2), were exported from the TPS 3D dose matrix for each treatment plan. Planar doses were calculated for a  $13 \times 13 \text{ cm}^2$  square field with a resolution of 1mm.

## 2.2 Aim 2

The targeting accuracy of the Elekta with an Agility head (Elekta, Stockholm, Sweden, one located at Mary Bird Perkins Cancer Center in Baton Rouge, Serial Number: 151892 and one located at the MBPCC Gonzales site, Serial Number: 151785) linear accelerator system as well as the Elekta Versa HD™ linear accelerator system (located at the MBPCC Baton Rouge site, Serial Number: 153187) were tested through geometric testing in the form of a Winston-Lutz type test and end-to-end testing in which the plans from Aim 1 were delivered. Moreover, the reproducibility of the experimental set up was also evaluated in this aim.

### 2.2.1 MV Isocenter Accuracy Test

In order to test the mechanical component of targeting accuracy for the Elekta linear accelerator, geometric testing was performed with a vendor-supplied Winston-Lutz type test (called the MV Isocenter Accuracy Test in this work), which followed the vendor-supplied protocol for Customer Acceptance Tests for MV Isocenter Accuracy. Following the stated workflow (Clements, 2016), the steps for the Winston-Lutz test were as follows:

1. A small high-density (typically tungsten or steel) ball bearing (BB) is placed at a location in the treatment room that is defined to be the mechanical isocenter point. This definition can refer to: coincidence of room lasers, coincidence of light-field crosshairs, or location of the tip of a front-pointer device. Typically, the BB is placed on the treatment table such that it rotates and translates with the table.
2. A small radiation field is projected through the BB onto an image receptor, such as film or electronic portal imaging device (EPID), using an aperture defined by MLC, primary collimator (jaws), or stereotactic cone.
3. Projection images of the above are acquired for various gantry rotations and table rotations. Generally a total of eight images are acquired at varying gantry and couch angles in order to encompass the largest range of motion during a stereotactic treatment.
4. For each projection image, the 2D deviation between the center of the BB and the center of the radiation field is found.

For the purposes of this research, the geometric phantom consisted of the kV x-ray volume imaging (XVI) ball-bearing (BB) phantom (Elekta, Stockholm, Sweden) made of steel with a diameter of 8mm. The steel ball is located at the tip of a plastic tube that is connected to a plate, which attaches to the treatment table so that the BB is suspended off the table. The base plate is equipped with a set of vernier adjustments that allow the position of the BB to be adjusted by 0.01 mm increments. A circular collimator of 50-mm diameter was attached to the treatment head. The service cone was equipped with a set of micrometers to adjust the position of the stereotactic collimator. The gantry was set at 0° to verify the cone was

centered with respect to the central axis and the BB was aligned to the room crosshairs. EPID images were acquired with the collimator at  $0^\circ$  and  $180^\circ$ . A 6MV energy beam was used to collect all images for the MV Isocenter Accuracy Test. Adjustments to the micrometers were made until there was no apparent movement between the images and the difference in pixel position was zero (Figure 2.5). This step verified that the cone alignment remained the same for varying angles, therefore the collimator was left at  $0^\circ$  for subsequent image acquisitions.

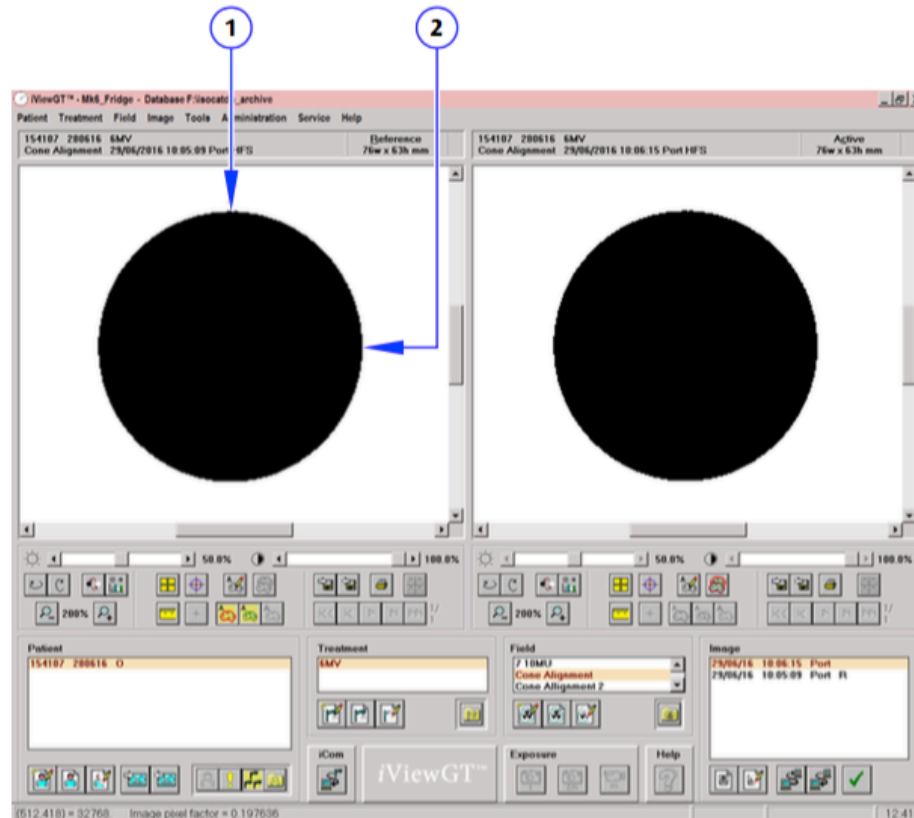


Figure 2.5. Comparison of the longitudinal (1) or lateral (2) edge of EPID images of the collimator aperture collected at collimator angles of  $0^\circ$  and  $180^\circ$  with the gantry placed at  $0^\circ$ . Adjustments to the collimator micrometers were made until the pixel value for the edge of the field were the same.

The position of the ball-bearing phantom was set by acquiring four EPID images of the phantom at the cardinal gantry angles using the iViewGT system (Elekta, Stockholm, Sweden). These images were then analyzed using commercial analysis software (RIT Isocenter Analysis Tool software V.6.3.1, Radiological Imaging Technology, Colorado Springs, CO) as recommended by the protocol of the vendor-supplied MV Isocenter Accuracy Test. The software calculated the systemic displacement on each principal axis using the method described in Low's paper on minimization of target localization error in accelerator based radiosurgery (Low *et al.*, 1995). Adjustments were made to the three micrometers on

the phantom based on the deviation results from the software analysis. Images at the four cardinal angles were re-acquired until the deviation between the MV isocenter and center of the ball-bearing phantom were less than or equal to the isocenter position tolerance of 0.1 mm. Four additional images were acquired with treatment table isocentric rotation angles of  $-90^\circ$ ,  $-45^\circ$ ,  $45^\circ$ , and  $90^\circ$ . The projections and standard deviation of the field-ball offset for each of the principal axes for were then calculated from the set of eight images using the analysis software.

## 2.2.2 Diode Array Measurements

In order to test the therapeutic delivery accuracy of the Elekta linear accelerator, a two-dimensional diode array (MapCHECK2 serial number: 76352038; Sun Nuclear Corporation, Melbourne, FL) was selected as the dosimeter to measure delivered dose because of its detector sensitivity. The 2D diode array contained 1527 diodes and an active detector area of  $0.64 \text{ mm}^2$  spanning a field size of  $32.0 \times 26.0 \text{ cm}$ . A distance of 10.0 mm separates the diodes horizontally and vertically with a spacing of 7.1 mm diagonally.

As previously mentioned (Section 2.1.3), treatment plans were copied to a CT scan of the diode array so that calculated dose values could be compared to delivered doses for assessment of end-to-end testing. Due to the calibration limitations of the array, in which only one photon energy can be used for calibration before a measurement session, the lung SBRT treatment plan was adjusted so that the plan only utilized 6 MV photon beams rather than a combination of 6MV and 10MV photon beam energies. This enabled the correct calibration dose to be applied to the collection of one plan with the same energy for each beam. Calibrations were performed before each measurement session. The diode array was also limited in its spatial resolution, with diodes spaced 1 cm apart along the horizontal and vertical axis of the device. For the purposes of this project, we required a resolution of 1 mm in order to assess the delivery accuracy of high dose to small target volumes. To achieve 1-mm resolution, the A40 Series UniSlide stage (Velmex, Inc. Bloomfield, NY) was employed that allowed for incremental shifts to the diode array using an aluminum, vernier scale-controlled stage that moved in one direction. According to the manufacturer, the stage had a repeatability of 4 microns with straight-line accuracy of 0.076mm.

Planar dose distributions of each treatment plan were measured using the diode array as shown in Figures 2.6, 2.7, 2.8, and 2.9. The electronic section of the diode array was centered over the moving

stage of the stepper motor and weighed down with steel weights so that the active detective area was suspended over the end of the treatment table. This configuration was used to prevent any treatment beams from passing through the aluminum apparatus of the electronic portion of the array. The solid water enclosure (MapPHAN, Sun Nuclear Corporation, Melbourne, FL) that is often used in combination with the diode array was not used for this study due to the additional weight it would have introduced.



Figure 2.6. Patient left lateral view of x-axis (coronal right/left) shifting mechanism.



Figure 2.7. Patient right lateral view of x-axis (coronal right/left) shifting mechanism.



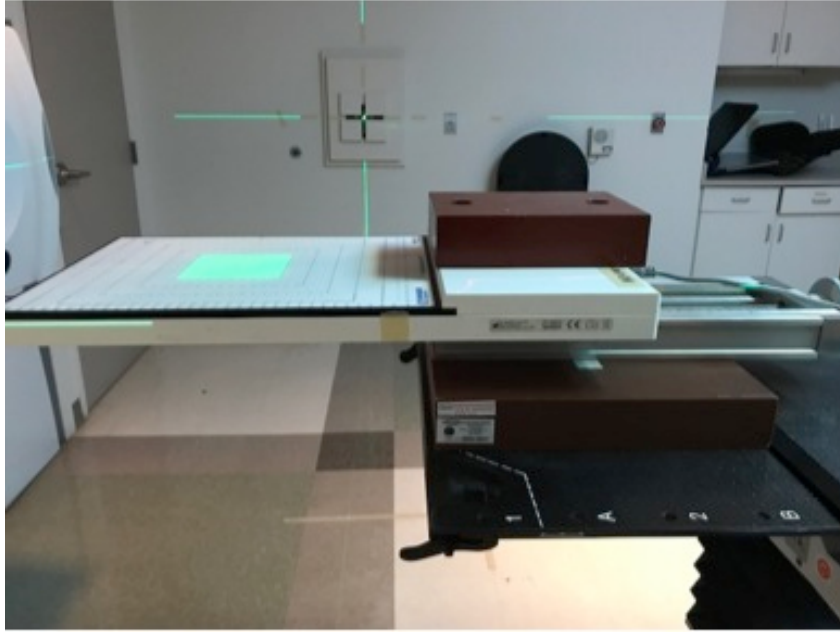


Figure 2.8. Patient right lateral view of the setup for y-axis (coronal inferior/superior) shifting mechanism.

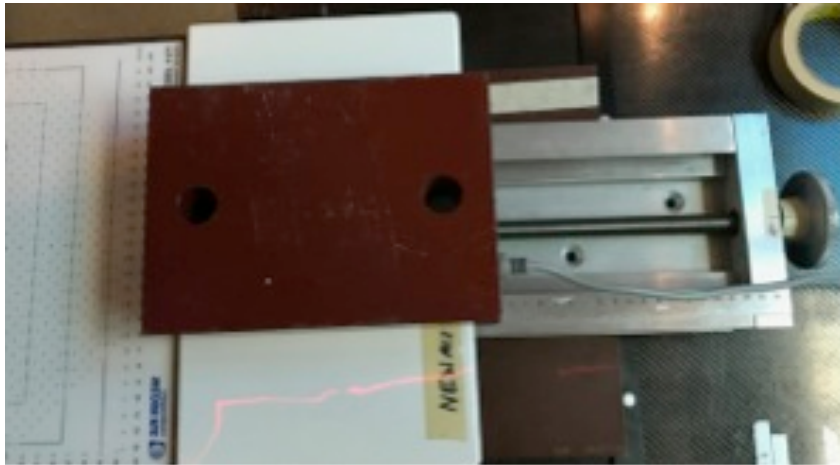


Figure 2.9. Beam's eye view for the setup for y-axis (coronal inferior/superior) shifting mechanism.

All measurements of the lung SBRT and spine SRS plans were taken in the coronal plane. For those deliveries in which the diode array was positioned at isocenter, shifts were made along the x-axis and y-axis, defined as patient left and patient right; and patient superior and inferior, respectively. These measurements are referred to as coronal left/right and coronal superior/inferior in this work. In addition to the plane through the isocenter for the SSRS case, two supplementary coronal planes were evaluated in the posterior direction of the patient (i.e. the diode array was shifted vertically down). These additional positions represent the coronal plane along the z-axis for the SSRS case. Since the array orientation was in the coronal plane, shifts along the x-axis using the aluminum stage were performed in order to assess

the dose delivery to the steepest dose gradients in the plan. These areas are characterized by the horseshoe shape isodose lines encompassing the vertebral column and excluding the spinal cord so that dose can be limited to the spinal cord. One of the coronal posterior positions was taken at 2 cm and the other at 2.7 cm (Figure 2.10). These points were chosen to represent the coronal plane approximately through the juncture of the vertebral PTV and spinal cord contour (a high dose gradient region) and the coronal plane directly through the spinal cord and adjacent vertebral pedicles, respectively (Figures 2.11 and 2.12).

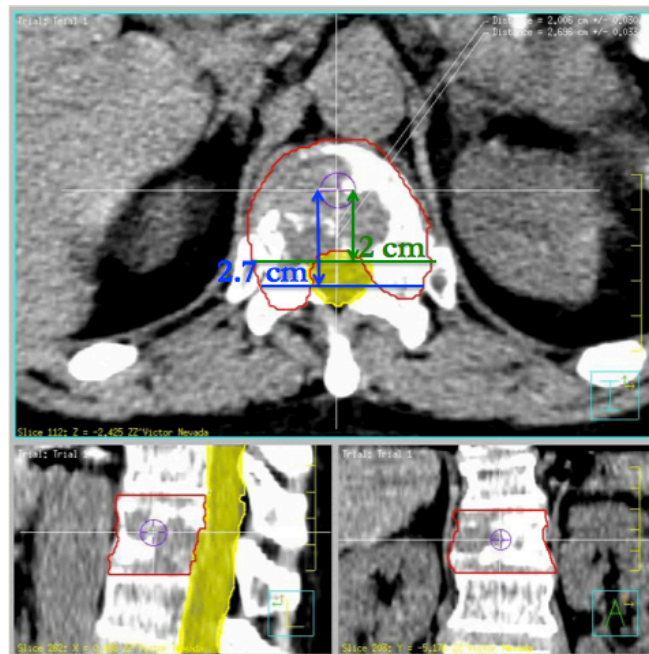


Figure 2.10. SSRS plan with 2cm and 2.7cm distance measured from CTV isocenter displayed in the axial plane with corresponding sagittal (bottom left) and coronal (bottom right) planes displayed. The CTV is outlined in red and the OAR (spinal cord) is contoured in yellow.

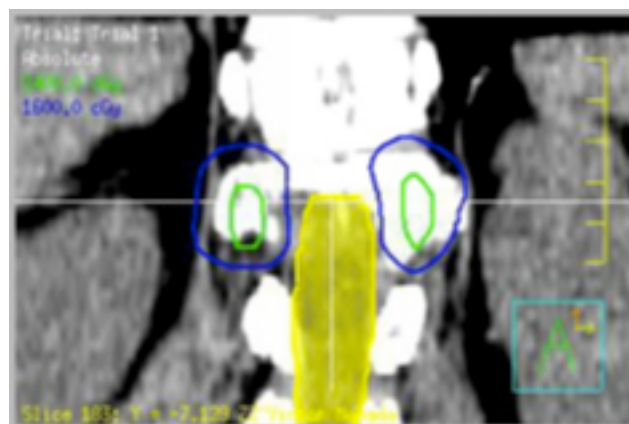


Figure 2.11. SSRS coronal plane of 2 cm posterior shift from CTV isocenter. The OAR (spinal cord) is contoured in yellow with the 16 Gy isodose line targeting the CTV outlined in blue and the 24 Gy isodose line targeting the GTV in green.

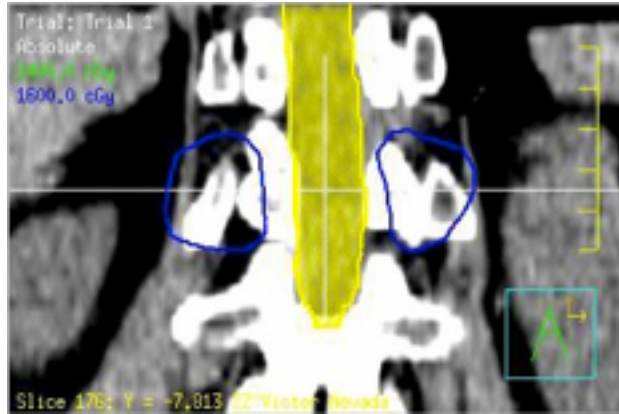


Figure 2.12. SSRS coronal plane of 2.7 cm posterior shift from CTV isocenter. The OAR (spinal cord) is contoured in yellow with the 16 Gy isodose line targeting the CTV outlined in blue and the 24 Gy isodose line targeting the GTV in green.

### 2.2.3 Diode Array Positioning with kV-CBCT

These additional vertically positioned measurements were also designed to test the IGRT capabilities of the Elekta Infinity platform. For those measurements of the lung SBRT and spine SRS plan taken through the isocentric coronal plane, the diode array was aligned using the room lasers so that the plane of diodes was parallel to the coronal plane of a supine patient. Rather than moving the treatment table to the desired posterior offset for the spine SRS plan by referencing the monitor readouts with 0.1 cm precision, IGRT capabilities provided images before and after posterior positioning that allowed for comparison and confirmation of the applied alignment with 0.01 cm precision. To position the MapCHECK2 to its specified positions of 2 cm and 2.7 cm posteriorly, a kilovoltage cone beam computed tomography (kV-CBCT) image was taken using the x-ray volume imaging system (XVI) to align the diode array position with that in the planning CT data set of the phantom exported from the TPS. Each kV-CBCT was acquired using the “S20 Head and Neck” MBPCC protocol where a cone-beam is taken without a filter (F0) using a small collimator field of view with an axial length of 26 cm (S20). The protocol uses a small field-of-view, kV tube potential of 100kV, and current of 10 mA. Once the kV-CBCT was acquired, it was automatically registered to the reference CT image set using grey-scale matching (Figure 2.13). A clipbox was set to only include the central diodes of the array so as to avoid any misalignment due to image artifacts from the outer edges of the kV-CBCT. However, the perimeter of the diode array, as seen in the coronal image window in Figure 2.13 and 2.14, was used to confirm that the row alignment of the diodes was correct. The registration was visually evaluated using a dual-image system that

overlays the images. After the diode array was aligned to the reference image, the table was then positioned the calculated amount and a kV-CBCT was re-acquired in order to ensure the adjusted position was within  $\pm 0.05$  cm of what was expected (Figure 2.14). For the spine SRS treatment plan only, the posterior offset was achieved once the Elekta Infinity software automatically translated the treatment table by the specified amounts. The SSRS plan was then delivered to the diode array after the desired posterior position was achieved.

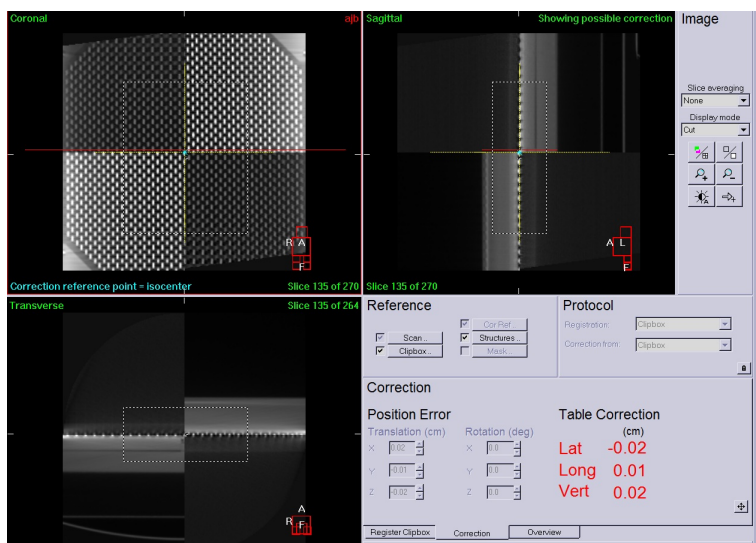


Figure 2.13. Screenshot of XVI 3D-kVCBCT registration window. The kVCBCT was aligned to the planning CT at isocenter in this figure. (Cross sections represent the overlaid intersection of the acquired CBCT, shown here as the lighter contrasted image, and the Pinnacle Export reference image, shown here as the darker contrasted image).

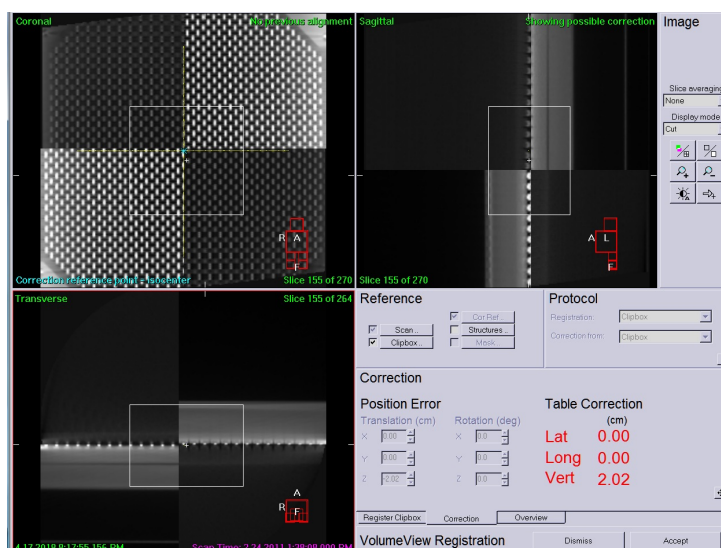


Figure 2.14. Screenshot of XVI 3D-kVCBCT registration window. The kVCBCT was aligned to the planning CT at isocenter in this figure after a 2cm posterior shift. (Cross sections represent the overlaid intersection of the acquired CBCT, shown here as the lighter contrasted image, and the Pinnacle Export reference image, shown here as the darker contrasted image).

## 2.2.4 Concatenation of Measurements

An in-house MATLAB (MathWorks Inc., Natick, Massachusetts) code was developed to concatenate the 1-mm shifted data into one file to be analyzed by the commercial software that supports the diode array (SNC Patient<sup>TM</sup> software, version 6.2.2, Sun Nuclear Corporation, Melbourne, FL). The aggregate data file was then analyzed along the axis in which the diode array was shifted. For example, the typical data dimensions for a diode array text file are  $65 \times 53$ , which corresponds to the number of diodes in each direction with 1-cm spacing along vertical and horizontal axes. With the 1-mm shift applied in one direction along one of the axes in 2-D space, the number of columns expanded to 270 for the coronal left/right shift and the number of rows expanded to 330 for the superior/inferior shift. This represents the initial position of the diodes with an additional 9 data points to fill in the 1-cm gap between diodes along a given axis.

## 2.2.5 Reproducibility

Measurement sessions occurred on separate days and therefore required repeated construction of the experimental setup; therefore, assuring reproducibility in setup was crucial to the developed design. Measurements taken through isocenter for the lung SBRT and SSRS plans were replicated for shifts along the coronal left/right axis and the coronal superior/inferior axis. For the posteriorly positioned 2.0 cm and 2.7 cm SSRS plan deliveries, shifts in the diode array were only applied along the coronal left/right axis. Reproducibility was only assessed using the aggregate data files of the coronal left/right axis for the posteriorly positioned SSRS plans. Experimental reproducibility was assessed by overlaying the aggregate measured dose distributions for a given shift within the coronal plane and calculating the positional alignment error and shift in isodose levels, which are described in the following section.

## 2.3 Aim 3

Delivery accuracy was quantified using three analysis metrics: percent difference between measured and planned dose values, positioning alignment, and difference in isodose levels. After the measurements were analyzed, additional tests were required to explain the results from the delivery of the treatment plans.

### 2.3.1 Analysis Metrics

#### Percent Difference

Due to a noticeable dose discrepancy in the center of the SSRS profile between the measured dose delivery and that generated by the treatment planning system, the percent difference between the measured and planned value for the center point in the MapCHECK2 array was calculated using the standard formula:

$$\% \text{ Difference} = \frac{(\text{measured dose value} - \text{planned dose value})}{\text{planned dose value}} \times 100 \quad (1)$$

The percent difference of the measured and planned center point dose value was only calculated for the SSRS coronal left/right plane with a 2 cm and 2.7 cm posterior shift. The center point in these planes represents the approximate location of the spinal cord in the plan, specifically where it abuts to the vertebral column (2cm profile) and the center of the spinal cord (2.7 cm profile). Percent difference was calculated for this point, in particular, due to the strict dose tolerance of the spinal cord and the potential for large overdoses due to inaccurate treatment delivery. Percent difference between measured and calculated dose points was not calculated for the deliveries of the lung SBRT or spine SRS plans through the coronal plane at isocenter.

#### Positional Alignment Error

The positional alignment error ( $\Delta c$ ) for those measurements taken at isocenter with no posterior shift applied was defined as the displacement between the center of the planned and measured profiles (defined as the midpoint between the 75% dose levels on each side of the profile):

$$\Delta c = \frac{1}{2} (X_{75\%, \text{TPS}+} + X_{75\%, \text{TPS}-}) - \frac{1}{2} (X_{75\%, \text{Meas}+} + X_{75\%, \text{Meas}-}) \quad (2)$$

Where  $X_{75\%}$  refers to the position of the 75% maximum dose point as calculated by the TPS and subscripts (+) and (-) refer to the slopes of the profile while moving across the profile from patient left to patient right or patient inferior to patient superior respectively. The 75% dose value was selected as it is located near the point of steepest dose gradient. Because 100% dose refers to an absolute maximum dose of 2046 cGy as calculated by the TPS for the lung SBRT plan transferred to the diode array phantom, the 75% dose correspond to an absolute dose of 1535 cGy. Similarly, the 100% dose refers to an absolute maximum dose of 3784 cGy as calculated by the TPS for the spine SRS plan, which makes

the 75% dose corresponds to 2838 cGy. The 75% dose point was used to calculate the positional alignment error those profiles taken along the patient left-right axis and the patient superior-inferior axis for the lung SBRT and spine SRS treatment delivery profiles of the coronal plane taken through isocenter.

The positional alignment error ( $\Delta c$ ) for the SSRS measurements taken at additional posterior alignments of 2cm and 2.7cm was defined as the displacement between the center of the planned and measured profiles (defined as the midpoint between the 60% dose levels on each outer side of the profile):

$$\Delta c = \frac{1}{2} (X_{60\%, \text{TPS}+} + X_{60\%, \text{TPS}-}) - \frac{1}{2} (X_{60\%, \text{Meas}+} + X_{60\%, \text{Meas}-}) \quad (3)$$

Where  $X_{60\%}$  refers to the position of the 60% maximum dose point as calculated by the TPS and subscripts (+) and (-) refer to the slopes of the profile while moving across it from patient left to patient right respectively. The 60% maximum dose point was used for the posteriorly offset SSRS profiles because the 75% maximum dose point was not applicable for one or more profiles as they did not receive this dose during delivery due to the high dose gradient across profiles. Rather, a lower percentage of the maximum dose point was chosen because it similarly corresponds to the approximate point of the sharpest dose gradient as the 60% maximum dose value corresponds to 2270 cGy of the SSRS absolute maximum dose. Positional alignment error was only calculated for the patient left-right axis for the posteriorly offset SSRS treatment delivery, as shifts in the diode array were not made along the patient superior-inferior axis.

Overall, the value of  $\Delta c$  is a degree of the alignment error in a measurement, where positive values indicate a shift of the measured profile in the left or inferior direction and negative values indicate a shift in the right or superior direction relative to the planned profile (Sutton *et al.*, 2014).

#### Difference in the 75% and 60% Dose Levels

Shifts in the 75% dose level ( $\Delta 75$ ) represented the asymmetric deviations in the 75% isodose lines within the profiles of the coronal plane of delivered lung SBRT and SSRS plans taken through isocenter. Moreover, the shift in dose point served as an evaluation of coverage of the tumor volume. The 75% dose level shifts were defined as:

$$\Delta 75_{\text{Right}} = 75\%_{\text{TPS,R}} - 75\%_{\text{Meas,R}} \quad (4)$$

$$\Delta 75_{\text{Left}} = 75\%_{\text{Meas,L}} - 75\%_{\text{TPS,L}} \quad (5)$$

$$\Delta 75_{\text{Superior}} = 75\%_{\text{TPS,S}} - 75\%_{\text{Meas,S}} \quad (6)$$

$$\Delta 75_{\text{Inferior}} = 75\%_{\text{Meas,I}} - 75\%_{\text{TPS,I}} \quad (7)$$

Where the subscripts R, L, S, and I denote the right, left, superior, and inferior sides of the profile, respectively. Positive values of  $\Delta 75$  indicated that the position of the measured 75% isodose fell inside the calculated (planned) 75% isodose line. Conversely, negative values of  $\Delta 75$  indicated that the measured 75% isodose line fell outside the calculated (planned) 75% isodose line.

Differences in the 60% isodose levels ( $\Delta 60$ ) represented the asymmetric deviation and the coverage of the target volume in the 60% isodose lines within the profiles of the delivered SSRS plan posteriorly offset by 2cm and 2.7cm. Shifts in the 60% dose level were defined as:

$$\Delta 60_{\text{Right}} = 60\%_{\text{TPS,R}} - 60\%_{\text{Meas,R}} \quad (8)$$

$$\Delta 60_{\text{Left}} = 60\%_{\text{Meas,L}} - 60\%_{\text{TPS,L}} \quad (9)$$

With the same defining characteristics as  $\Delta 75$ . Of note,  $\Delta 60_{\text{Superior}}$  and  $\Delta 60_{\text{Inferior}}$  were not calculated for the posteriorly aligned diode array for the delivery of the SSRS treatment plan because shifts were made only along the patient left-right axis.

A sample profile has been provided that demonstrates the metrics previously described, including the positional alignment error and the difference in isodose levels (Figure 2.15). For the chosen profile, Figure 2.15 displays  $\Delta 75$  for one of the lung SBRT treatment plan deliveries.

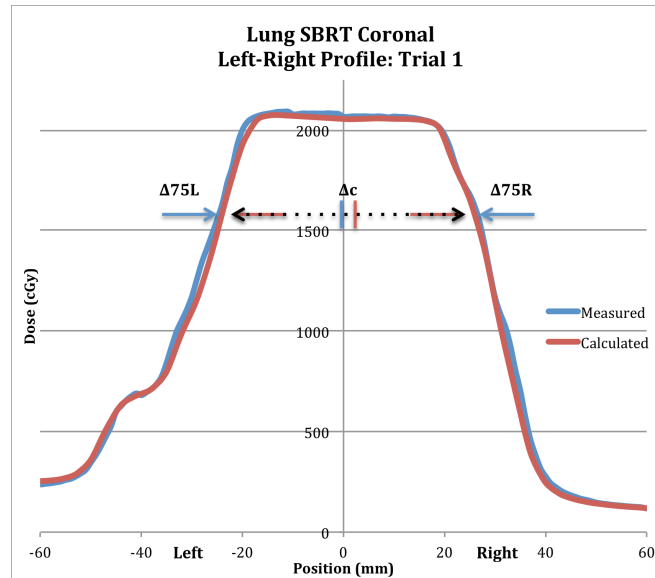


Figure 2.15. Sample profile illustrating the positional alignment error and difference in 75% isodose level metrics on a profile of the delivered and calculated lung SBRT treatment.



### 2.3.2 Delivery of Treatment Plans on Additional Linear Accelerators

Additional measurements were collected across three linear accelerators to test for differences between the delivery capabilities and performance of each unit. Using the same methods previously described (Section 2.2.2), the lung SBRT treatment plan and the SSRS treatment plan offset posteriorly by 2.0 cm and 2.7 cm were delivered on two additional linear accelerators: the Elekta Versa HD™ linear accelerator and an additional Elekta Infinity™ with Agility head linear accelerator. Measurement sessions utilized the XVI system to acquire kV-CBCT images to aid in positioning the MapCHECK2 diode array (Section 2.2.3).

### 2.3.3 Individual Gantry Beam Measurements

To further assess the dose discrepancy in treatment delivery of the spine SRS plan, each treatment field was delivered at the prescribed gantry angle as well as at 0° to the MapCHECK2 with MapPHAN for the 2.0 cm and 2.7 cm posteriorly shifted measurement sessions. The planar dose for each beam with the corresponding posterior offset of either 2.0 or 2.7 cm was generated with the same method as described in section 2.1.3. Additionally, to isolate the planar dose for each beam at its planned gantry and collimator angle, the number of monitor units was set to zero for all beams but one before exporting the file. For the delivery of the beams at gantry and collimator angle 0, the orientation of the beams were manually modified while leaving the MLC control points the same, which resulted in the delivery of the same number of monitor units and MLC leaf configuration for each beam.

Individual beam measurements were taken with the diode array posteriorly offset by 2.0 and 2.7 cm and the fields delivered at their planned angle. An additional measurement consisted of the treatment beams delivered at 0° for the gantry and collimator angles. By delivering the beams at gantry angle 0° and collimator angle 0°, the potential for over-response from the diodes resulting from oblique gantry angles was minimized. Analysis of the data was performed using the aforementioned percent difference formula for the center point of the measured and calculated treatment plan.

### 2.3.4 Ion Chamber Measurements

Because diodes have been reported to exhibit directional dependence (Jursinic, 2009; Keeling *et al.*, 2013; Jursinic *et al.*, 2010), additional measurements were required to determine the cause of a specific discrepancy between the TPS calculated dose and the measured dose to the (0,0) point in the

SSRS plan with an applied posterior offset of 2 cm and 2.7 cm. To establish whether the measured dose at this point was actually being delivered or the potential result of over-responding diodes, the absolute dose was measured with an Exradin A1SL ion chamber (Standard Imaging, Inc., Middleton, WI; SN: XW120896) inserted in a cylindrical, solid water “cheese” phantom with radius of 15 cm and a width of 18 cm (Accuray, Inc. TomoTherapy®, Sunnyvale, CA). Measurement readings were recorded from the CNMC Instruments Inc. Model 206 Dosimetry Electrometer. The SSRS treatment plan was copied to an image set of the “cheese” phantom, and the dose to the approximate active detector volume of the A1SL ion chamber located 2 cm and 2.7 cm posterior to the isocenter point was calculated for each treatment beam using the TPS. The volume of the A1SL ion chamber is 0.053 cm<sup>3</sup> and the volume contoured was 0.063 cm<sup>3</sup>; the exact volume of the chamber could not be contoured since the CT slice is 2.5 mm, therefore limiting the range of volume that could be contoured. The ion chamber was then placed in the 2-cm posterior insert within the phantom and three measurements for each beam were acquired and averaged for dose calculations (Figure 2.25). Since no insert exists for a 2.7 cm shift, the table was shifted down by 0.7 cm for this additional measurement. Using an adaptation of the TG-51 formalism (Almond *et al.*, 1999) to determine the photon dose, the absorbed dose to water was calculated and converted to absorbed dose for muscle using the formula below:

$$Dose (muscle) = (P_{ion} * P_{TP} * P_{elec} * P_{pol} * M_{raw}) * k_q * N_{D,w}^{Co-60} \times \left( \frac{\mu}{\rho} \right)_{water}^{muscle} \quad (10)$$

Where  $M_{raw}$  represents the uncorrected ion chamber reading,  $P_{ion}$  is the recombination correction factor that takes into account the incomplete collection of charge from an ion chamber,  $P_{TP}$  is the temperature-pressure correction factor which makes the charge correspond to the standard environmental conditions for which the calibration factor applies,  $P_{elec}$  represents the electrometer correction factor, and  $P_{pol}$  is the polarity correction factor which takes into account any polarity effect in the response of the ion chamber. Additionally,  $k_q$  is the quality conversion factor that accounts for the change in the absorbed-dose to water calibration factor between the beam quality of interest, Q, and the beam quality of Co-60 for which the absorbed-dose calibration factor applies.  $N_{D,w}^{Co-60}$  represents the absorbed-dose to water calibration factor for an ion chamber located under reference conditions in a radiation beam of Co-60 beam quality. Since dose to muscle is the quantity of interest in clinical dosimetry, absorbed dose to water must be

converted to absorbed dose to muscle in order to compare those values generated by the TPS to what was measured. The mass energy absorption coefficient ratio between muscle and water,  $(\frac{\mu}{\rho})_{water}^{muscle}$ , was used to convert the absorbed dose in water to the absorbed dose in muscle.

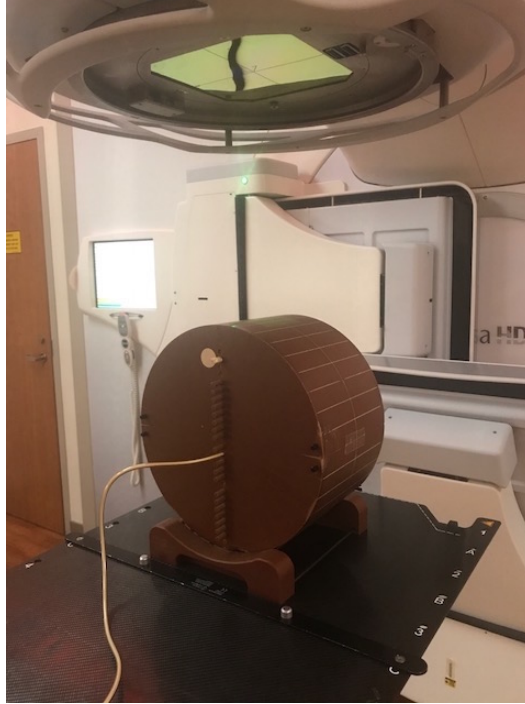


Figure 2.16. Solid water “cheese” phantom with ion chamber placed in 2cm patient posterior insert.

## Chapter 3. Results

### 3.1 Results of Treatment Planning

#### 3.1.1 Lung SBRT Treatment Plan

The lung SBRT treatment plan was designed to follow dose constraints outlined by RTOG Report 0813, which can be found in Table 3.1. Specifically, the maximum dose of the treatment plan requires that 100% corresponds to the maximum dose delivered to the patient that must occur within the PTV. The prescription isodose surface had to be  $\geq 60\%$  and  $\leq 90\%$  of the maximum dose. The prescription isodose surface coverage constraint requires at least 95% of the PTV receive the prescription dose ( $V_{100} \geq 95\%$ ) and that 99% of the PTV receive a minimum of 90% of the prescription dose ( $V_{90} \geq 99\%$ ). Lastly, the constraint for high dose spillage limited the volume of tissue outside the PTV to be no greater than 15% of the PTV volume that received a dose  $>105\%$  of the prescription dose.

Table 3.1: RTOG 0813 Protocol Requirements

| Criteria                              | Constraint  |
|---------------------------------------|---|
| Maximum Dose                          | 100% corresponds to the maximum dose delivered to the patient; point must exist within the PTV                        |
| Prescription Isodose                  | $\geq 60\%$ and $\leq 90\%$   |
| Prescription Isodose Surface Coverage | PTV $V_{100} = 95\%$ and PTV $V_{90} > 99\%$  |
| High Dose Spillage                    | Cumulative volume of all tissue outside the PTV receiving $>105\%$ of prescription dose $\leq 15\%$ of the PTV volume |

Additionally, the generated lung SBRT treatment plan also met the requirements for conformality of prescribed dose described subsequently. With a PTV of  $57.45 \text{ cm}^3$ , the RTOG 0813 requirements were met (Figure 3.1). Specifically, the ratio of prescription isodose volume to the PTV volume did not exceed the ratio requirement of 1.5 for the PTV volume. Also, the ratio of 50% prescription isodose volume to the PTV volume ( $R_{50\%}$ ) and maximum dose in percent of dose prescribed at 2 cm from PTV in any direction [ $D_{2\text{cm}} (\%)$ ] did not exceed the requirements as listed in RTOG Report 0813. With all constraints and requirements met, the lung SBRT treatment plan met all stated RTOG requirements.

| ROI            | Type                       | Primary Goal |                      | Secondary Goal |                      | Dose cGy | Volume at Primary Goal Dose | Result |
|----------------|----------------------------|--------------|----------------------|----------------|----------------------|----------|-----------------------------|--------|
|                |                            | Dose cGy     | Volume               | Dose cGy       | Volume               |          |                             |        |
| PTV            | Min DVH (%)                | 5000         | 95 %                 | 5000           | 94 %                 | 3373.7   | Min 95.824 %                | Met    |
| PTV            | Min DVH (%)                | 4500         | 99 %                 | 4500           | 98 %                 | 3373.7   | Min 99.005 %                | Met    |
| SpinalCord     | Max Dose                   | 3000         |                      | 0              |                      | 2393.7   | Max                         | Met    |
| Esophagus      | Max Dose                   | 3250         |                      | 0              |                      | 995.9    | Max                         | Met    |
| BrachialPlexus | Max Dose                   | 3000         |                      | 0              |                      | 2154.7   | Max                         | Met    |
| Heart          | Max Dose                   | 3500         |                      | 0              |                      | 172.6    | Max                         | Met    |
| Trachea        | Max Dose                   | 3250         |                      | 0              |                      | 918.6    | Max                         | Met    |
| Skin           | Max Dose                   | 4000         |                      | 0              |                      | 2171.2   | Max                         | Met    |
| Lungs          | Max DVH (cm <sup>3</sup> ) | 1160         | 1500 cm <sup>3</sup> | 1240           | 1000 cm <sup>3</sup> | 7377.3   | Max 301.476 cm <sup>3</sup> | Met    |
| Great Vessels  | Max Dose                   | 5500         |                      | 0              |                      | 1288.8   | Max                         | Met    |
| Rib            | Max DVH (%)                | 3250         | 8 %                  | 3250           | 9 %                  | 6529.3   | Max 7.871 %                 | Met    |

Figure 3.1. Scorecard containing objectives for the lung SBRT plan.

### 3.1.2 SSRS Treatment Plan

The SSRS treatment plan met the protocol requirements of RTOG Report 0631 as shown in Table 3.2. Figure 3.2 displays the scorecard from the treatment planning system. Of note, the maximum dose to the spinal cord was 1011.2 cGy, which was well below the maximum dose constraint of 1400 cGy. Moreover, the treatment plan design achieved a prescribed dose of 16 Gy in one fraction to cover at least 90% of the CTV as well as 90% coverage to the GTV that received 24 Gy. Since all goals and constraints were met, the SSRS treatment plan was considered clinically acceptable and used for end-to-end testing to assess the delivery accuracy of multiple Elekta linear accelerators.

Table 3.2. RTOG 0631 Protocol Requirements and MBPCC Constraints

| Organ at Risk (OAR) | Constraint                |
|---------------------|---------------------------|
| Spinal Cord         | Max Dose $\leq$ 14 Gy     |
| Spinal Cord         | 12 Gy to less than 0.01cc |
| Kidney              | Max Dose of 10 Gy         |
| Liver               | Max Dose of 10 Gy         |
| Stomach             | Max Dose of 11 Gy         |
| Bowel               | Max Dose of 15 Gy         |

| ROI         | Type                       | Primary Goal |                      | Secondary Goal |                   | Dose cGy | Volume at Primary Goal Dose | Result |
|-------------|----------------------------|--------------|----------------------|----------------|-------------------|----------|-----------------------------|--------|
|             |                            | Dose cGy     | Volume               | Dose cGy       | Volume            |          |                             |        |
| Kidney_L    | Max Dose                   | 1000         |                      | 0              |                   | 931.6    | Max                         | Met    |
| Kidney_R    | Max Dose                   | 1000         |                      | 0              |                   | 909.0    | Max                         | Met    |
| Spinal Cord | Max Dose                   | 1400         |                      | 0              |                   | 1010.3   | Max                         | Met    |
| CTV         | Min DVH (%)                | 1600         | 90 %                 | 0              | 0 %               | 605.0    | Min 94.771 %                | Met    |
| Liver       | Max Dose                   | 1000         |                      | 0              |                   | 991.9    | Max                         | Met    |
| Stomach     | Max Dose                   | 1100         |                      | 0              |                   | 597.1    | Max                         | Met    |
| Bowel       | Max Dose                   | 1500         |                      | 0              |                   | 542.5    | Max                         | Met    |
| Spinal Cord | Max DVH (cm <sup>3</sup> ) | 1200         | 0.01 cm <sup>3</sup> | 0              | 0 cm <sup>3</sup> | 1010.3   | Max 0.000 cm <sup>3</sup>   | Met    |

Figure 3.2. Scorecard containing objectives for the spine SRS plan.

### 3.2 MV Isocenter Accuracy Test Results

Table 3.3 contains the results of the MV Isocenter Accuracy test for the three linear accelerators used for this study. Infinity 1 refers to the Elekta Infinity™ with Agility head located at the MBPCC Baton Rouge site. Versa HD refers to the Elekta Versa HD™ linear accelerator, also located at the MBPCC Baton Rouge site. Moreover, Infinity 2 refers to the additional Elekta Infinity™ with Agility head linear accelerator located at the MBPCC Gonzales site. Per the 6 MV Isocenter Customer Acceptance protocol, MV isocenter radius for gantry rotation has a limit of  $\leq 0.70$  mm. Additionally, the limit of the MV isocenter radius for the combined gantry and treatment table rotation is  $\leq 1.00$  mm. For the Infinity 1 and Versa HD linear accelerators, the maximum MV isocenter radius for both the gantry and treatment table rotation was a result of the gantry rotation, which is why the radius for gantry rotation and combined gantry and treatment table rotation are the same. Since the results of the MV isocenter accuracy test was within tolerance for the MV isocenter radius for the combined gantry and treatment table rotation and only a maximum of 0.01 mm from being within tolerance for the gantry rotation for all three linear accelerators, no adjustments were made to the mechanical aspects of the delivery system to improve the radius of isocenter.

Table 3.3. Results of the MV Isocenter Accuracy Test for three linear accelerators.

| Linear Accelerator | MV Isocenter Radius for Gantry Rotation (mm) | MV Isocenter Radius for Combine Gantry and Treatment Table Rotation (mm) |
|--------------------|--|--|
| Infinity 1         | 0.71   | 0.71   |
| Versa HD           | 0.69   | 0.69   |
| Infinity 2         | 0.65   | 0.87   |

### 3.3 Results of Treatment Deliveries

#### 3.3.1 Reproducibility of Diode Array Setup

The reproducibility of the experimental setup was evaluated by overlaying repeated delivered treatment plans that were shifted in the same direction. Table 3.4 contains the average positional alignment error between two measured trials of the treatment delivery of the lung SBRT and spine SRS plan. Equations 2 and 3 were used to calculate the positional alignment ( $\Delta c$ ) between the two measured profiles, where the midpoint value for the TPS-calculated value was replaced with the midpoint value from trial 1 and the midpoint value of trial 2 was subtracted. Positive  $\Delta c$  values indicated a left or inferior shift of trial 2 relative to trial 1. Tables 3.5 and 3.6 display values for the shift in 75% isodose levels between measured deliveries. Equations 4-7 were used to calculate the difference in isodose levels.  $\Delta 75_{\text{Right}}$  and  $\Delta 75_{\text{Superior}}$  were calculated by subtracting the 75% dose level position of trial 2 from the 75% isodose level position of trial 1.  $\Delta 75_{\text{Left}}$  and  $\Delta 75_{\text{Inferior}}$  were calculated by subtracting the 75% isodose level position of trial 1 from that of trial 2. Similarly, the values for  $\Delta 60$  in Table 3.7 were calculated in the same manner for those profiles that were posteriorly offset. Positive  $\Delta 75$  and  $\Delta 60$  values indicate that the profile of trial 2 fell within the profile of trial 1. Conversely, negative  $\Delta 75$  and  $\Delta 60$  values indicate that the profile for trial 2 fell outside that of trial 1. Ideally, positional alignment and shifts in the isodose levels would be zero if there were no uncertainties within the setup. However, the values from Tables 3.4 - 3.7 indicate that the uncertainty in the reproducibility of the setup was less than 1mm on average. Figures 3.3 - 3.8 display sample overlaid profiles taken through the central axis of the measured deliveries. Overall, the precision of repeated measurements of the same plan with device setup re-constructed for each session was quantified and deemed acceptable based on the slight deviances from one measurement session to the next.

Table 3.4. Average positional alignment comparison between two measured treatment delivery trials demonstrating reproducibility of setup for treatment deliveries on the Elekta Infinity linear accelerator with Agility head. Positive values of  $\Delta c$  indicate a left or inferior shift of trial 2 relative to trial 1. Conversely, negative values of  $\Delta c$  indicate a right or superior shift of trial 2 relative to trial 1.

| Treatment Plan | Direction of Profile | Average $\Delta c$ (mm) | Minimum $\Delta c$ (mm) | Maximum $\Delta c$ (mm) |
|----------------|----------------------|-------------------------|-------------------------|-------------------------|
| Lung SBRT      | Left-Right           | 0.13                    | 0.08                    | 0.17                    |
| Lung SBRT      | Superior-Inferior    | -0.13                   | -0.24                   | -0.04                   |
| SSRS           | Left-Right           | 0.08                    | -0.03                   | 0.15                    |
| SSRS           | Superior-Inferior    | -0.21                   | -0.62                   | -0.07                   |
| SSRS, 2 cm     | Left-Right           | -0.61                   | -0.69                   | -0.55                   |
| SSRS, 2.7 cm   | Left-Right           | -0.16                   | -2.46                   | 0.56                    |

Table 3.5. Average shift in 75% isodose level comparison between two measured treatment delivery trials demonstrating reproducibility of setup for treatment deliveries on the Elekta Infinity linear accelerator with Agility head. Values are for profiles of 1-mm resolution along the patient left-right axis, where a positive  $\Delta 75_{\text{Left}}$  or  $\Delta 75_{\text{Right}}$  indicates the trial 2 isodose level fell within the trial 1 profile. Conversely, a negative  $\Delta 75_{\text{Left}}$  or  $\Delta 75_{\text{Right}}$  indicates the trial 2 isodose level fell outside the trial 1 profile.

| Treatment Plan | Average $\Delta 75_{\text{Left}}$ (mm) | Minimum $\Delta 75_{\text{Left}}$ (mm) | Maximum $\Delta 75_{\text{Left}}$ (mm) | Average $\Delta 75_{\text{Right}}$ (mm) | Minimum $\Delta 75_{\text{Right}}$ (mm) | Maximum $\Delta 75_{\text{Right}}$ (mm) |
|----------------|--|--|--|---|---|---|
| Lung SBRT      | -0.14                                  | -0.30                                  | -0.01                                  | 0.12                                    | -0.03                                   | 0.32                                    |
| SSRS           | -0.04                                  | -0.16                                  | 0.13                                   | 0.12                                    | 0.05                                    | 0.20                                    |

Table 3.6. Average shift in 75% isodose level comparison between two measured treatment delivery trials demonstrating reproducibility of setup for treatment deliveries on the Elekta Infinity linear accelerator with Agility head. Values are for profiles of 1-mm resolution along the patient superior-inferior axis, where a positive  $\Delta 75_{\text{Inferior}}$  or  $\Delta 75_{\text{Superior}}$  indicates the trial 2 isodose level fell within the trial 1 profile. Conversely, a negative  $\Delta 75_{\text{Inferior}}$  or  $\Delta 75_{\text{Superior}}$  indicates the trial 2 isodose level fell outside the trial 1 profile.

| Treatment Plan | Average $\Delta 75_{\text{Inferior}}$ (mm) | Minimum $\Delta 75_{\text{Inferior}}$ (mm) | Maximum $\Delta 75_{\text{Inferior}}$ (mm) | Average $\Delta 75_{\text{Superior}}$ (mm) | Minimum $\Delta 75_{\text{Superior}}$ (mm) | Maximum $\Delta 75_{\text{Superior}}$ (mm) |
|----------------|--|--|--|--|--|--|
| Lung SBRT      | 0.05                                       | -0.06                                      | 0.12                                       | -0.24                                      | -0.37                                      | -0.13                                      |
| SSRS           | 0.29                                       | 0.05                                       | 0.71                                       | -0.13                                      | -0.53                                      | 0.07                                       |

Table 3.7. Average shift in 60% isodose level comparison between two measured treatment delivery trials with posterior offsets demonstrating reproducibility of setup for treatment deliveries on the Elekta Infinity linear accelerator with Agility head. Values are for profiles of 1-mm resolution along the patient left-right axis, where a positive  $\Delta 60_{\text{Left}}$  or  $\Delta 60_{\text{Right}}$  indicates the trial 2 isodose level fell within the trial 1 profile. Conversely, a negative  $\Delta 60_{\text{Left}}$  or  $\Delta 60_{\text{Right}}$  indicates the trial 2 isodose level fell outside the trial 1 profile.

| Treatment Plan | Average $\Delta 60_{\text{Left}}$ (mm) | Minimum $\Delta 60_{\text{Left}}$ (mm) | Maximum $\Delta 60_{\text{Left}}$ (mm) | Average $\Delta 60_{\text{Right}}$ (mm) | Minimum $\Delta 60_{\text{Right}}$ (mm) | Maximum $\Delta 60_{\text{Right}}$ (mm) |
|----------------|--|--|--|---|---|---|
| SSRS, 2cm      | 0.40                                   | 0.26                                   | 0.49                                   | -0.82                                   | -0.89                                   | -0.73                                   |
| SSRS, 2.7cm    | -0.41                                  | -0.77                                  | -0.13                                  | 0.55                                    | 0.21                                    | 1.32                                    |



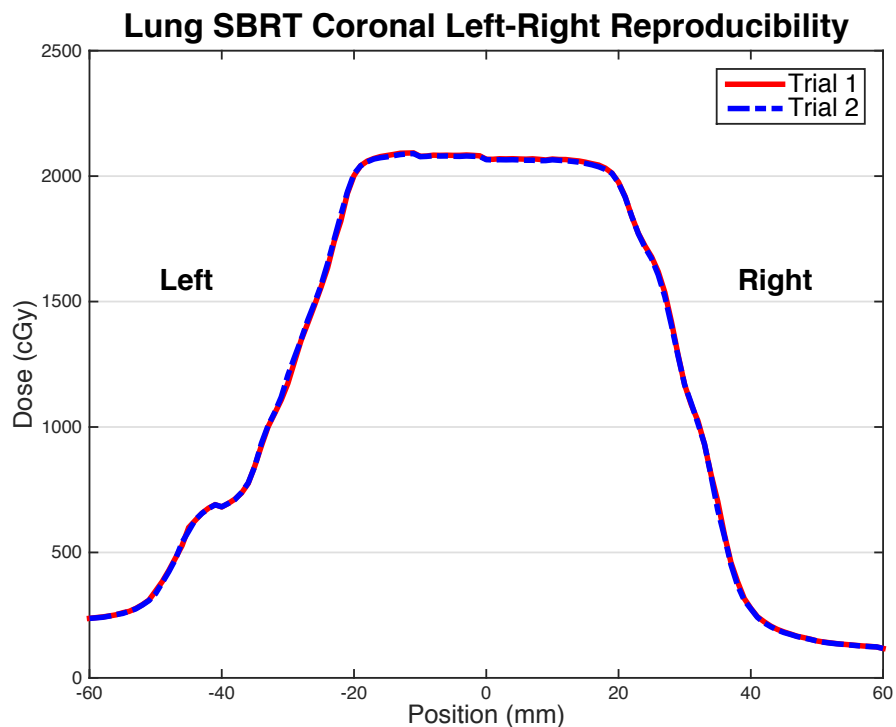


Figure 3.3. Profiles of repeated measurements for the lung SBRT plan in the coronal plane taken at 0 cm along the superior-inferior axis; used for determining reproducibility of the experimental setup.

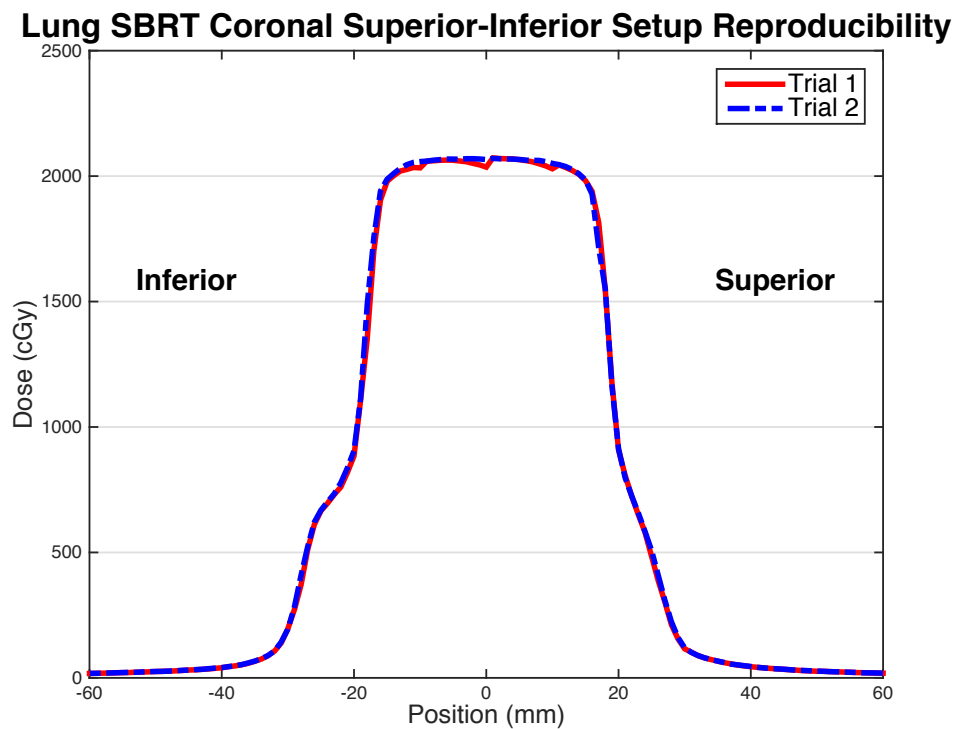


Figure 3.4. Profiles of repeated measurements for the lung SBRT plan in the coronal plane taken at 0 cm along the left-right axis; used for determining reproducibility of the experimental setup.

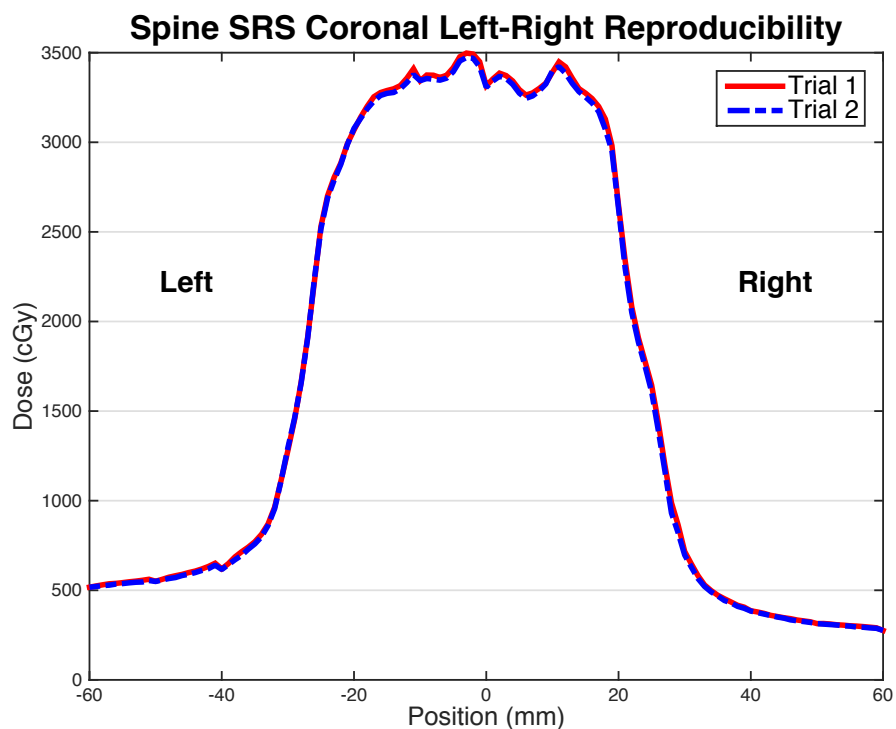


Figure 3.5. Profiles of repeated measurements for the spine SRS plan in the coronal plane taken at 0 cm along the superior-inferior axis; used for determining reproducibility of the experimental setup.

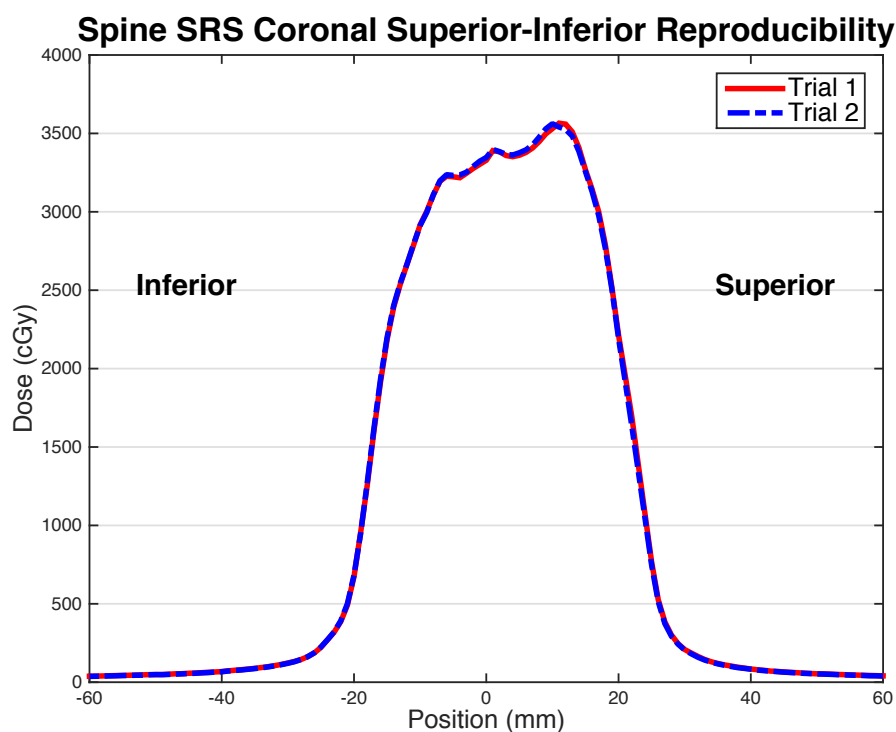


Figure 3.6. Profiles of repeated measurements for the spine SRS plan in the coronal plane taken at 0 cm along the left-right axis; used for determining reproducibility of the experimental setup.

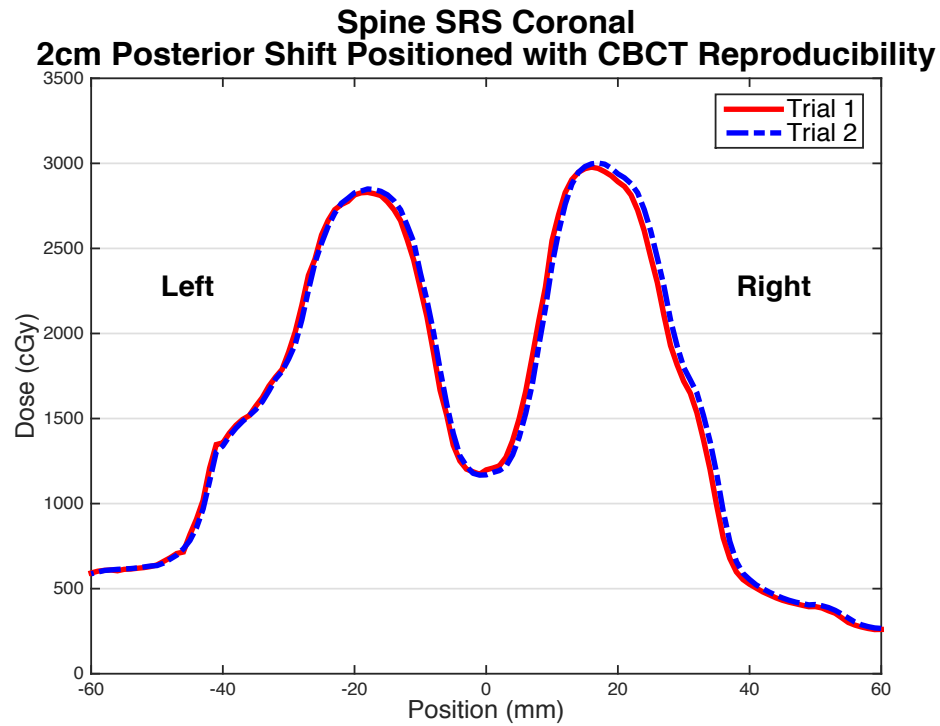


Figure 3.7. Profiles of repeated measurements for the spine SRS plan posteriorly offset by 2 cm in the coronal plane taken at 0 cm along the superior-inferior axis; used for determining reproducibility of the experimental setup.

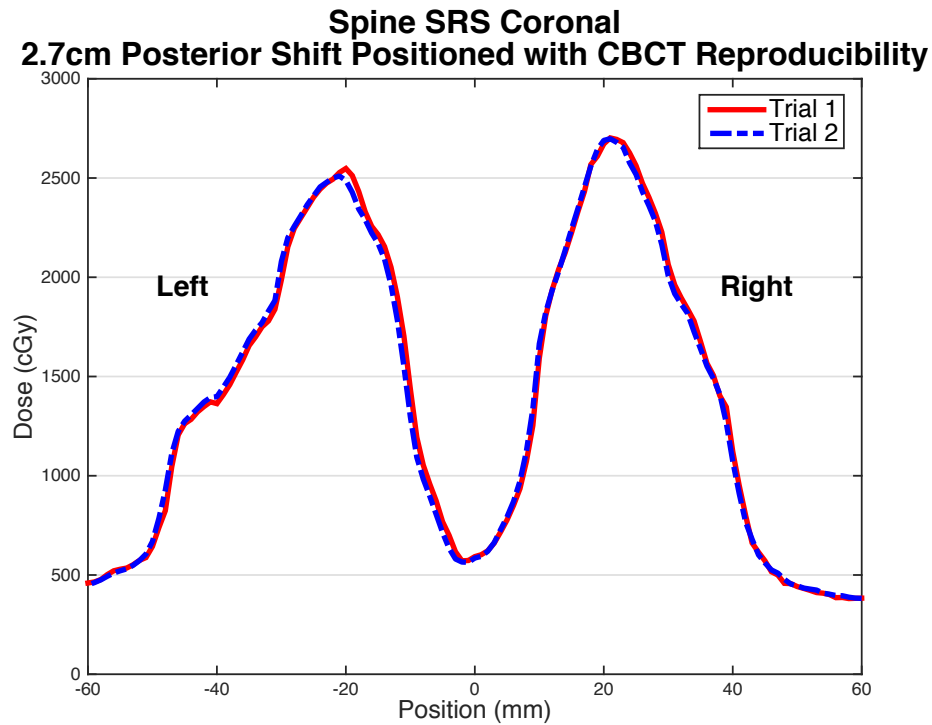


Figure 3.8. Profiles of repeated measurements for the spine SRS plan posteriorly offset by 2.7 cm in the coronal plane taken at 0 cm along the superior-inferior axis; used for determining reproducibility of the experimental setup.

An example profile taken from Appendix A has been included to illustrate a feature that resulted from the aggregate file of the combined 1-mm shifts of the diode array. Shown in Figure 3.9 is a profile from the delivery of the lung SBRT treatment plan on the Elekta Infinity linear accelerator taken through the superior-inferior point of 0.5cm ( $Y = 0.5\text{cm}$ ). Figure 3.9 (A) is an analysis performed by the SNC Patient Software of one of the nine individual files that were combined to form the aggregate data file with 1-mm resolution along a single axis, Figure 3.9 (B). The diode within the green circle (A) measured a higher dose than the diodes directly adjacent to it. When the individual files were combined to form the aggregate this resulted in an artifact resembling a plateau that is highlighted with the green circle in Figure 3.9 (B). These characteristics are found in several of the measured profiles that were used for analysis in this research. The data points in Figure 3.9 (A) represent distinct measured diode doses that when they were combined created a smearing effect seen in Figure 3.9 (B).

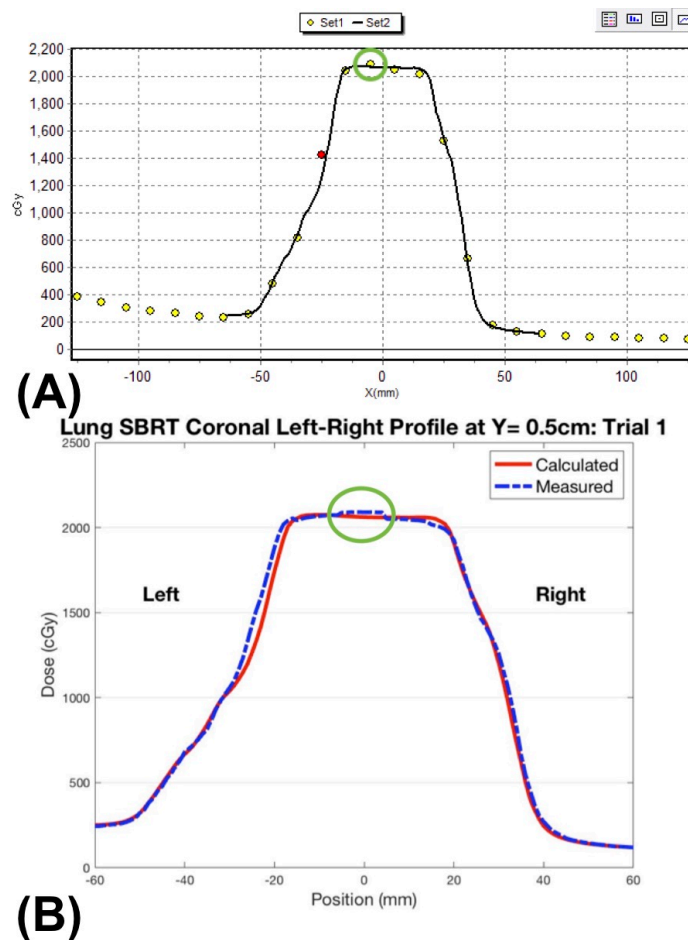


Figure 3.9. (A) SNC Patient Software profile of a single delivery of the lung SBRT plan analyzed at the native resolution of the diode array. (B) Sample plotted profile of the aggregate data file for 9 sequential deliveries of the lung SBRT plan, including that of (A).

### 3.3.2 Analysis of Treatment Delivery

Figures 3.10, 3.11, and 3.12 are comparisons between the calculated and delivered treatment plans created in Aim 1 and delivered with the methods described for Aim 2. Specifically, Figure 3.10 shows lung SBRT profiles taken through  $Y = 0$  cm for three linear accelerators as well as the calculated profile from the TPS. Measurement sessions for the delivery of the lung SBRT plan did not utilize kV-CBCT imaging for setup. Overall, agreement between the planned and delivered lung plan profiles was similar across all linear accelerators. Quantitative comparisons follow in the subsequent sections.

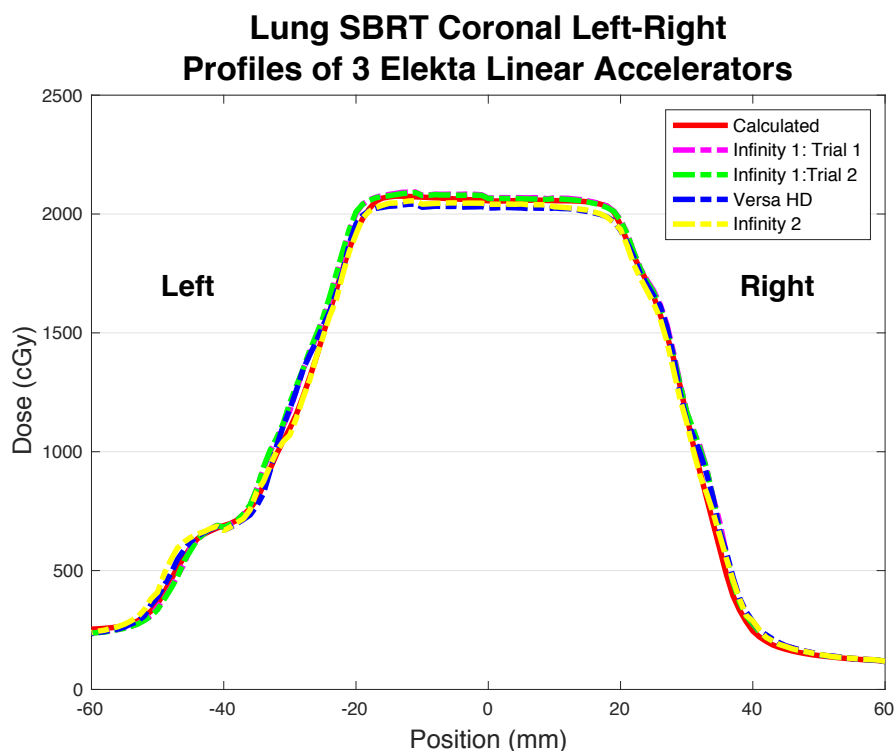


Figure 3.10. Comparison of profiles the planned and delivered lung SBRT treatment plan on three linear accelerators; profiles were taken through  $Y = 0$  cm on superior-inferior axis.

Conversely, the agreement across linear accelerators for the delivery of the SSRS plan varied, as seen in Figures 3.11 and 3.12. Both measurement sessions for the posteriorly offset diode array for the SSRS delivery utilized kV-CBCT imaging for experimental setup. Figure 3.11 displays the overlaid profiles taken through  $Y = 0$  cm for the three linear accelerators as well as the calculated TPS profile for the SSRS treatment plan through the 2-cm posterior coronal plane. Upon visual inspection, large discrepancies can be seen at the center of the profile, which represents the area where the spinal cord is adjacent to the vertebral column. As previously stated, this profile falls within a high dose gradient region

so variability was expected due to the fact that a sub-millimeter misalignment in the anterior-posterior direction could result in a drastically different dose. However, the degree of variability (see Table 3.8) that resulted from the treatment deliveries led to further analysis described in the following sections. Similar results can be seen in Figure 3.12 that displays the overlaid profiles taken through  $Y = 0$  cm for the calculated and delivered SSRS treatment plan through the 2.7-cm posterior coronal plane. A similar dose discrepancy between planned and calculated values at the center of the profile for the 2.7 cm posterior offset coronal plane (representing the region of the spinal cord) can be seen in Figure 3.12.

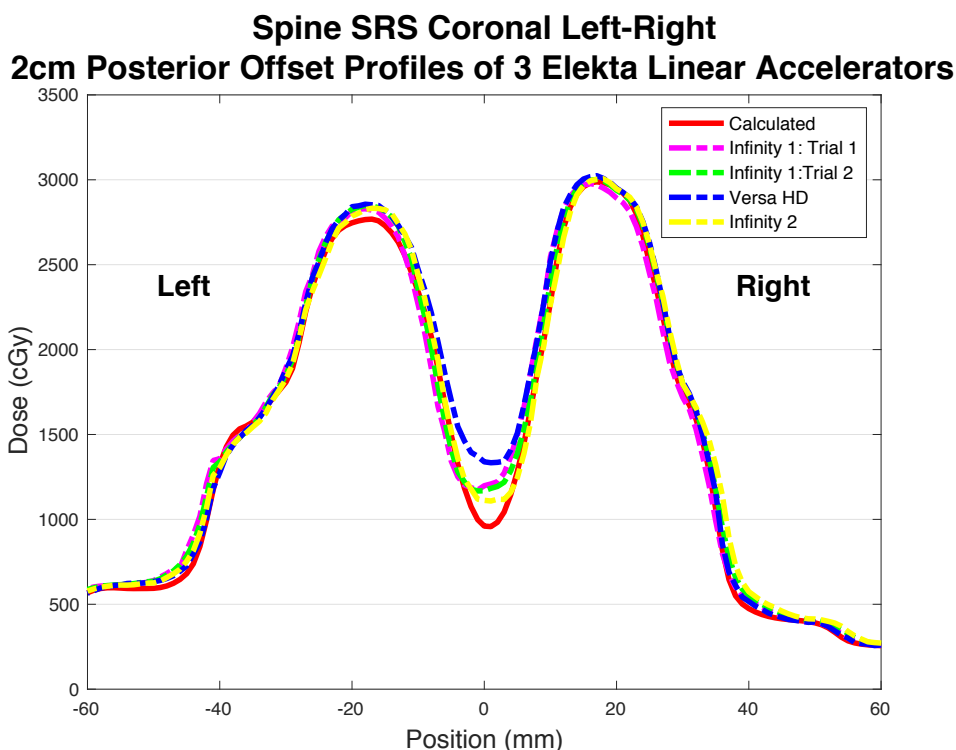


Figure 3.11. Comparison of the center profiles of the planned and delivered spine SRS treatment plan posteriorly shifted by 2 cm on three linear accelerators profiles; were taken through  $Y = 0$  cm on superior-inferior axis.

#### Percent Difference

Table 3.8 shows the percent difference calculated for the central diode of the delivered SSRS treatment plans shifted posteriorly by 2 cm and 2.7 cm as compared to the planned dose for the central diode on the TPS-generated planar dose. As previously stated, the central diode was chosen in the coronal left-right profile to represent the approximate position of the junction of the spinal cord and vertebral column, at the 2 cm profile, and the center of the spinal cord, at the 2.7 cm profile. The

measured dose at the center point of the profile was consistently higher than that which was planned, suggesting a systematic difference between measurement and calculation.

### Spine SRS Coronal Left-Right 2.7cm Posterior Offset Profiles of 3 Elekta Linear Accelerators

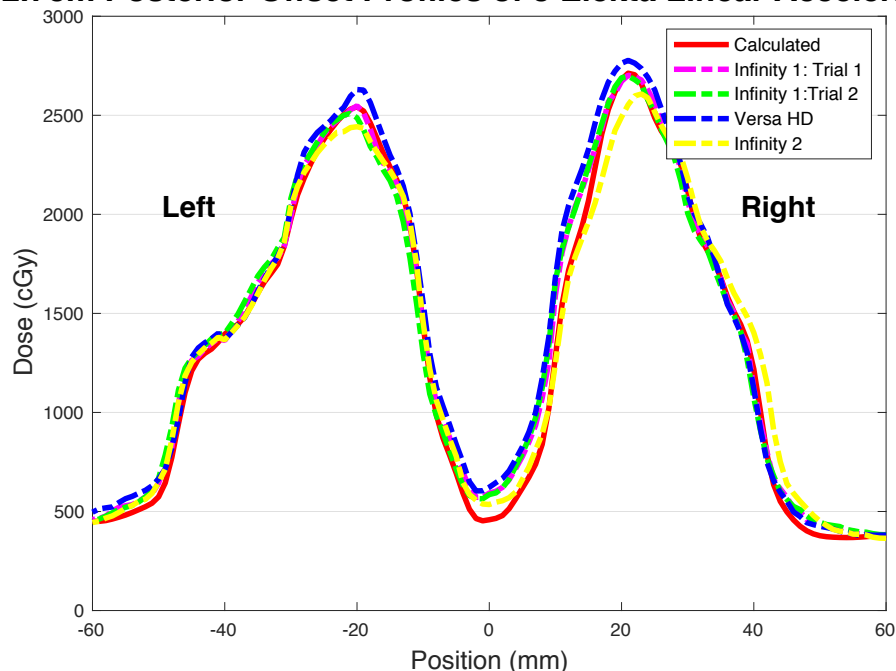


Figure 3.12. Comparison of the center profiles of the planned and delivered spine SRS treatment plan posteriorly shifted by 2.7 cm on three linear accelerators; profiles were taken through Y = 0 cm on superior-inferior axis.

Table 3.8. Percent Difference between TPS calculated dose and delivery of the treatment plan measured dose at the central point of the MapCHECK2 diode array. All measurements were taken in the coronal plane along the right-left direction.

| Linear Accelerator | Trial | Posterior Offset (cm) | Measured Value at Center Point (cGy) | TPS Value at Center Point (cGy) | Percent Difference |
|--------------------|-------|-----------------------|--------------------------------------|---------------------------------|--------------------|
| Infinity 1         | 1     | 2.0                   | 1198.2                               | 960.5                           | 24.75%             |
| Infinity 1         | 2     | 2.0                   | 1168.7                               | 960.5                           | 21.67%             |
| Versa HD           | 1     | 2.0                   | 1339.0                               | 960.5                           | 39.41%             |
| Infinity 2         | 1     | 2.0                   | 1112.2                               | 960.5                           | 15.79%             |
| Infinity 1         | 1     | 2.7                   | 592.6                                | 485.3                           | 29.32%             |
| Infinity 1         | 2     | 2.7                   | 585.6                                | 485.3                           | 27.78%             |
| Versa HD           | 1     | 2.7                   | 622.4                                | 485.3                           | 35.83%             |
| Infinity 2         | 1     | 2.7                   | 535.3                                | 485.3                           | 16.81%             |

#### Positional Alignment Error

Table 3.9 contains the data corresponding to the average positional alignment error ( $\Delta c$ ) between the measured and planned lung SBRT and SSRS profiles taken through Y = 0, -0.5, -1, 0.5, and 1 cm for

the left-right direction and  $X = 0, -0.5, -1, 0.5, \text{ and } 1 \text{ cm}$  for the superior-inferior direction (see Appendix A). The range, displayed as minimum and maximum values, was also calculated. The meanings of positive and negative values of  $\Delta c$  were described in Section 2.3.1. 2-mm accuracy has been achieved for lung SBRT treatment delivery with a 1-mm accuracy achieved for spine SRS treatments (see Section 1.2), therefore these values served as the standard for the positional alignment error of the delivered treatment plans. Ideally, all data points would align on the central axis specific to the direction of the increased resolution. For example, those measurements with 1-mm resolution in the left-right direction would ideally have a positional alignment error of zero along the y-axis and vice versa for those measurements with 1-mm resolution in the superior-inferior direction. Overall, average positional alignment indicated a shift of the measured profile in the left or inferior direction due to the primarily positive values.

Table 3.9. Summary of  $\Delta c$  analysis metric for the delivery of the lung SBRT and SSRS treatment plans delivered on three linear accelerators. Positive values of  $\Delta c$  indicate a shift of the measured profile in the left or inferior direction relative to the planned profile. Negative values of  $\Delta c$  indicate a shift in the right or superior direction relative to the planned profile.

| Linear Accelerator | Treatment Plan | Direction of Profile | Average $\Delta c$ (mm) | Minimum $\Delta c$ (mm) | Maximum $\Delta c$ (mm) |
|--------------------|----------------|----------------------|-------------------------|-------------------------|-------------------------|
| Infinity 1         | Lung SBRT      | Left-Right           | 0.3                     | -0.1                    | 1.2                     |
| Infinity 1         | Lung SBRT      | Superior-Inferior    | 0.2                     | -0.7                    | 0.6                     |
| Versa HD           | Lung SBRT      | Left-Right           | 0.5                     | 0.0                     | 1.6                     |
| Infinity 2         | Lung SBRT      | Left-Right           | 0.4                     | 0.0                     | 1.0                     |
| Infinity 1         | SSRS           | Left-Right           | -0.1                    | -0.5                    | 0.4                     |
| Infinity 1         | SSRS           | Superior-Inferior    | 0.4                     | -0.5                    | 1.3                     |
| Infinity 1         | SSRS, 2 cm     | Left-Right           | 0.5                     | -0.2                    | 1.3                     |
| Versa HD           | SSRS, 2 cm     | Left-Right           | 0.2                     | -0.3                    | 0.8                     |
| Infinity 2         | SSRS, 2 cm     | Left-Right           | 0.0                     | -0.4                    | 0.4                     |
| Infinity 1         | SSRS, 2.7 cm   | Left-Right           | 0.6                     | -0.8                    | 1.7                     |
| Versa HD           | SSRS, 2.7 cm   | Left-Right           | 0.4                     | -0.4                    | 1.1                     |
| Infinity 2         | SSRS, 2.7 cm   | Left-Right           | -0.6                    | -1.9                    | 0.2                     |

#### Shift in 75% and 60% Isodose Level

Table 3.10 and 3.11 show the average values of the shifts in the 75% dose points ( $\Delta 75$ ) for the profiles of the delivered lung SBRT and SSRS plans with isocentric setup. Profiles were taken through  $Y = 0, -0.5, -1, 0.5, \text{ and } 1 \text{ cm}$  for the evaluation of  $\Delta 75_{\text{Left}}$  and  $\Delta 75_{\text{Right}}$  with profiles taken through  $X = 0, -0.5, -1, 0.5, \text{ and } 1 \text{ cm}$  for the evaluation of  $\Delta 75_{\text{Superior}}$  and  $\Delta 75_{\text{Inferior}}$  (see Appendix A). Specifically, Table 3.10 displays the values for  $\Delta 75_{\text{Left}}$  and  $\Delta 75_{\text{Right}}$  as well as the minimum and maximum of calculated values corresponding to the measurements with a resolution of 1 mm in the left-right direction, while Table 3.11



contains values for  $\Delta 75_{\text{Superior}}$  and  $\Delta 75_{\text{Inferior}}$  as well as the minimum and maximum values, which correspond to the measurements with a resolution of 1 mm in the superior-inferior direction. The values of  $\Delta 75$  represent the asymmetric deviations in the 75% isodose lines between the measured and planned profiles (Section 2.3.1).

Table 3.10.  $\Delta 75_{\text{Left}}$  and  $\Delta 75_{\text{Right}}$  for lung SBRT and spine SRS profiles on three linear accelerators. Positive values of  $\Delta 75_{\text{Left}}$  and  $\Delta 75_{\text{Right}}$  indicated that the position of the measured 75% isodose line fell inside the planned 75% isodose line. Negative values of  $\Delta 75_{\text{Left}}$  and  $\Delta 75_{\text{Right}}$  indicated that the measured 75% isodose line fell outside the planned 75% isodose line.

| Linear Accelerator | Treatment Plan | Average $\Delta 75_{\text{Left}}$ (mm) | Minimum $\Delta 75_{\text{Left}}$ (mm) | Maximum $\Delta 75_{\text{Left}}$ (mm) | Average $\Delta 75_{\text{Right}}$ (mm) | Minimum $\Delta 75_{\text{Right}}$ (mm) | Maximum $\Delta 75_{\text{Right}}$ (mm) |
|--------------------|----------------|--|--|--|---|---|---|
| Infinity 1         | Lung SBRT      | -1.2                                   | -2.1                                   | -0.4                                   | -0.5                                    | -1.4                                    | 0.4                                     |
| Versa HD           | Lung SBRT      | -0.8                                   | -1.9                                   | 0.4                                    | 0.2                                     | -0.7                                    | 1.3                                     |
| Infinity 2         | Lung SBRT      | -0.2                                   | -0.6                                   | 0.1                                    | 0.6                                     | 0.2                                     | 1.5                                     |
| Infinity 1         | Spine SRS      | -0.7                                   | -1.7                                   | 0.2                                    | -0.8                                    | -1.3                                    | -0.3                                    |

Table 3.11.  $\Delta 75_{\text{Superior}}$  and  $\Delta 75_{\text{Inferior}}$  for lung SBRT and spine SRS profiles on an Elekta Infinity linear accelerator. Positive values of  $\Delta 75_{\text{Superior}}$  and  $\Delta 75_{\text{Inferior}}$  indicated that the position of the measured 75% isodose line fell inside the planned 75% isodose line. Negative values of  $\Delta 75_{\text{Superior}}$  and  $\Delta 75_{\text{Inferior}}$  indicated that the measured 75% isodose line fell outside the planned 75% isodose line.

| Linear Accelerator | Treatment Plan | Average $\Delta 75_{\text{Superior}}$ (mm) | Minimum $\Delta 75_{\text{Superior}}$ (mm) | Maximum $\Delta 75_{\text{Superior}}$ (mm) | Average $\Delta 75_{\text{Inferior}}$ (mm) | Minimum $\Delta 75_{\text{Inferior}}$ (mm) | Maximum $\Delta 75_{\text{Inferior}}$ (mm) |
|--------------------|----------------|--|--|--|--|--|--|
| Infinity 1         | Lung SBRT      | -0.6                                       | -1.9                                       | 0.2  | -0.9                                       | -1.1                                       | -0.5                                       |
| Infinity 1         | Spine SRS      | 0.0  | -1.3                                       | 1.3  | -0.9                                       | -2.4                                       | 0.7  |

Table 3.12 contains the values of  $\Delta 60_{\text{Left}}$  and  $\Delta 60_{\text{Right}}$  that correspond to the delivery of the spine SRS treatment plan shifted posteriorly by 2.0 or 2.7 cm on three different linear accelerators. For either data session, 1 mm resolution was achieved in only the left-right direction.

Table 3.12.  $\Delta 60_{\text{Left}}$  and  $\Delta 60_{\text{Right}}$  for posteriorly offset spine SRS profiles on three linear accelerators. Positive values of  $\Delta 60_{\text{Left}}$  and  $\Delta 60_{\text{Right}}$  indicated that the position of the measured 60% isodose line fell inside the planned 60% isodose line. Negative values of  $\Delta 60_{\text{Left}}$  and  $\Delta 60_{\text{Right}}$  indicated that the measured 60% isodose line fell outside the planned 60% isodose line.

| Linear Accelerator | Treatment Plan  | Average $\Delta 60_{\text{Left}}$ (mm) | Minimum $\Delta 60_{\text{Left}}$ (mm) | Maximum $\Delta 60_{\text{Left}}$ (mm) | Average $\Delta 60_{\text{Right}}$ (mm) | Minimum $\Delta 60_{\text{Right}}$ (mm) | Maximum $\Delta 60_{\text{Right}}$ (mm) |
|--------------------|-----------------|--|--|--|---|---|---|
| Infinity 1         | Spine SRS, 2 cm | -0.9                                   | -1.6                                   | -0.1                                   | 0.1                                     | -0.5                                    | 1.0                                     |
| Versa HD           | Spine SRS, 2 cm | -0.7                                   | -1.2                                   | 0.2                                    | -0.2                                    | -0.5                                    | 0.5                                     |

(table continued)

| Linear Accelerator | Treatment Plan    | Average $\Delta 60_{\text{Left}}$ (mm) | Minimum $\Delta 60_{\text{Left}}$ (mm) | Maximum $\Delta 60_{\text{Left}}$ (mm) | Average $\Delta 60_{\text{Right}}$ (mm) | Minimum $\Delta 60_{\text{Right}}$ (mm) | Maximum $\Delta 60_{\text{Right}}$ (mm) |
|--------------------|-------------------|--|--|--|---|---|---|
| Infinity 2         | Spine SRS, 2cm    | -0.5                                   | -0.9                                   | 0.0                                    | -0.5                                    | -0.8                                    | 0.0                                     |
| Infinity 1         | Spine SRS, 2.7 cm | -0.7                                   | -2.3                                   | 0.4                                    | -0.1                                    | -2.8                                    | 1.7                                     |
| Versa HD           | Spine SRS, 2.7 cm | -1.1                                   | -2.0                                   | 1.1                                    | -0.3                                    | -2.7                                    | 0.9                                     |
| Infinity 2         | Spine SRS, 2.7 cm | 1.2                                    | -0.7                                   | 3.3                                    | 0.0                                     | -0.9                                    | 1.9                                     |

### 3.4 Individual Gantry Beam Measurement Results

Tables 3.13 and 3.14 contain data for the delivery of individual gantry beams to the MapCHECK2 diode array at its native resolution with MapPHAN shifted posteriorly in comparison with the TPS-generated planar dose. These measurements were taken to provide more insight concerning the diode array's performance and whether or not angular dependence and over-response were potential causes for dose discrepancies in the region of the spinal cord. Specifically, Table 3.13 corresponds to data taken at the approximate region where the spinal cord ROI is adjacent to the vertebral body, whereas Table 3.14 corresponds to measurements taken at the approximate region representing the center of the spinal cord. Both measurement sessions displayed in Tables 3.13 and 3.14 resulted in overall high percent differences indicating that there was a systematically higher dose delivered to the region of the spinal cord for every prescribed gantry beam. Additional measurements were taken with the gantry and collimator placed at 0° to determine if angular dependence was the cause of the consistently higher dose delivered than planned.

Table 3.13. SSRS beams at planned gantry angles delivered to a diode array shifted posteriorly by 2 cm on Versa HD linear accelerator.

| Gantry Angle | Measured Dose (cGy) at (0,0) | Planned Dose (cGy) at (0,0) | Percent Difference |
|--------------|------------------------------|-----------------------------|--------------------|
| 100          | 85.19                        | 38.93                       | 118.83%            |
| 120          | 159.73                       | 88.12                       | 81.26%             |
| 140          | 207.98                       | 171.87                      | 21.01%             |
| 160          | 165.97                       | 125.75                      | 31.98%             |
| 180          | 59.83                        | 51.97                       | 15.12%             |
| 200          | 179.92                       | 152.65                      | 17.86%             |
| 220          | 241.16                       | 175.19                      | 37.66%             |
| 240          | 128.39                       | 51.67                       | 148.48%            |
| 260          | 91.69                        | 31.79                       | 188.42%            |
| <b>Total</b> | <b>1319.86</b>               | <b>887.94</b>               | <b>48.64%</b>      |

Table 3.14. SSRS beams at planned gantry angles delivered to a diode array shifted posteriorly by 2.7 cm on Versa HD linear accelerator.

| <b>Gantry Angle</b> | <b>Measured Dose (cGy) at (0,0)</b> | <b>Planned Dose (cGy) at (0,0)</b> | <b>Percent Difference</b> |
|---------------------|-------------------------------------|------------------------------------|---------------------------|
| 100                 | 13.69                               | 10.81                              | 26.64%                    |
| 120                 | 42.11                               | 23.76                              | 77.23%                    |
| 140                 | 67.30                               | 38.70                              | 73.90%                    |
| 160                 | 149.19                              | 120.37                             | 23.94%                    |
| 180                 | 61.31                               | 52.86                              | 15.99%                    |
| 200                 | 145.86                              | 133.06                             | 9.62%                     |
| 220                 | 85.33                               | 45.43                              | 87.83%                    |
| 240                 | 32.15                               | 19.84                              | 62.05%                    |
| 260                 | 16.94                               | 14.27                              | 18.71%                    |
| <b>Total</b>        | <b>613.88</b>                       | <b>459.10</b>                      | <b>33.71%</b>             |

Table 3.15 displays the comparison between the TPS-generated planar dose and the data collected for the individual beams of the SSRS treatment plan delivered at gantry and collimator angles of 0°. Delivering the treatment beams at these angles ostensibly eliminated any angular dependence of the diode array since the beams were delivered perpendicularly to the diode array. However, these measurements resulted in varying percent differences ranging from approximately -35% to 37% when the beams were delivered perpendicularly incident to the diode array, as is its intended use. The results from Table 3.15 suggest that angular dependence was not the cause of the systematic error seen in Tables 3.13 and 3.14 where the beams were delivered at the prescribed angles.

Table 3.15. SSRS beams delivered at gantry angle 0 and collimator angle 0 to a diode array on Versa HD linear accelerator.

| <b>Gantry Angle</b> | <b>Measured Dose (cGy) at (0,0)</b> | <b>Planned Dose (cGy) at (0,0)</b> | <b>Percent Difference</b> |
|---------------------|-------------------------------------|------------------------------------|---------------------------|
| 100                 | 124.12                              | 90.09                              | 37.77%                    |
| 120                 | 312.27                              | 252.31                             | 23.76%                    |
| 140                 | 752.61                              | 773.76                             | -2.73%                    |
| 160                 | 207.68                              | 322.82                             | -35.67%                   |
| 180                 | 49.00                               | 47.79                              | 2.53%                     |
| 200                 | 327.35                              | 428.34                             | -23.58%                   |
| 220                 | 683.63                              | 696.94                             | -1.91%                    |
| 240                 | 325.30                              | 324.9                              | 0.12%                     |
| 260                 | 326.42                              | 343.92                             | -5.09%                    |
| <b>Total</b>        | <b>3108.38</b>                      | <b>3208.87</b>                     | <b>-5.26%</b>             |

Further analysis of the SSRS treatment beams delivered at 0° for the gantry and collimator angle led to the discovery that a 1-mm applied shift of the planar dose along the patient superior-inferior axis resulted in smaller percent differences, as seen in Table 3.16. This shift most likely accounted for gantry

sag that is prominent when the gantry is at 0° and 180°. With this shift applied, the delivery performance of the SSRS beams were closer to what was expected based on the treatment planning system.

However, there was still variability as high as -12% between what was planned and what was measured on the diode array. In order to confirm if this finding was a result of the chosen diode array dosimeter or a result of an inaccuracy in the treatment planning system, a different experimental setup utilizing an ion chamber dosimeter was used to measure the delivered dose for the same set of gantry angle configurations as previously described.

Table 3.16. SSRS beams delivered at gantry angle 0 and collimator angle 0 to a diode array on Versa HD linear accelerator. TPS Data was shifted by 1 mm along the Y-axis using SNC Patient™ Software, resulting in smaller percent differences.

| <b>Gantry Angle</b> | <b>Measured Dose (cGy) at (0,0)</b> | <b>Planned Dose (cGy) at (0,0)</b> | <b>Percent Difference</b> |
|---------------------|-------------------------------------|------------------------------------|---------------------------|
| 100                 | 124.12                              | 116.75                             | 6.31%                     |
| 120                 | 312.27                              | 291.41                             | 7.16%                     |
| 140                 | 752.61                              | 770.17                             | -2.28%                    |
| 160                 | 207.68                              | 237.45                             | -12.54%                   |
| 180                 | 49.00                               | 44.77                              | 9.44%                     |
| 200                 | 327.35                              | 351.66                             | -6.91%                    |
| 220                 | 683.63                              | 687.78                             | -0.60%                    |
| 240                 | 325.30                              | 329.42                             | -1.25%                    |
| 260                 | 326.42                              | 333.58                             | -2.15%                    |
| <b>Total</b>        | <b>3108.38</b>                      | <b>3162.99</b>                     | <b>-1.73%</b>             |

### 3.5 Ion Chamber Measurements

Tables 3.17 and 3.18 contain the data acquired using an ion chamber in the solid water “cheese” phantom at the specific points that represent the perimeter of the spinal cord ROI (Table 3.17) and center of the spinal cord (Table 3.18) as they compare to the TPS-generated values at the corresponding points of interest. These measurements were acquired with the beams at their planned gantry and collimator angles. The percent difference between the measured and planned values at both posterior positions was not negligible with regards to the anatomical point of interest they represent. Moreover, the consistently higher dose delivered agrees with the results from the central diode measurements seen in Tables 3.13 and 3.14. The data from the ion chamber measurements shown in Tables 3.17 and 3.18 confirmed that the delivered dose measured by the diode array was valid, therefore suggesting an error in the treatment planning system’s beam modeling algorithm.

Table 3.17. Ion chamber measurements for an active detector volume representing the approximate region where the spinal cord ROI is adjacent to the vertebral body (2 cm from the CTV isocenter). Beams were delivered at their planned gantry and collimator angles.

| Gantry Angle | Measured (cGy) | TPS Minimum (cGy) | TPS Maximum (cGy) | TPS Mean Dose (cGy) | TPS Standard Deviation (cGy) | Percent Difference |
|--------------|----------------|-------------------|-------------------|---------------------|------------------------------|--------------------|
| 100          | 93.33          | 30.1              | 132.9             | 72.2                | 27.5                         | 29.27%             |
| 120          | 150.43         | 41.4              | 253.1             | 120.9               | 51.3                         | 24.43%             |
| 140          | 151.98         | 77.8              | 221.3             | 134.0               | 30.7                         | 13.42%             |
| 160          | 118.33         | 56.8              | 128.6             | 89.2                | 23.6                         | 32.66%             |
| 180          | 47.48          | 38.3              | 49.7              | 43.3                | 3.4                          | 9.65%              |
| 200          | 133.37         | 94.4              | 171.8             | 123.9               | 18.2                         | 7.64%              |
| 220          | 163.78         | 56.7              | 280.5             | 147.6               | 54.5                         | 10.96%             |
| 240          | 100.32         | 31.1              | 191.8             | 75.9                | 39.0                         | 32.17%             |
| 260          | 107.04         | 27.8              | 156.9             | 60.0                | 27.0                         | 78.40%             |
| <b>Total</b> | <b>1066.06</b> |                   |                   | <b>867.0</b>        |                              | <b>22.96%</b>      |

Table 3.18. Ion chamber measurements for an active detector volume representing the approximate center of the spinal cord (2.7 cm from the CTV isocenter). Beams were delivered at their planned gantry and collimator angles.

| Gantry Angle | Measured (cGy) | TPS Minimum (cGy) | TPS Maximum (cGy) | TPS Mean Dose (cGy) | TPS Standard Deviation (cGy) | Percent Difference |
|--------------|----------------|-------------------|-------------------|---------------------|------------------------------|--------------------|
| 100          | 16.02          | 11.4              | 18.2              | 14.0                | 1.5                          | 14.46%             |
| 120          | 28.26          | 15.9              | 37.3              | 21.8                | 4.0                          | 29.62%             |
| 140          | 44.89          | 22.7              | 69.0              | 39.3                | 8.4                          | 14.21%             |
| 160          | 97.73          | 59.6              | 118.6             | 85.9                | 15.5                         | 13.77%             |
| 180          | 49.62          | 39.9              | 51.8              | 45.1                | 3.6                          | 10.02%             |
| 200          | 115.05         | 86.7              | 125.8             | 105.2               | 8.9                          | 9.36%              |
| 220          | 59.48          | 29.9              | 84.0              | 43.3                | 10.2                         | 37.37%             |
| 240          | 22.60          | 14.8              | 22.9              | 17.8                | 1.7                          | 4.80%              |
| 260          | 20.09          | 14.2              | 23.4              | 17.6                | 1.9                          | 14.16%             |
| <b>Total</b> | <b>453.73</b>  |                   |                   | <b>390.0</b>        |                              | <b>16.34%</b>      |

To further test the accuracy of the SSRS treatment plan beams' delivery, the beams were overridden to be delivered at gantry and collimator angles of 0° with the ion chamber placed 2.7 cm posterior to isocenter to represent the center of the spinal cord. Table 3.19 displays the result of this experiment where an improvement between the percent difference of the measured and calculated dose to this region of interest can be seen. The results in Table 3.19 suggest that the prescribed gantry and collimator angles for the SSRS treatment plan, in combination with the optimized modulation, are the cause for the error in the TPS beam model.

Table 3.19. Ion chamber measurements for an active detector volume representing the approximate center of the spinal cord (2.7 cm from the CTV isocenter). Beams were overridden to be delivered at gantry and collimator angles of 0°.

| <b>Gantry Angle</b> | <b>Measured (cGy)</b> | <b>TPS Minimum (cGy)</b> | <b>TPS Maximum (cGy)</b> | <b>TPS Mean Dose (cGy)</b> | <b>TPS Standard Deviation (cGy)</b> | <b>Percent Difference</b> |
|---------------------|-----------------------|--------------------------|--------------------------|----------------------------|-------------------------------------|---------------------------|
| 100                 | 64.60                 | 26.4                     | 89.6                     | 59.0                       | 22.2                                | 9.49%                     |
| 120                 | 176.80                | 109.4                    | 216.0                    | 161.6                      | 37.0                                | 9.41%                     |
| 140                 | 437.40                | 408.1                    | 443.5                    | 428.1                      | 10.2                                | 2.17%                     |
| 160                 | 158.40                | 70.7                     | 267.1                    | 164.8                      | 60.6                                | -3.88%                    |
| 180                 | 35.50                 | 29.6                     | 37.7                     | 33.3                       | 2.5                                 | 6.61%                     |
| 200                 | 225.30                | 150.2                    | 309.5                    | 229.7                      | 59.3                                | -1.92%                    |
| 220                 | 409.90                | 368.2                    | 416.9                    | 396.7                      | 12.2                                | 3.33%                     |
| 240                 | 195.90                | 177.8                    | 203.0                    | 188.7                      | 7.3                                 | 3.82%                     |
| 260                 | 200.98                | 183.4                    | 212.4                    | 196.7                      | 9.8                                 | 2.18%                     |
| <b>Total</b>        | <b>1904.78</b>        |                          |                          | <b>1858.6</b>              |                                     | <b>2.48%</b>              |

## Chapter 4. Discussion

### 4.1 Summary of Results

This project provided quantitative data regarding the accuracy and precision of high-dose treatments delivered with the Elekta Infinity and Versa HD linear accelerators. Baseline geometric accuracy was established across all three linear accelerators through the MV isocenter accuracy test, which produced results for the radius of isocenter within the limits of the vendor-provided protocol for two of the three tested linear accelerators with the third linear accelerator's isocenter radius varying by only 0.01 mm from the limit. Accuracy of dose delivery for two stereotactic treatment plans was assessed through a novel quality assurance platform that allowed for the diode array to achieve 1-mm resolution along one axis. The reproducibility of the experimental design was measured and found to have acceptable positional alignment errors and shift in isodose levels of less than 1 mm.

Variability in delivery accuracy of the treatment plans occurred across all three linear accelerators. Profile comparisons of the calculated and measured data from these measurements were analyzed for characteristic positional alignment ( $\Delta c$ ). For the delivery of lung SBRT treatment plans, 2-mm accuracy for patient setup with the use of immobilization devices has previously been achieved (Benedict *et al.*, 2010; Wulf *et al.*, 2000; Nagata *et al.*, 2002). Our study proved the Elekta Infinity and Versa HD linear accelerators were able to achieve 2-mm positional accuracy. The delivery of the spine SRS treatment plan across all linear accelerators achieved less than a 1-mm accuracy on average that has previously been reported for spine SBRT treatments (Guckenberger *et al.*, 2007; Wang *et al.*, 2008; Chang *et al.*, 2004). Yenice *et al.* reported that errors of 2 mm in magnitude can result in a significantly greater (>100%) dose to the spinal cord than planned (Yenice *et al.*, 2003). The calculated percent difference between measured and calculated dose values at the region representative of the spinal cord reflected these findings. Even with kV-CBCT positioning, the difference between calculated and measured doses showed a delivered dose to the region of the spinal cord as much as 39% higher than intended. Therefore, achieving 1-mm positional accuracy is necessary when treating spine SRS cases so as to avoid delivering a greater dose to OARs than planned.

Where the positional alignment varied among each linear accelerator, analysis of the differences in specific isodose levels ( $\Delta 75$  and  $\Delta 60$ ) showed that, overall, the measured profile point fell outside the

planned isodose line, meaning that the target volume was consistently covered with the prescribed dose compared to the TPS calculation. The values of  $\Delta 75$  and  $\Delta 60$  varied by approximately 1.2 mm at most for the lung SBRT and spine SRS, suggesting variable coverage of the target volume for the delivered plan compared to that generated by the treatment planning system.

After analysis of the measured and planned profiles, consistently higher delivered doses were seen for those planes taken through the region of interest representing the spinal cord. This was particularly noteworthy as a dose exceeding the maximum limit to the spinal cord could lead to paralysis. Further investigation was required to identify the reason for discrepancy between the planned and measured dose at the spinal cord region of interest. Angular dependence was ruled out by individually delivering the SSRS beams to the diode array and comparing the delivered dose to the calculations performed by the treatment planning system. Consistently higher doses were measured when the beams were at their prescribed gantry and collimator angles. Variable doses were measured when the beams were overridden to be delivered at gantry and collimator angles of  $0^\circ$ . Once a millimeter shift was applied to the data, presumably to account for gantry sag when the gantry is placed at  $0^\circ$ , the magnitude of the percent difference between measured and calculated dose points decreased for most delivered beams. The evaluation of the delivery of individual SSRS beams proved that the delivery system was capable of delivering the planned beams when the gantry and collimator angles were set to  $0^\circ$ , which indicates that the treatment planning system is possibly incapable of modeling the beam accurately for the combination of the prescribed gantry and collimator angles as well as the optimized modulation required for the SSRS plan.

To confirm the discrepancy between the measured and calculated dose, a different experimental setup was adopted to repeat the measurements of the individual beams delivered to the diode array. Ion chamber measurements were taken at the approximate position of the spinal cord, specifically its perimeter proximal to the vertebral column and its center. Results confirmed the difference in the measured and delivered dose at the level of the spinal cord for the SSRS plan in that doses delivered were consistently higher for the prescribed gantry angles. The results from both the diode array and ion chamber experiments suggest an inaccuracy in the treatment planning system as it was utilized for the SSRS treatment plan.



## **4.2 Limitations of Work**

This work was limited by 1-mm resolution along one axis. This prevented the use of 2-dimensional metrics, such as gamma analysis, in assessing the delivery accuracy of the treatment systems. Additionally, artifacts were produced in the profiles due to over-responding diodes when measured files were combined for the aggregate file. These artifacts created a “smearing” effect that was a direct result of the dosimeter despite dose calibrations performed on the diode array before every measurement session. Lastly, this project lacks complete sets of data for the SSRS treatment delivery at 2 and 2.7 cm posterior offsets along the patient superior-inferior axis.

## **4.3 Evaluation of Hypothesis**

Based on the findings of this project, the Elekta Infinity and Versa HD delivery systems were adequate for lung SBRT treatments but require further exploration for the commencement of spine SRS treatments at Mary Bird Perkins Cancer Center. The hypothesis of this project was that the Elekta Infinity and Versa HD linear accelerators would be sufficient for lung SBRT and spine SRS treatments as deemed by clinical standards. While both treatment deliveries achieved 1-mm accuracy on average in terms of positional alignment and isodose level coverage, the delivery of the SSRS treatment plan resulted in a consistently higher delivered dose to the region of the spinal cord at the prescribed gantry and collimator angles.

## **4.4 Future Work**

The data in this research was obtained using a diode array with a novel setup allowing for 1-mm resolution. With this research design, major dose discrepancies were found between the measured and planned treatment plans. Further analysis with a different dosimeter confirmed these findings to be true and not a result of experimental design. Therefore, these findings suggest an inconsistency between the treatment planning system and the delivery system. Assessment of the treatment planning system as it applies to high dose single fraction treatments could be evaluated further. Moreover, additional treatment plans utilizing techniques other than 3D conformal and step and shoot IMRT could be tested on these platforms using the novel design of this project.

## References

- Almond, P, Biggs P, Coursey B M, Hanson W F, Huq M S, Nath R and Rogers D W O 1999 AAPM's TG-51 protocol for clinical reference dosimetry of high-energy photon and electron beams Medical Physics 26 1847-70
- American Cancer Society 2018 American Cancer Society, Cancer Facts & Figures 2018.
- Amini, A, Yeh N, Gaspar L E, Kavanagh B and Karam S D 2014 Stereotactic Body Radiation Therapy (SBRT) for lung cancer patients previously treated with conventional radiotherapy: a review Radiation Oncology (London, England) 9
- Benedict, S H, Yenice K M, Followill D, Galvin J M, Hinson W, Kavanagh B, Keall P, Lovelock M, Meeks S, Papiez L, Purdie T, Sadagopan R, Schell M C, Salter B, Schlesinger D J, Shiu A S, Solberg T, Song D Y, Stieber V, Timmerman R, Tome W A, Verellen D, Wang L and Yin F F 2010 Stereotactic body radiation therapy: the report of AAPM Task Group 101 Med Phys 37 4078-101
- Berkovic, P, Gulyban A, Nguyen P V, Dechambre D, Martinive P, Jansen N, Lakosi F, Janvary L and Coucke P A 2017 Stereotactic Robotic Body Radiotherapy for Patients With Unresectable Hepatic Oligorecurrence Clinical colorectal cancer
- Chang, E L, Shiu A S, Lii M-F, Rhines L D, Mendel E, Mahajan A, Weinberg J S, Mathews L A, Brown B W, Maor M H and Cox J D 2004 Phase I clinical evaluation of near-simultaneous computed tomographic image-guided stereotactic body radiotherapy for spinal metastases International Journal of Radiation Oncology • Biology • Physics 59 1288-94
- Clements, M 2016 Isocenter Optimization Radiological Imaging Technology, Inc.
- Court, L E, Wolfsberger L, Allen A M, James S and Tishler R B 2008 Clinical experience of the importance of daily portal imaging for head and neck IMRT treatments Journal of applied clinical medical physics 9 26-33
- Greco, C, Pares O, Pimentel N, Moser E, Louro V, Morales X, Salas B and Fuks Z 2015 Spinal metastases: From conventional fractionated radiotherapy to single-dose SBRT Reports of Practical Oncology and Radiotherapy 20 454-63
- Guckenberger, M, Meyer J, Wilbert J, Baier K, Bratengeier K, Vordermark D and Flentje M 2007 Precision required for dose-escalated treatment of spinal metastases and implications for image-guided radiation therapy (IGRT) Radiotherapy and Oncology 84 56-63
- Hara, R, Itami J, Kondo T, Aruga T, Abe Y, Ito M, Fuse M, Shinohara D, Nagaoka T and Kobiki T 2002 Stereotactic single high dose irradiation of lung tumors under respiratory gating Radiotherapy and Oncology 63 159-63
- Hof, H, Herfarth K K, Munter M, Hoess A, Motsch J, Wannenmacher M and Debus J J 2003 Stereotactic single-dose radiotherapy of stage I non-small-cell lung cancer (NSCLC) International journal of radiation oncology, biology, physics 56 335-41
- Jursinic, P A 2009 Angular dependence of dose sensitivity of surface diodes Med Phys 36 2165-71
- Jursinic, P A, Sharma R and Reuter J 2010 MapCHECK used for rotational IMRT measurements: step-and-shoot, TomoTherapy, RapidArc Med Phys 37 2837-46
- Katagiri, H, Takahashi M, Inagaki J, Kobayashi H, Sugiura H, Yamamura S and Iwata H 1998 Clinical results of nonsurgical treatment for spinal metastases International journal of radiation oncology, biology, physics 42 1127-32

- Keeling, V P, Ahmad S and Jin H 2013 A comprehensive comparison study of three different planar IMRT QA techniques using MapCHECK 2 *Journal of applied clinical medical physics* 14 4398
- Khan, F M 2010 *The Physics of Radiation Therapy: Williams & Wilkins*
- Kong, F M, Zhao J, Wang J and Faivre-Finn C 2014 Radiation dose effect in locally advanced non-small cell lung cancer *Journal of Thoracic Disease* 6 336-47
- Lohr, F, Debus J, Frank C, Herfarth K, Pastyr O, Rhein B, Bahner M L, Schlegel W and Wannenmacher M 1999 Noninvasive patient fixation for extracranial stereotactic radiotherapy *International Journal of Radiation Oncology • Biology • Physics* 45 521-7
- Low, D A, Li Z and Drzymala R E 1995 Minimization of target positioning error in accelerator-based radiosurgery *Med Phys* 22 443-8
- Nagata, Y, Negoro Y, Aoki T, Mizowaki T, Takayama K, Kokubo M, Araki N, Mitsumori M, Sasai K, Shibamoto Y, Koga S, Yano S and Hiraoka M 2002 Clinical outcomes of 3D conformal hypofractionated single high-dose radiotherapy for one or two lung tumors using a stereotactic body frame *International Journal of Radiation Oncology • Biology • Physics* 52 1041-6
- Nalichowski, A, Kaufman I, Gallo J, Bossenberger T, Solberg T, Ramirez E, Yan Y, Fredrick J, Bichay T, Mayville A and Burmeister J 2017 Single fraction radiosurgery/stereotactic body radiation therapy (SBRT) for spine metastasis: A dosimetric comparison of multiple delivery platforms *Journal of applied clinical medical physics* 18 164-9
- Papiez, L and Timmerman R 2008 Hypofractionation in radiation therapy and its impact *Med Phys* 35 112-8
- Ryu, S I, Chang S D, Kim D H, Murphy M J, Le Q T, Martin D P and Adler J R, Jr. 2001 Image-guided hypo-fractionated stereotactic radiosurgery to spinal lesions *Neurosurgery* 49 838-46
- Sahgal, A, Larson D A and Chang E L Stereotactic Body Radiosurgery for Spinal Metastases: A Critical Review *International Journal of Radiation Oncology • Biology • Physics* 71 652-65
- Sharpe, M B, Moseley D J, Purdie T G, Islam M, Siewerdsen J H and Jaffray D A 2006 The stability of mechanical calibration for a kV cone beam computed tomography system integrated with linear accelerator *Med Phys* 33 136-44
- Sheehan, J P and Jagannathan J 2008 Review of spinal radiosurgery: a minimally invasive approach for the treatment of spinal and paraspinal metastases *Neurosurgical focus* 25 E18
- Solberg, T D, Medin P M, Mullins J and Li S 2008 Quality assurance of immobilization and target localization systems for frameless stereotactic cranial and extracranial hypofractionated radiotherapy *International journal of radiation oncology, biology, physics* 71 S131-5
- Song, C, Cho L, Yuan J, E Dusenbery K, Griffin R and Levitt S 2013 Radiobiology of Stereotactic Body Radiation Therapy/Stereotactic Radiosurgery and the Linear-Quadratic Model vol 87
- Sutton, M W, Fontenot J D, Matthews K L, 2nd, Parker B C, King M L, Gibbons J P and Hogstrom K R 2014 Accuracy and precision of cone-beam computed tomography guided intensity modulated radiation therapy *Practical radiation oncology* 4 e67-73
- Timmerman, R, Paulus R, Galvin J, Michalski J, Straube W, Bradley J, Fakiris A, Bezjak A, Videtic G, Johnstone D, Fowler J, Gore E and Choy H 2010 Stereotactic body radiation therapy for inoperable early stage lung cancer *Jama* 303 1070-6

- Verellen, D, Soete G, Linthout N, Van Acker S, De Roover P, Vinh-Hung V, Van de Steene J and Storme G 2003 Quality assurance of a system for improved target localization and patient set-up that combines real-time infrared tracking and stereoscopic X-ray imaging Radiotherapy and oncology : journal of the European Society for Therapeutic Radiology and Oncology 67 129-41
- Wambersie, A 1999 ICRU 62: Prescribing, Recording and Reporting Photon Beam Therapy (Supplement to ICRU Report 50) In: International Commission on Radiation Units and Measurements.
- Wang, H, Shiu A, Wang C, O'Daniel J, Mahajan A, Woo S, Liengsawangwong P, Mohan R and Chang E L 2008 Dosimetric Effect of Translational and Rotational Errors for Patients Undergoing Image-Guided Stereotactic Body Radiotherapy for Spinal Metastases International Journal of Radiation Oncology • Biology • Physics 71 1261-71
- Wang, L, Feigenberg S, Chen L, Pasklev K and Ma C C M 2006 Benefit of three-dimensional image-guided stereotactic localization in the hypofractionated treatment of lung cancer International Journal of Radiation Oncology • Biology • Physics 66 738-47
- Wulf, J, Hädinger U, Oppitz U, Olshausen B and Flentje M 2000 Stereotactic radiotherapy of extracranial targets: CT-simulation and accuracy of treatment in the stereotactic body frame Radiotherapy and Oncology 57 225-36
- Yenice, K M, Lovelock D M, Hunt M A, Lutz W R, Fournier-Bidoz N, Hua C-H, Yamada J, Bilsky M, Lee H, Pfaff K, Spirou S V and Amols H I 2003 CT image-guided intensity-modulated therapy for paraspinal tumors using stereotactic immobilization International Journal of Radiation Oncology • Biology • Physics 55 583-93
- Yu, C, Main W, Taylor D, Kuduvalli G, Apuzzo M L and Adler J R, Jr. 2004 An anthropomorphic phantom study of the accuracy of Cyberknife spinal radiosurgery Neurosurgery 55 1138-49
- Zhang, J, Yang F, Li B, Li H, Liu J, Huang W, Wang D, Yi Y and Wang J 2011 Which is the optimal biologically effective dose of stereotactic body radiotherapy for Stage I non-small-cell lung cancer? A meta-analysis International journal of radiation oncology, biology, physics 81 e305-16

## Appendix A. Profiles Comparing Measured and Calculated Treatment Plans

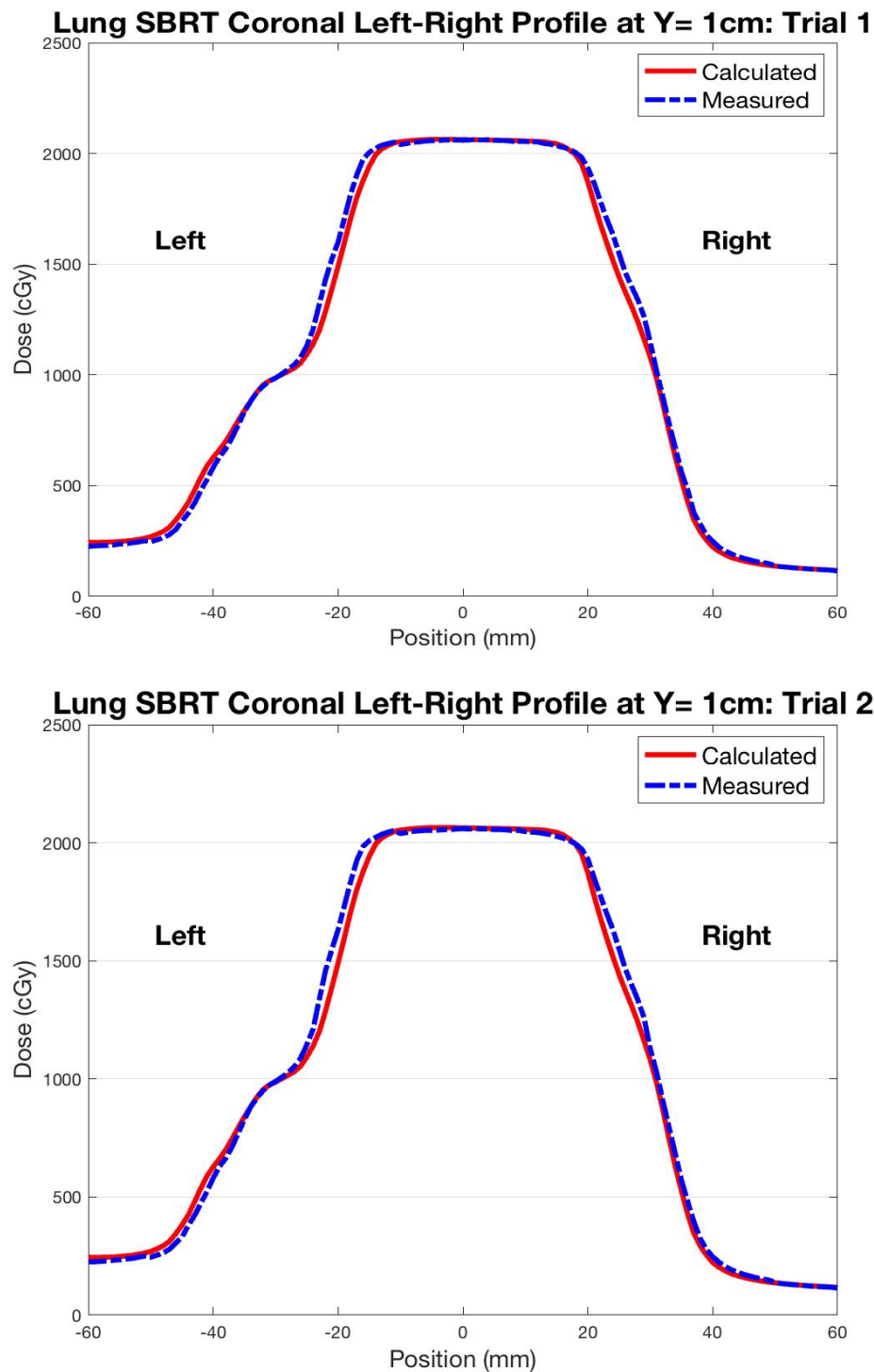
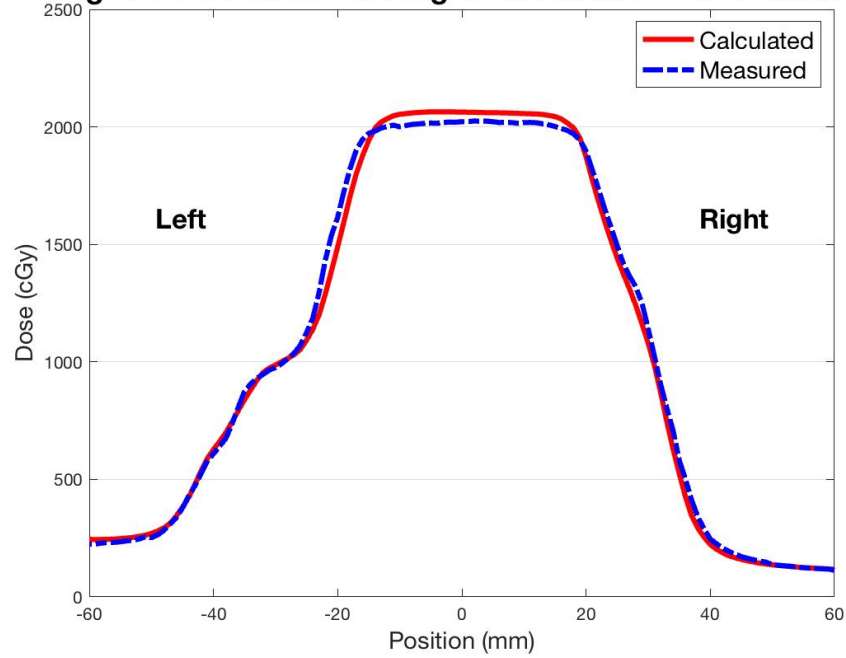


Figure A.1. Coronal left-right profile plots of Trials 1 and 2 taken through Y = 1 cm of the lung SBRT treatment plan delivered on the Elekta Infinity with Agility head at the MBPCC Baton Rouge facility.

**Lung SBRT Coronal Left-Right Profile at Y= 1cm: Versa HD**



**Lung SBRT Coronal Left-Right Profile at Y= 1cm: Infinity 2**

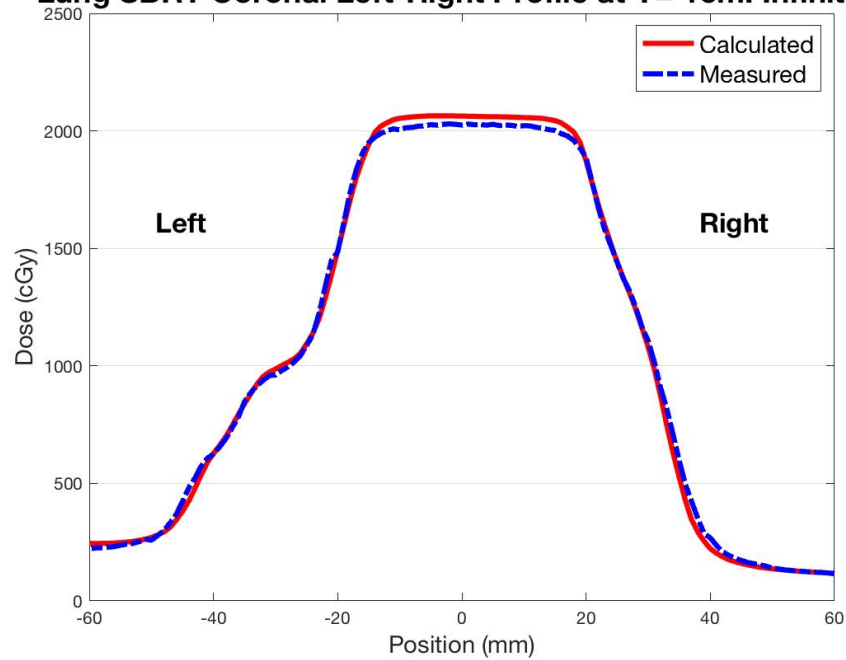


Figure A.2. Coronal left-right profile plots through Y = 1 cm of the lung SBRT treatment plan delivered on the Elekta Versa HD at the MBPCC Baton Rouge facility and the Elekta Infinity with Agility head located at the MBPCC Gonzales facility, respectively.

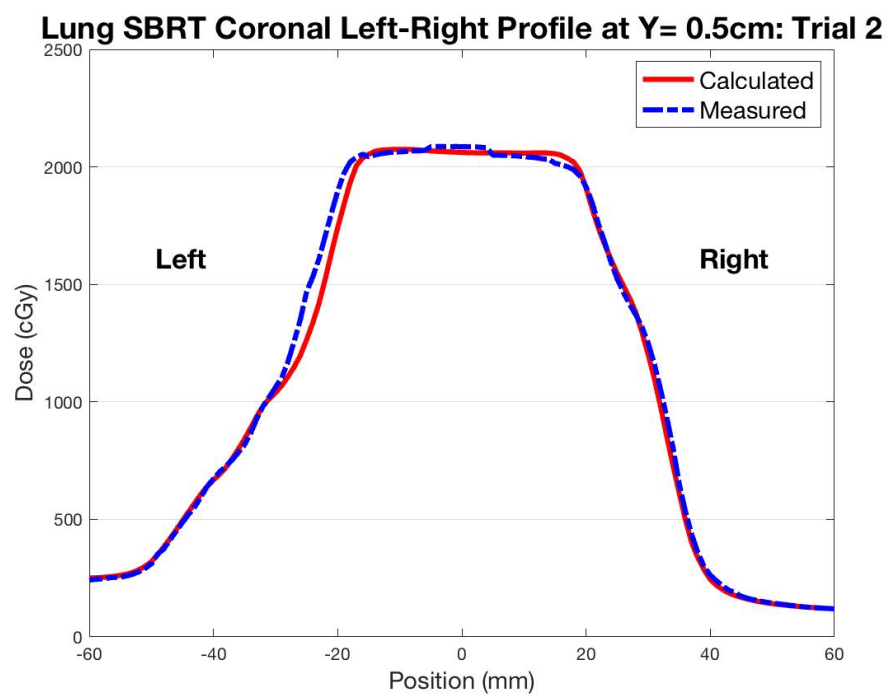
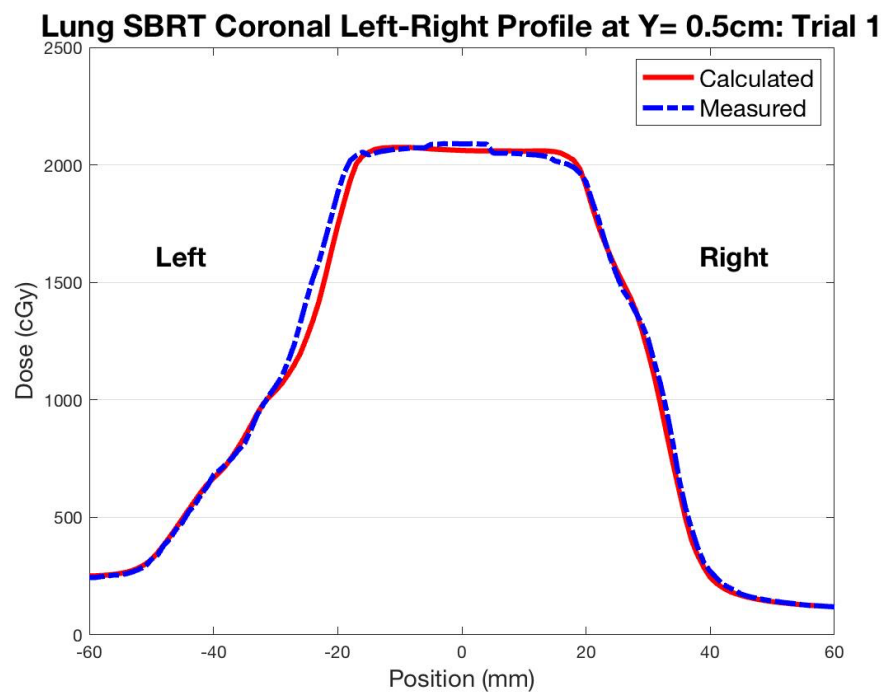
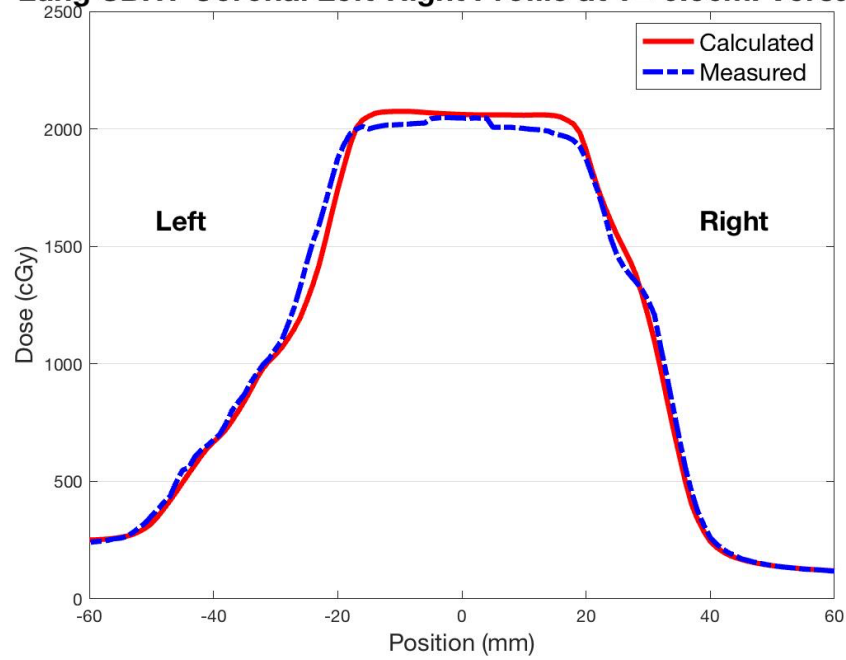


Figure A.3. Coronal left-right profile plots of Trials 1 and 2 taken through Y = 0.5 cm of the lung SBRT treatment plan delivered on the Elekta Infinity with Agility head at the MBPCC Baton Rouge facility.

**Lung SBRT Coronal Left-Right Profile at Y= 0.5cm: Versa HD**



**Lung SBRT Coronal Left-Right Profile at Y= 0.5cm: Infinity 2**

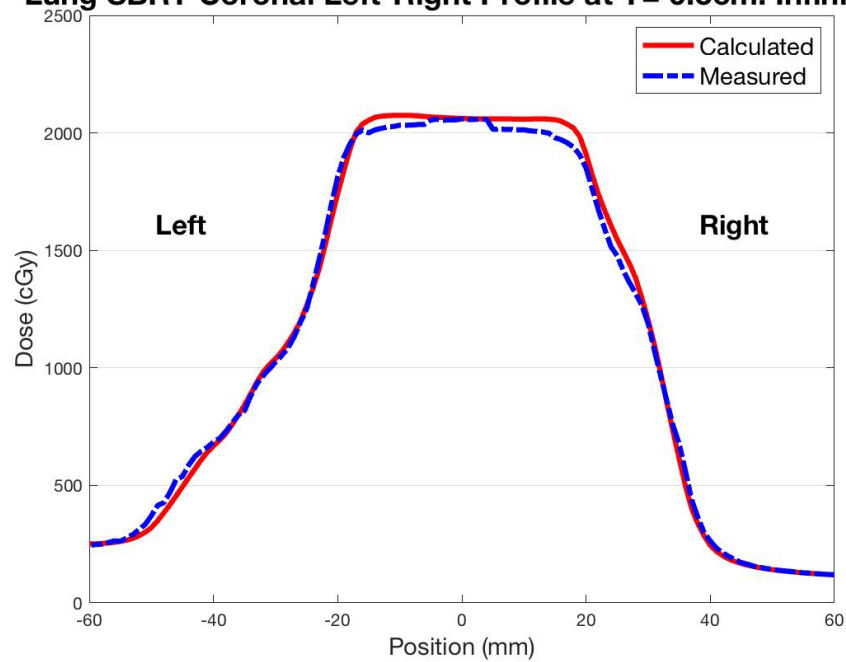


Figure A.4. Coronal left-right profile plots through Y = 0.5 cm of the lung SBRT treatment plan delivered on the Elekta Versa HD at the MBPCC Baton Rouge facility and the Elekta Infinity with Agility head located at the MBPCC Gonzales facility, respectively.



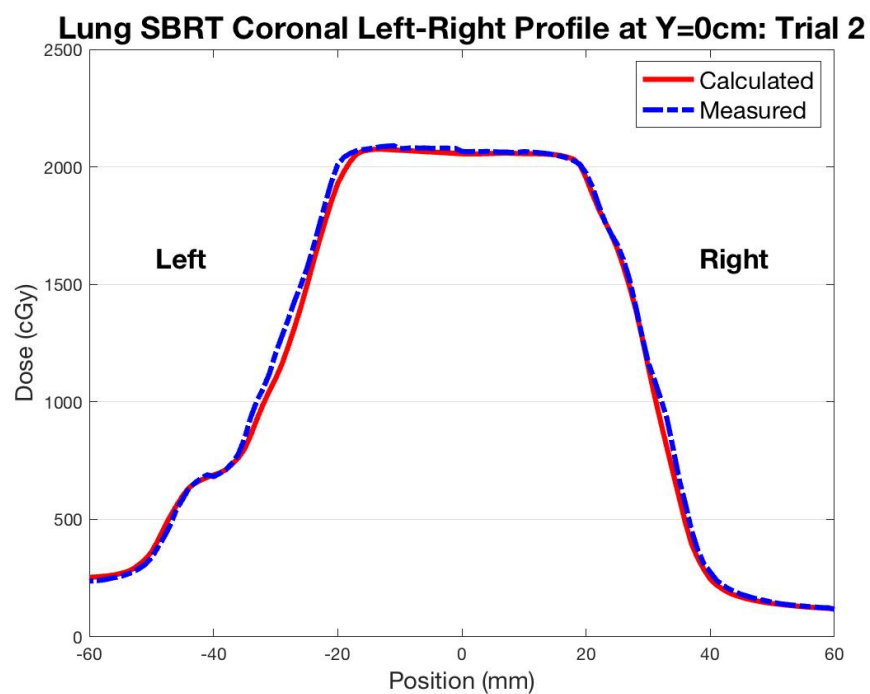
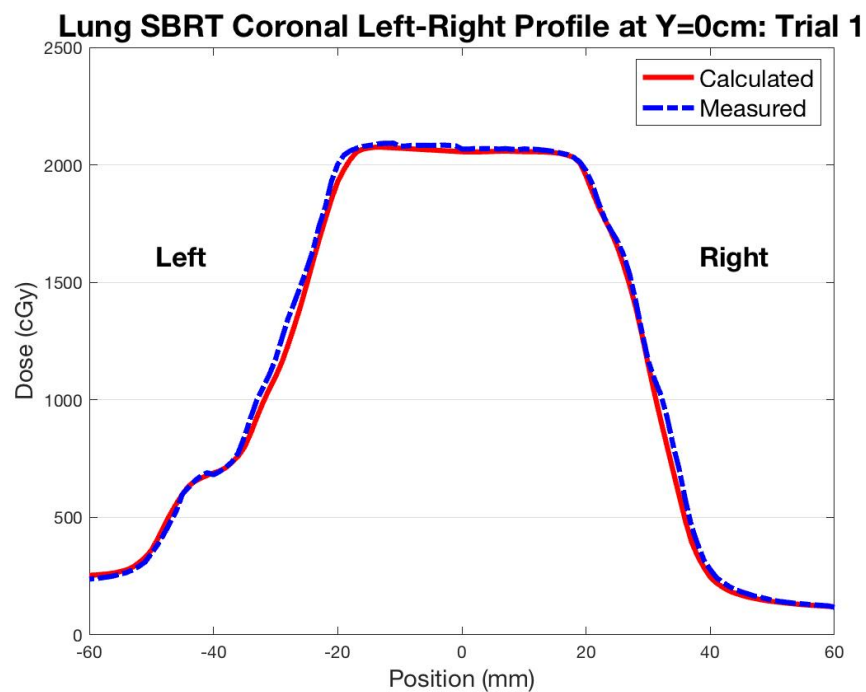


Figure A.5. Coronal left-right profile plots of Trials 1 and 2 taken through Y = 0 cm of the lung SBRT treatment plan delivered on the Elekta Infinity with Agility head at the MBPCC Baton Rouge facility.

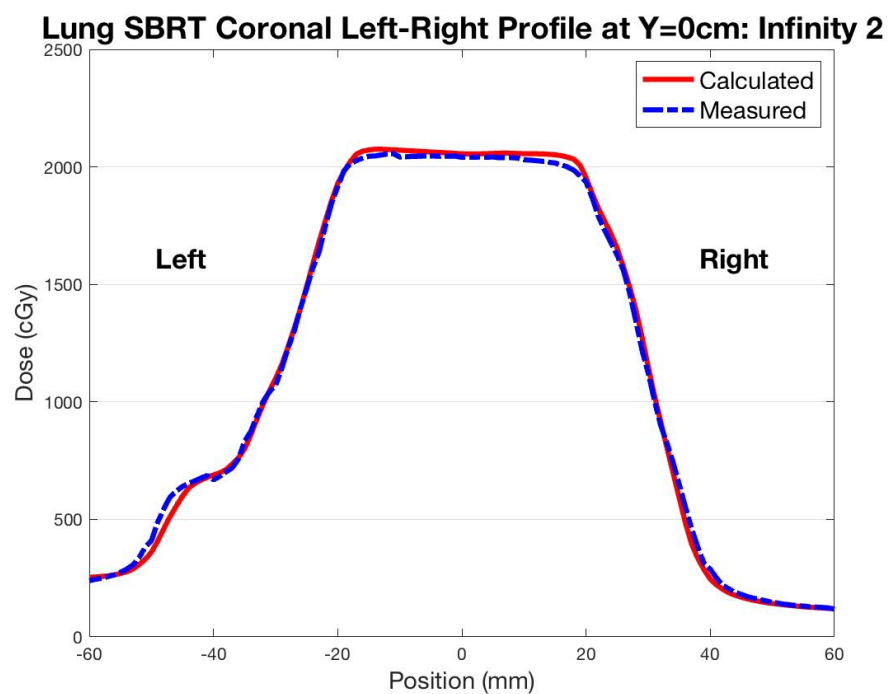
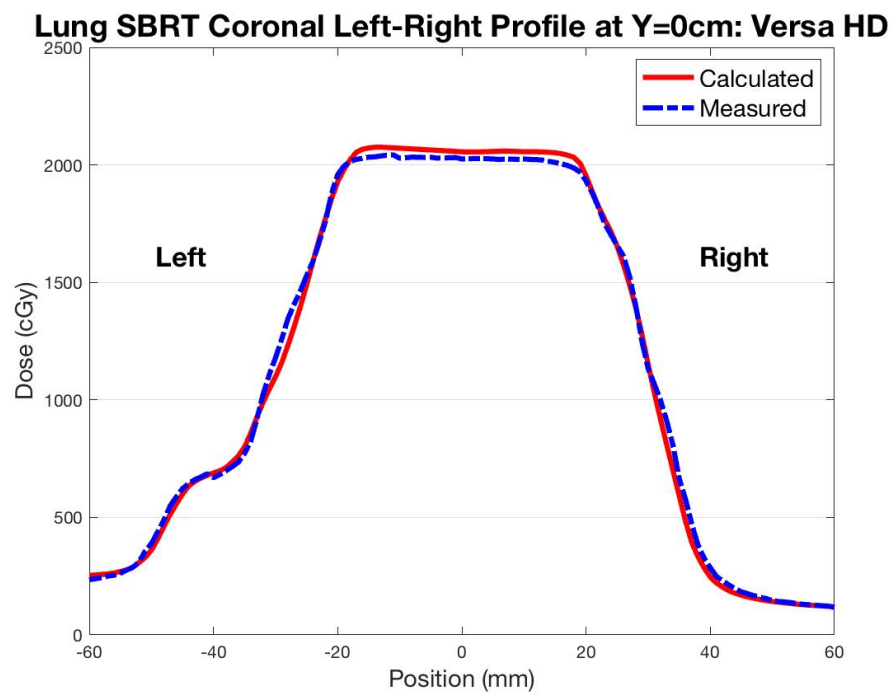


Figure A.6. Coronal left-right profile plots through Y = 0 cm of the lung SBRT treatment plan delivered on the Elekta Versa HD at the MBPCC Baton Rouge facility and the Elekta Infinity with Agility head located at the MBPCC Gonzales facility, respectively.

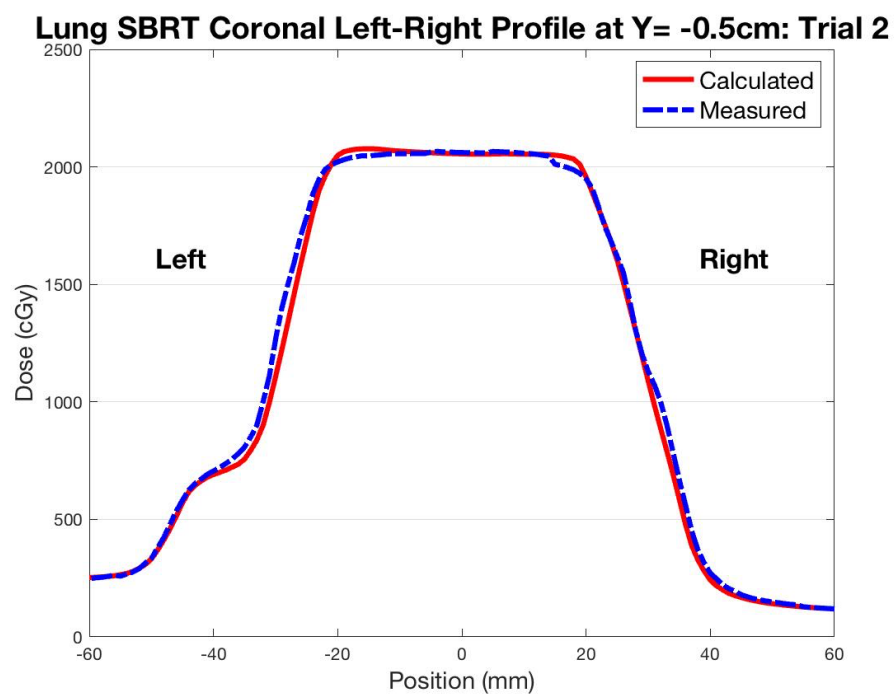
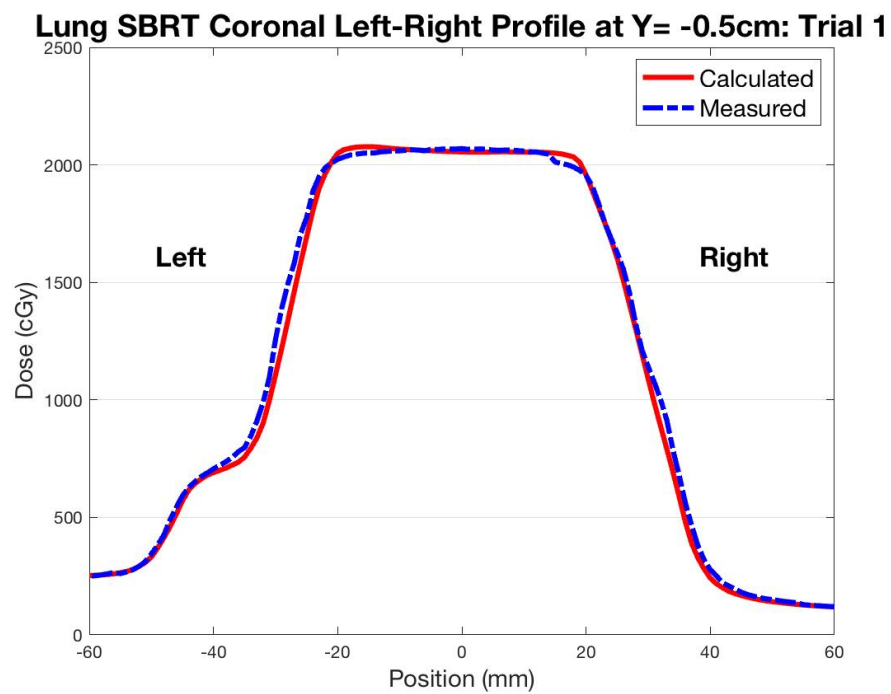
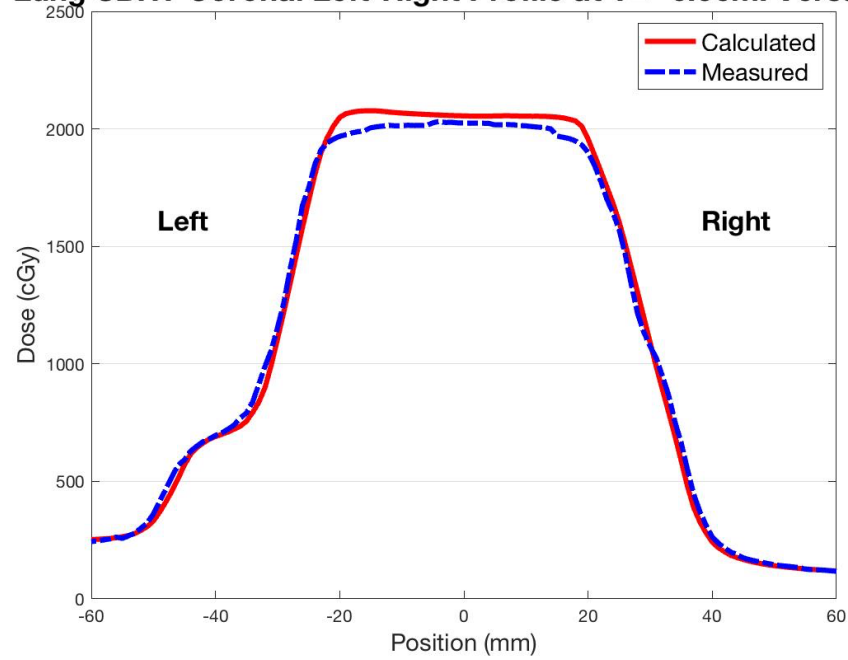


Figure A.7. Coronal left-right profile plots of Trials 1 and 2 taken through Y = -0.5 cm of the lung SBRT treatment plan delivered on the Elekta Infinity with Agility head at the MBPCC Baton Rouge facility.

**Lung SBRT Coronal Left-Right Profile at Y= -0.5cm: Versa HD**



**Lung SBRT Coronal Left-Right Profile at Y= -0.5cm: Infinity 2**

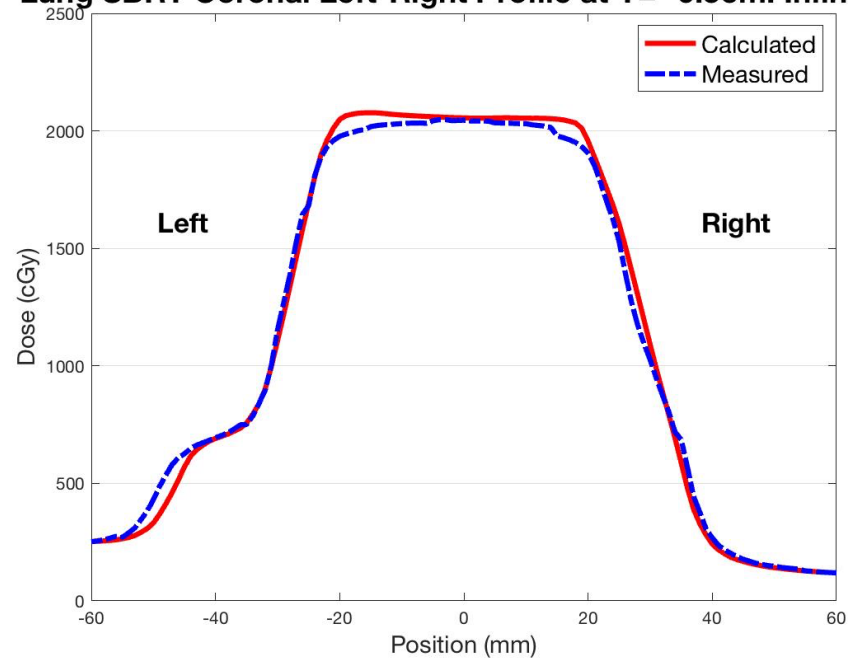


Figure A.8. Coronal left-right profile plots through Y = -0.5 cm of the lung SBRT treatment plan delivered on the Elekta Versa HD at the MBPCC Baton Rouge facility and the Elekta Infinity with Agility head located at the MBPCC Gonzales facility, respectively.

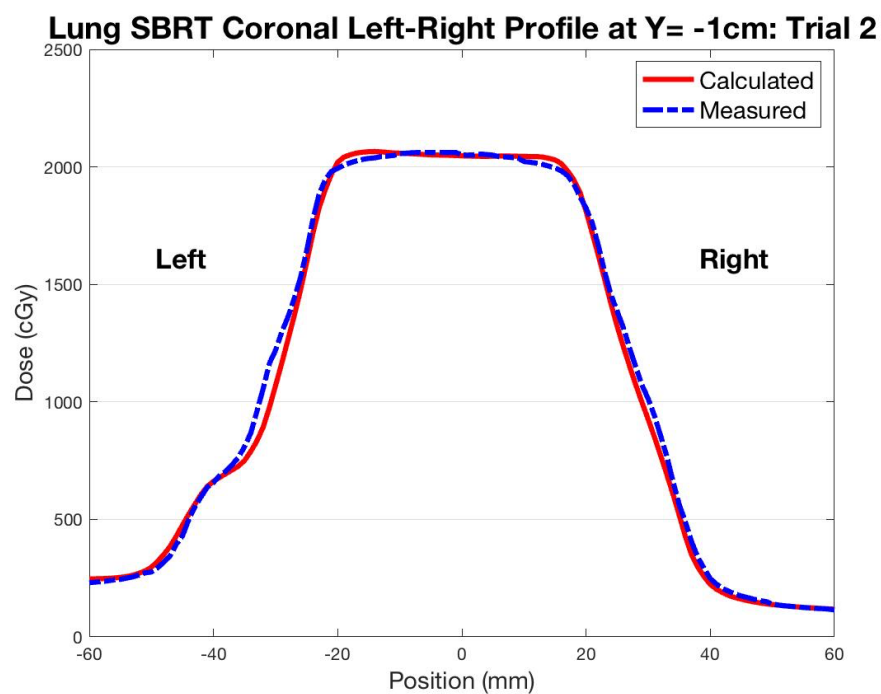
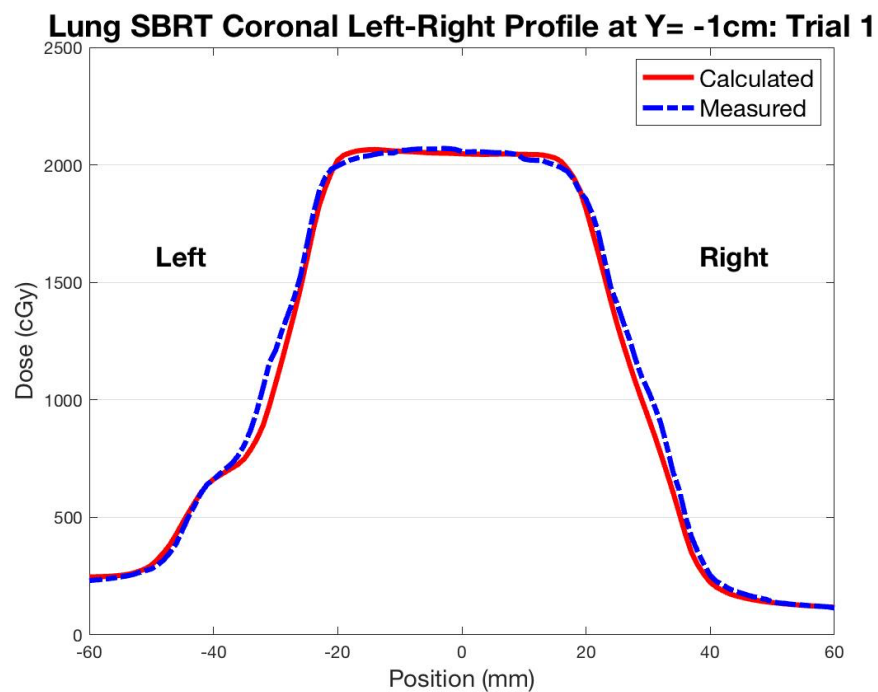
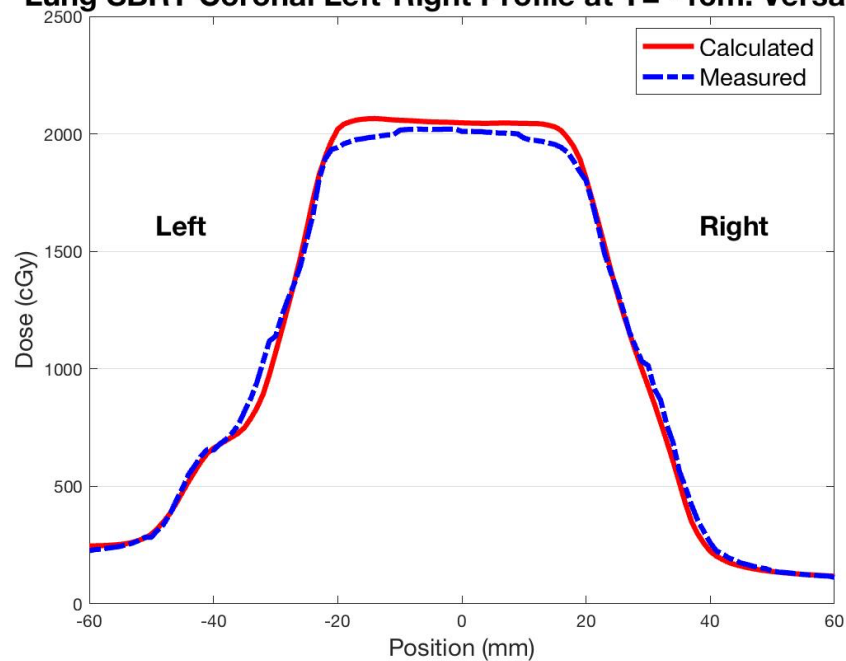


Figure A.9. Coronal left-right profile plots of Trials 1 and 2 taken through Y = -1 cm of the lung SBRT treatment plan delivered on the Elekta Infinity with Agility head at the MBPCC Baton Rouge facility.

**Lung SBRT Coronal Left-Right Profile at Y= -1cm: Versa HD**



**Lung SBRT Coronal Left-Right Profile at Y= -1cm: Infinity 2**

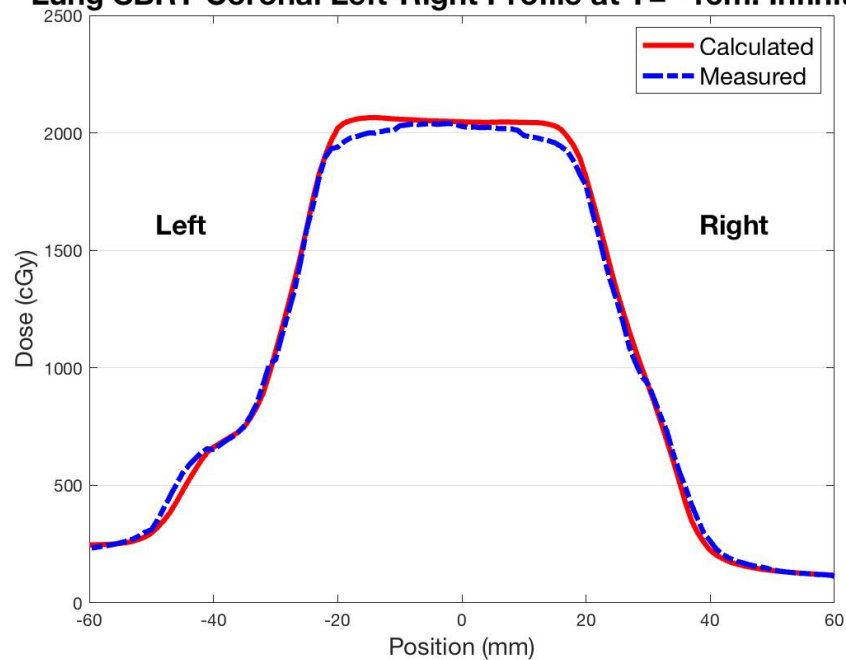
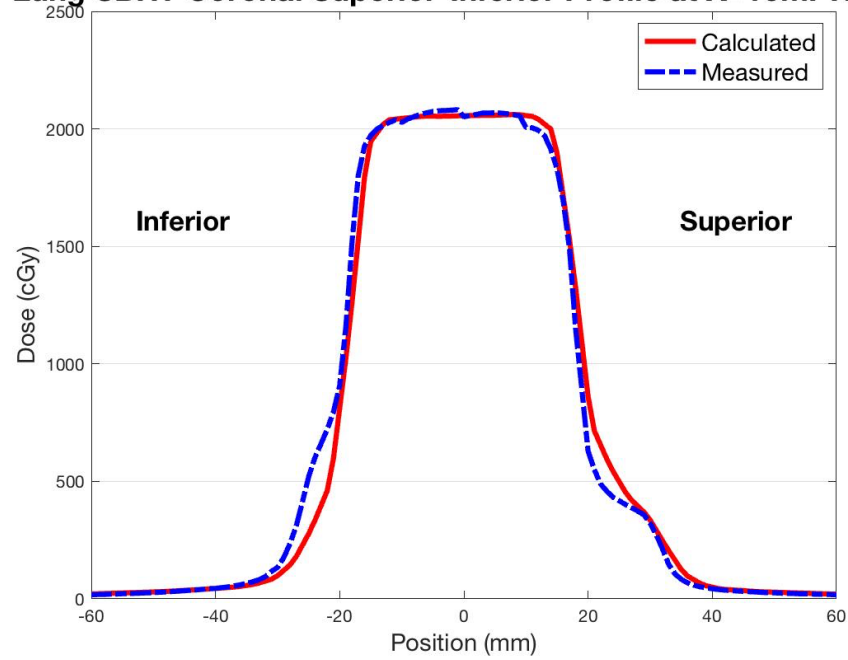


Figure A.10. Coronal left-right profile plots through Y = -1 cm of the lung SBRT treatment plan delivered on the Elekta Versa HD at the MBPCC Baton Rouge facility and the Elekta Infinity with Agility head located at the MBPCC Gonzales facility, respectively.

**Lung SBRT Coronal Superior-Inferior Profile at X=1cm: Trial 1**



**Lung SBRT Coronal Superior-Inferior Profile at X=1cm: Trial 2**

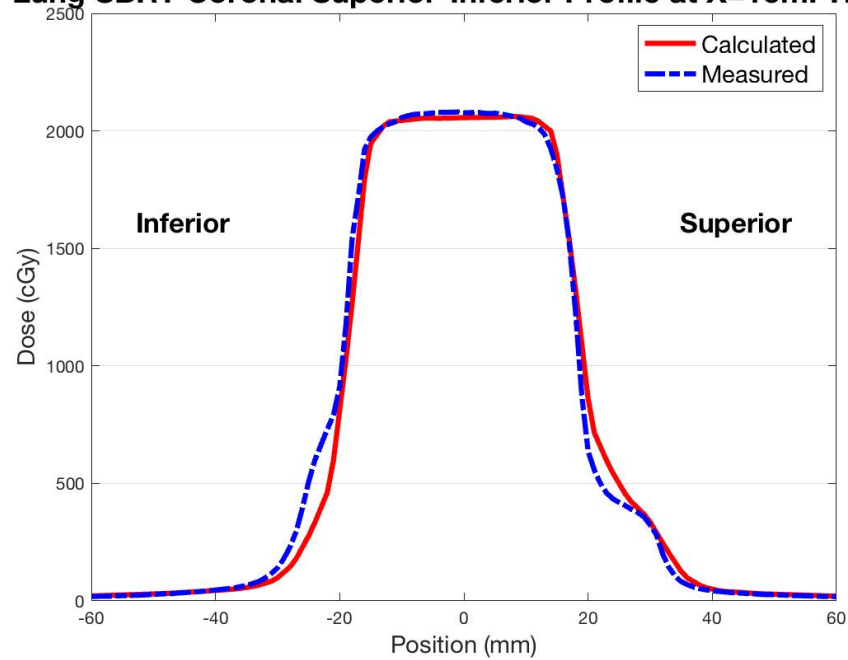


Figure A.11. Coronal superior-inferior profile plots of Trials 1 and 2 taken through X = 1 cm of the lung SBRT treatment plan delivered on the Elekta Infinity with Agility head at the MBPCC Baton Rouge facility.

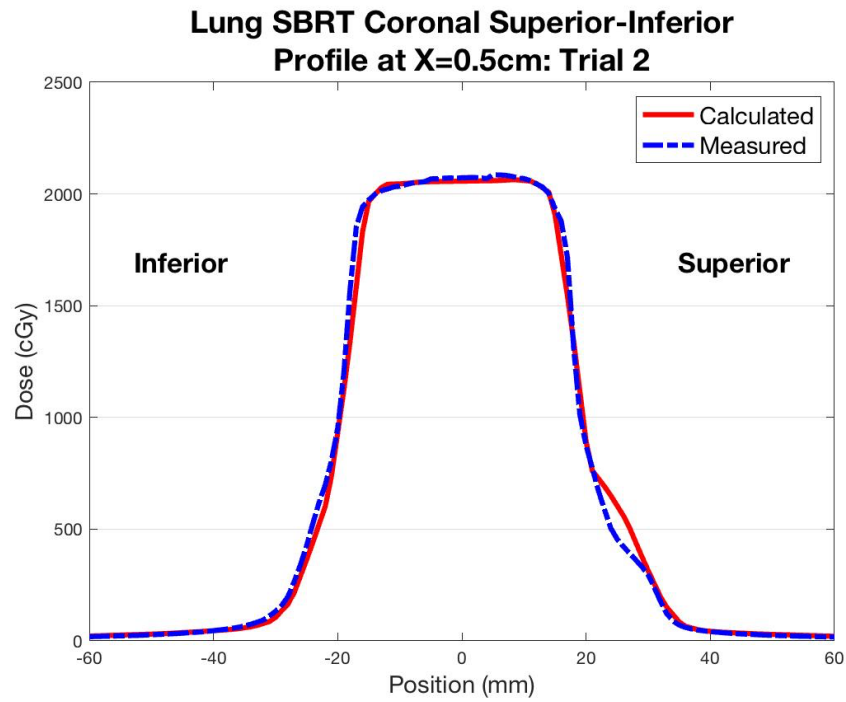
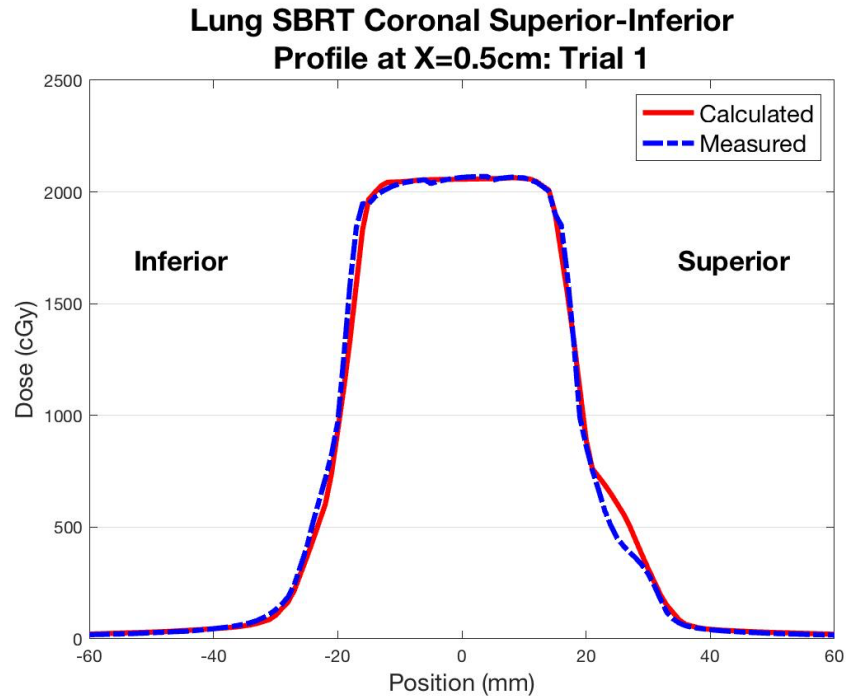
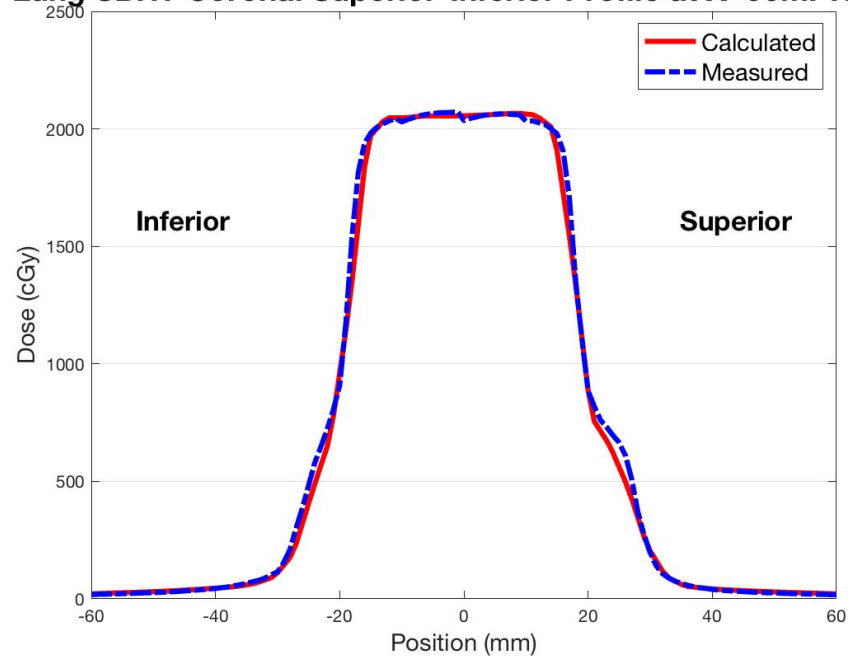


Figure A.12. Coronal superior-inferior profile plots of Trials 1 and 2 taken through X = 0.5 cm of the lung SBRT treatment plan delivered on the Elekta Infinity with Agility head at the MBPCC Baton Rouge facility.



**Lung SBRT Coronal Superior-Inferior Profile at X=0cm: Trial 1**



**Lung SBRT Coronal Superior-Inferior Profile at X=0cm: Trial 2**

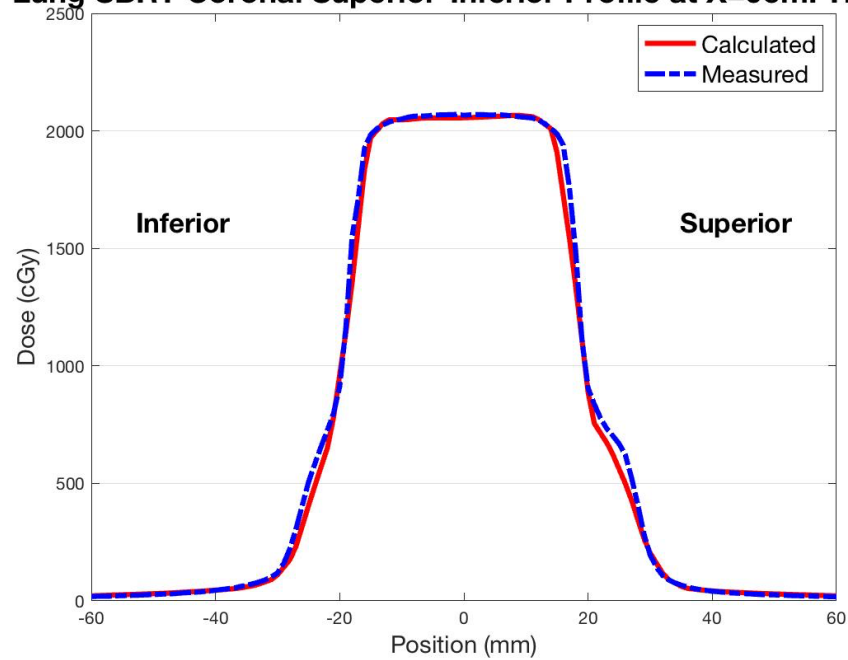


Figure A.13. Coronal superior-inferior profile plots of Trials 1 and 2 taken through X = 0 cm of the lung SBRT treatment plan delivered on the Elekta Infinity with Agility head at the MBPCC Baton Rouge facility.

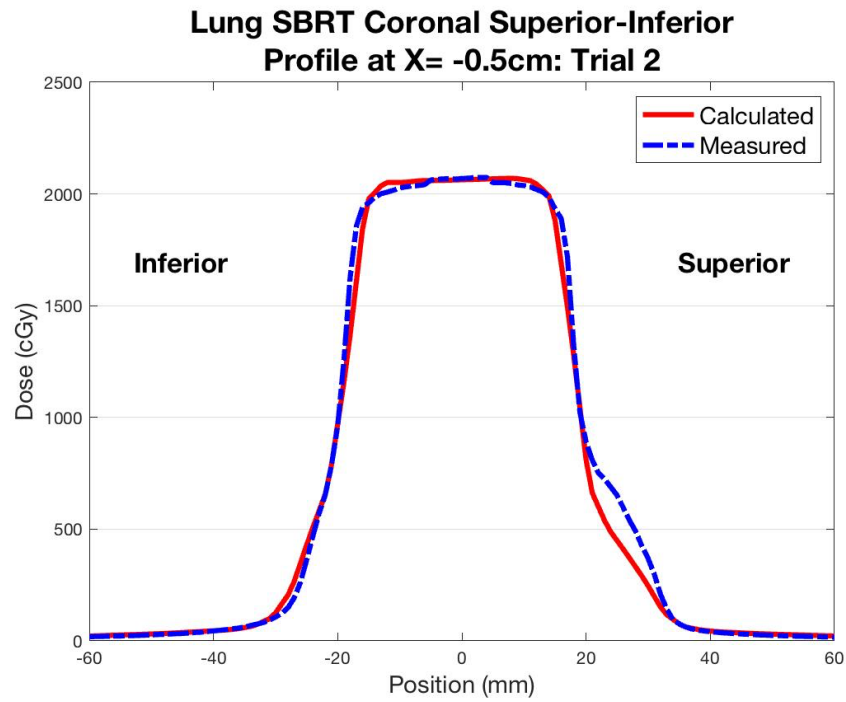
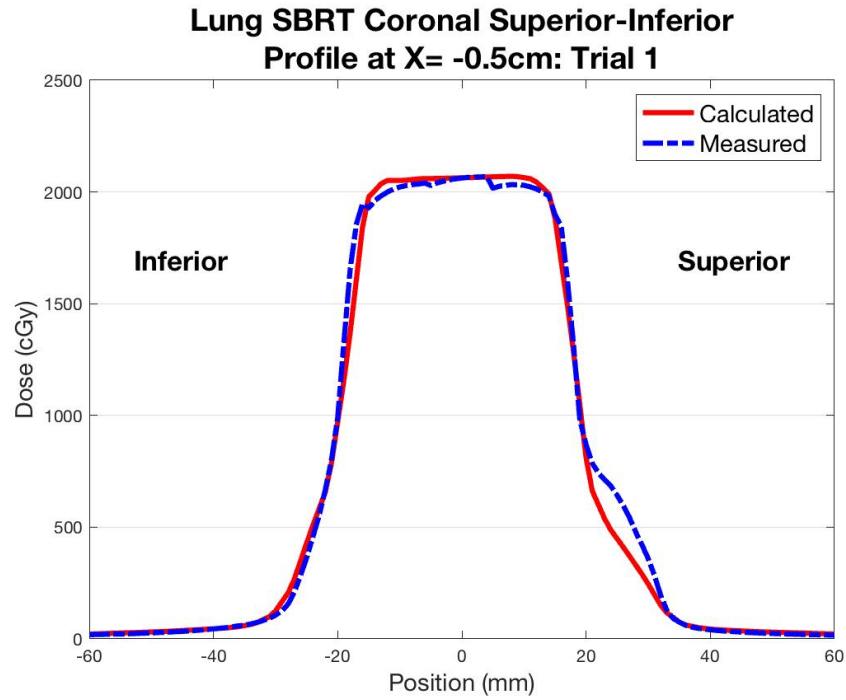
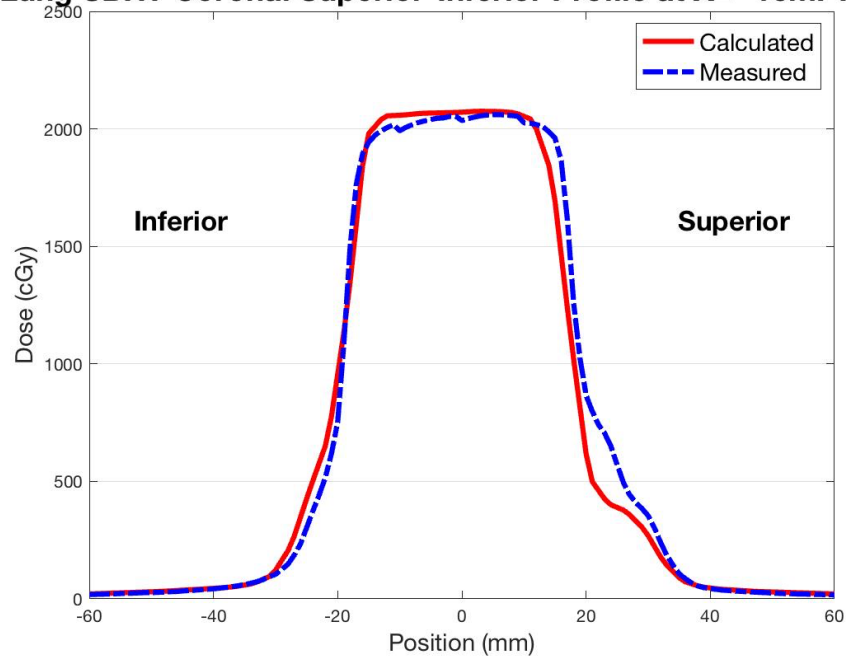


Figure A.14. Coronal superior-inferior profile plots of Trials 1 and 2 taken through X = -0.5 cm of the lung SBRT treatment plan delivered on the Elekta Infinity with Agility head at the MBPCC Baton Rouge facility.

**Lung SBRT Coronal Superior-Inferior Profile at X= -1cm: Trial 1**



**Lung SBRT Coronal Superior-Inferior Profile at X= -1cm: Trial 2**

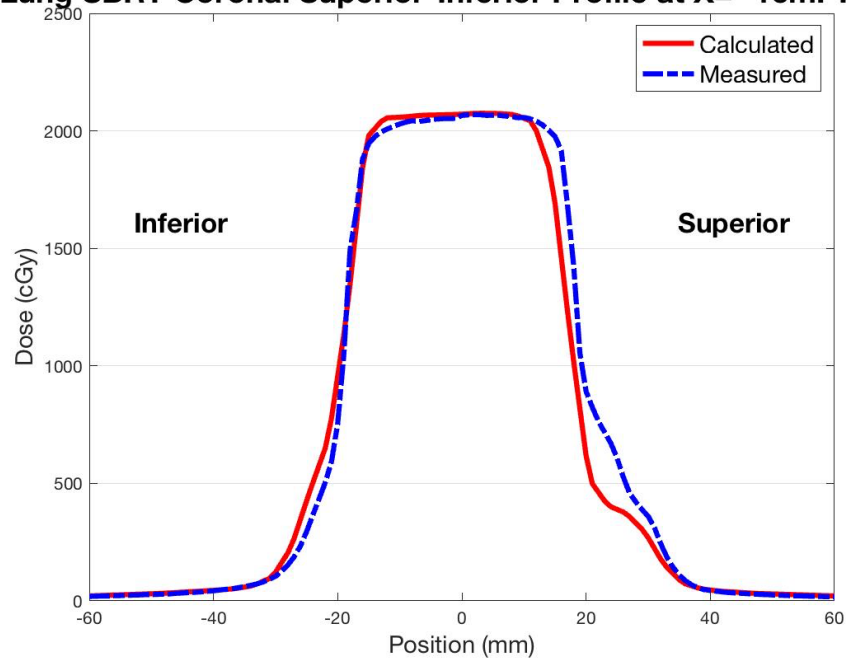


Figure A.15. Coronal superior-inferior profile plots of Trials 1 and 2 taken through X = -1 cm of the lung SBRT treatment plan delivered on the Elekta Infinity with Agility head at the MBPCC Baton Rouge facility.

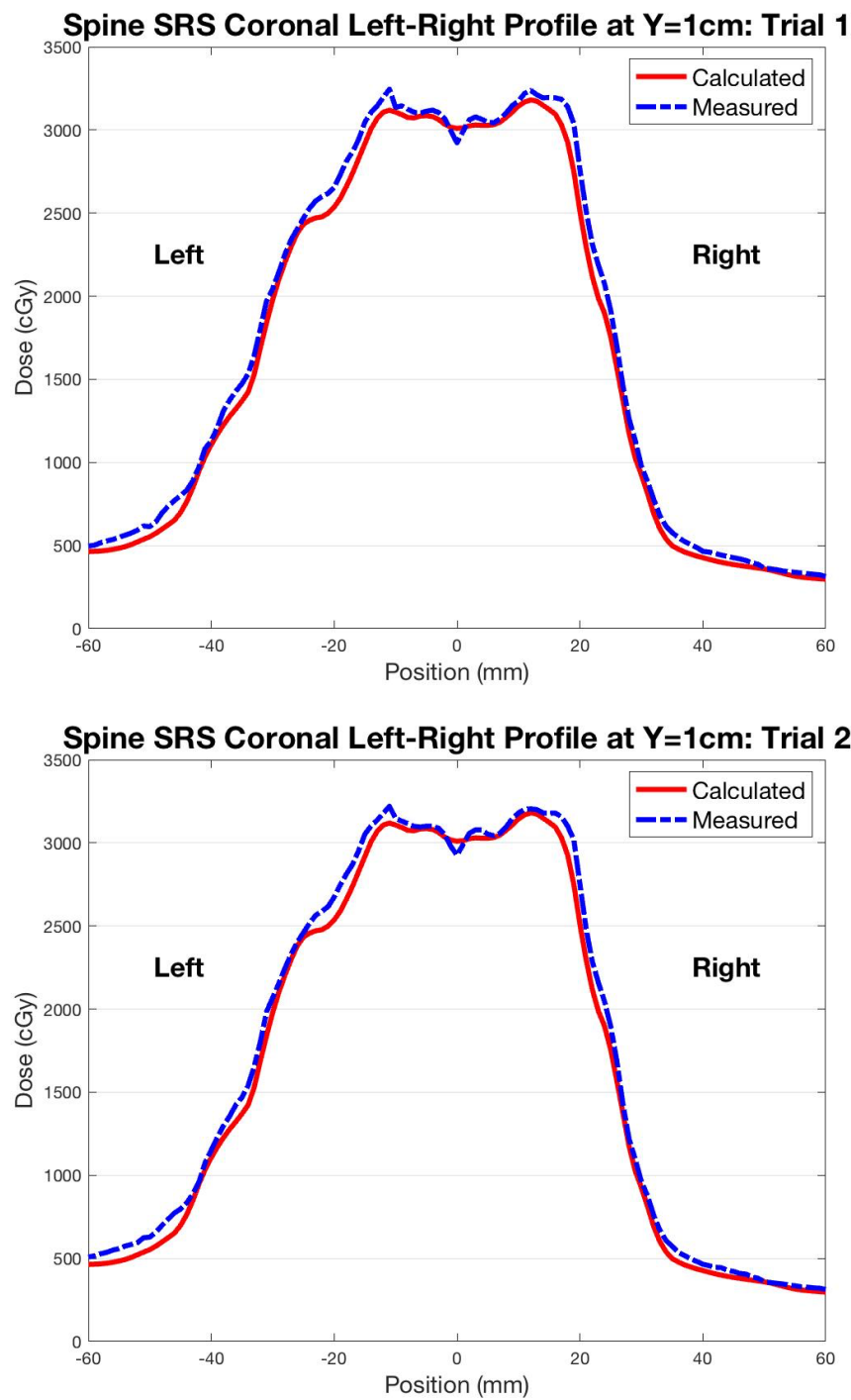


Figure A.16. Coronal left-right profile plots of Trials 1 and 2 taken through Y = 1 cm of the spine SRS treatment plan delivered on the Elekta Infinity with Agility head at the MBPCC Baton Rouge facility.

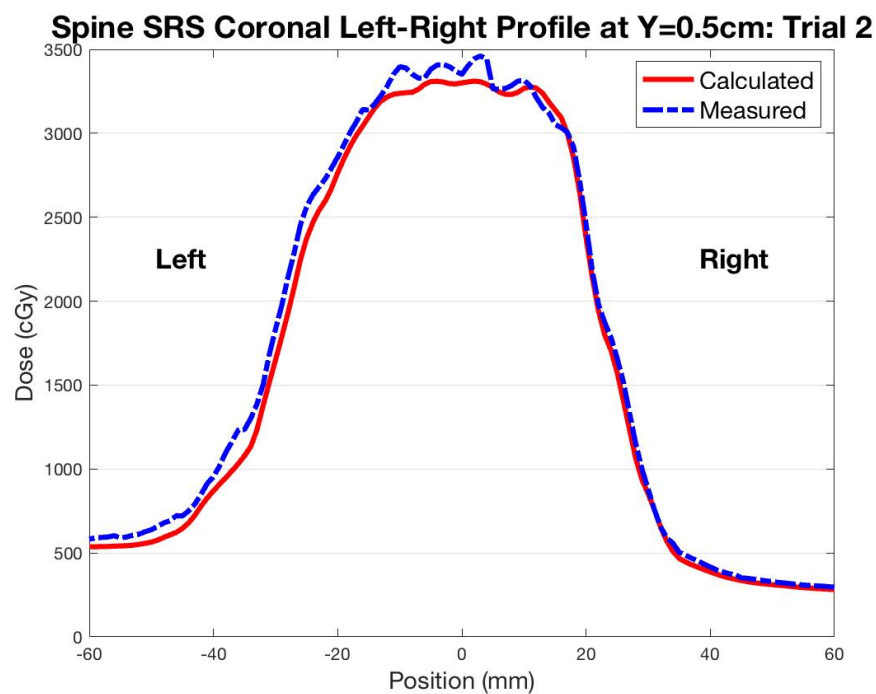
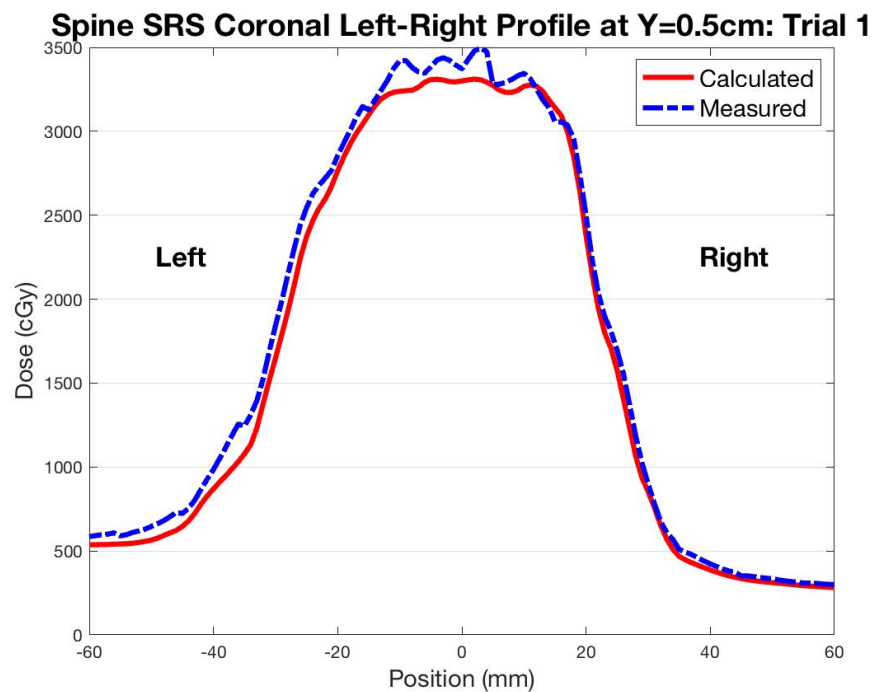


Figure A.17. Coronal left-right profile plots of Trials 1 and 2 taken through Y = 0.5 cm of the spine SRS treatment plan delivered on the Elekta Infinity with Agility head at the MBPCC Baton Rouge facility.

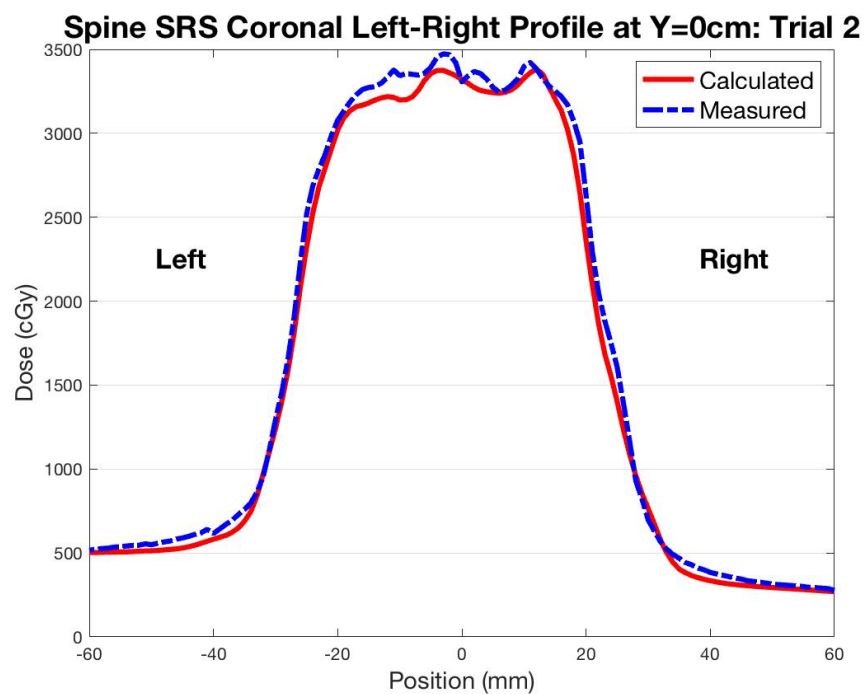
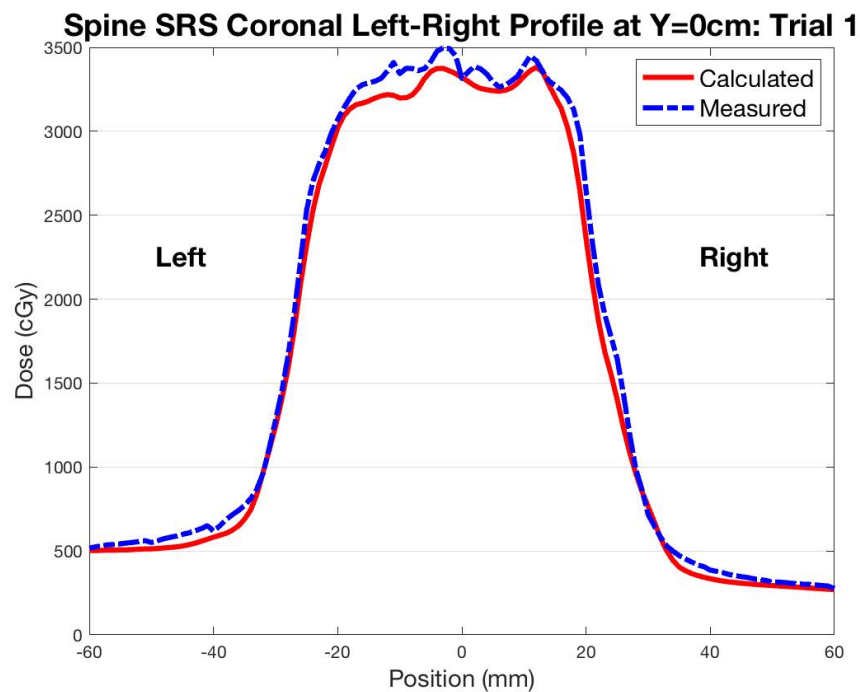


Figure A.18. Coronal left-right profile plots of Trials 1 and 2 taken through Y = 0 cm of the spine SRS treatment plan delivered on the Elekta Infinity with Agility head at the MBPCC Baton Rouge facility.

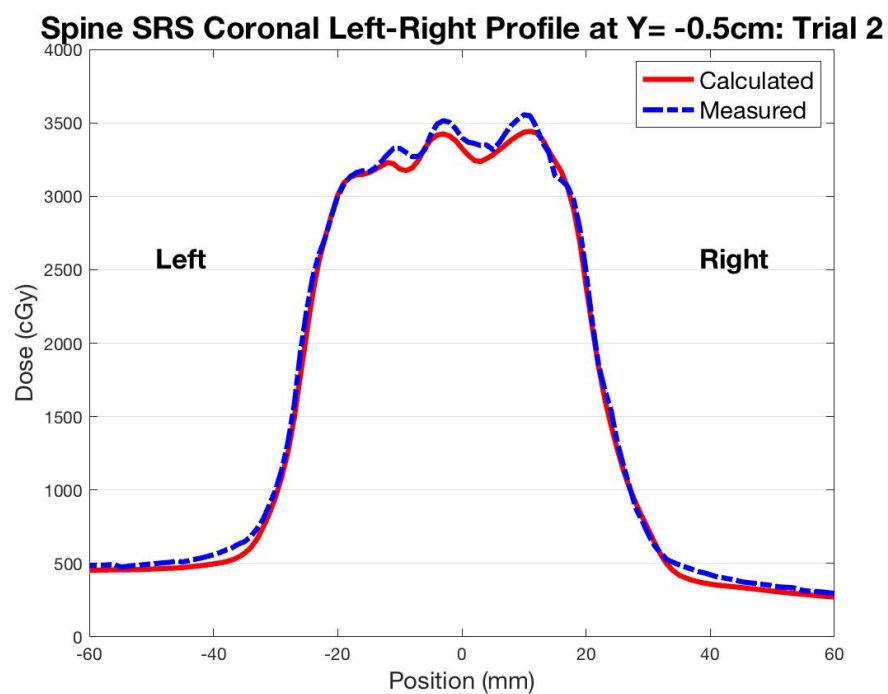
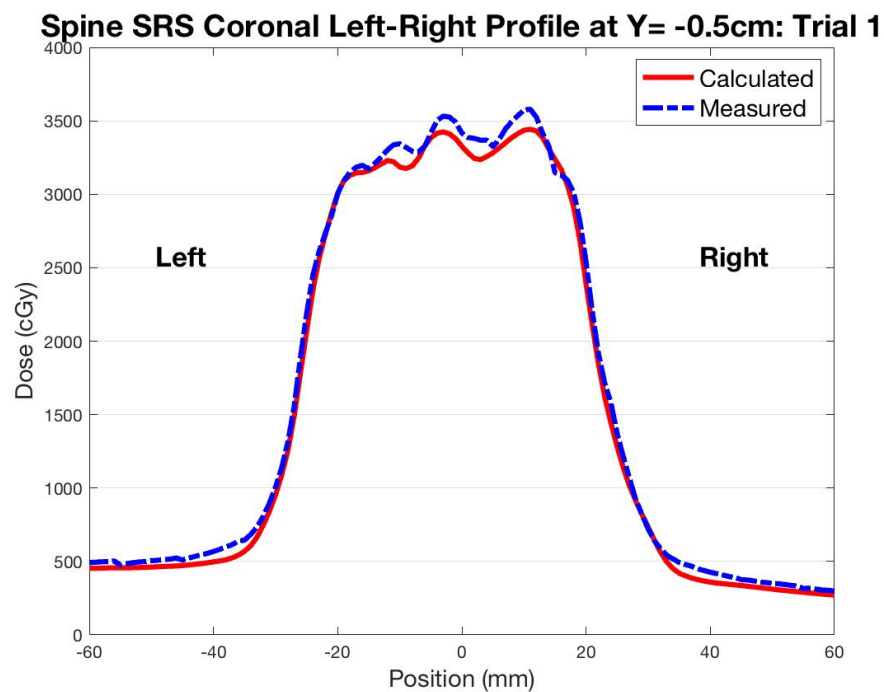


Figure A.19. Coronal left-right profile plots of Trials 1 and 2 taken through Y = -0.5 cm of the spine SRS treatment plan delivered on the Elekta Infinity with Agility head at the MBPCC Baton Rouge facility.

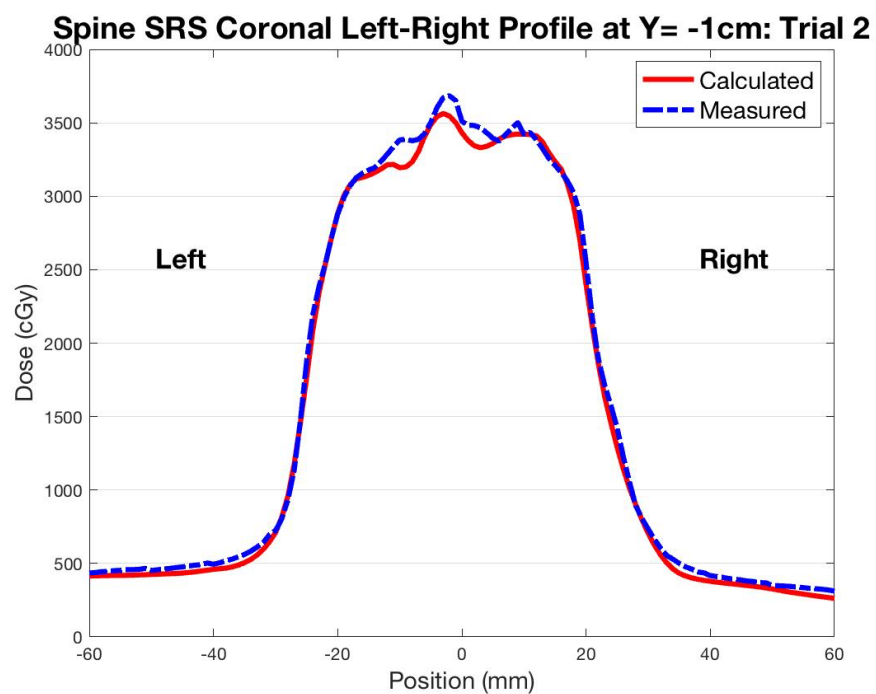
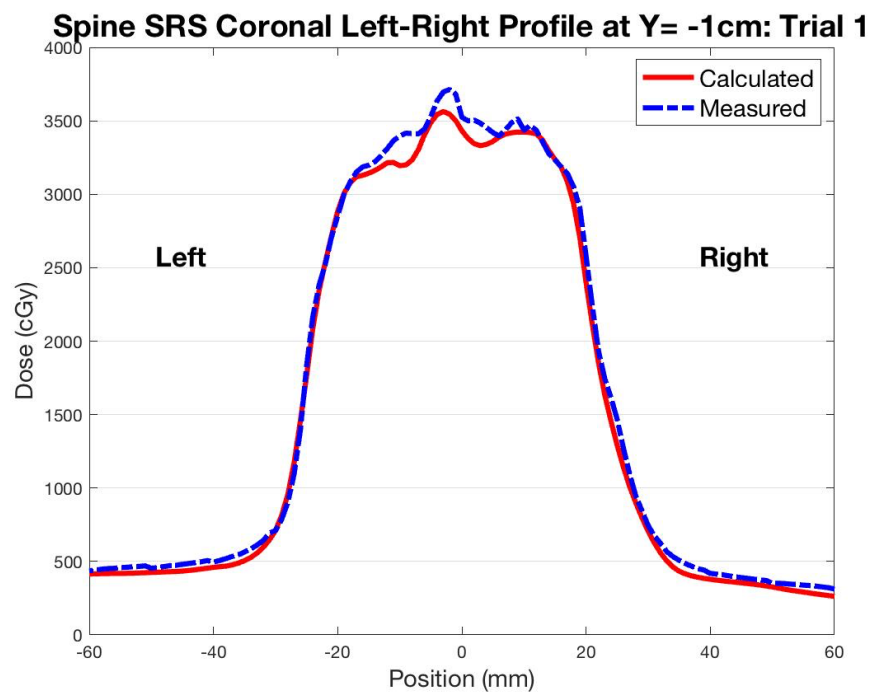
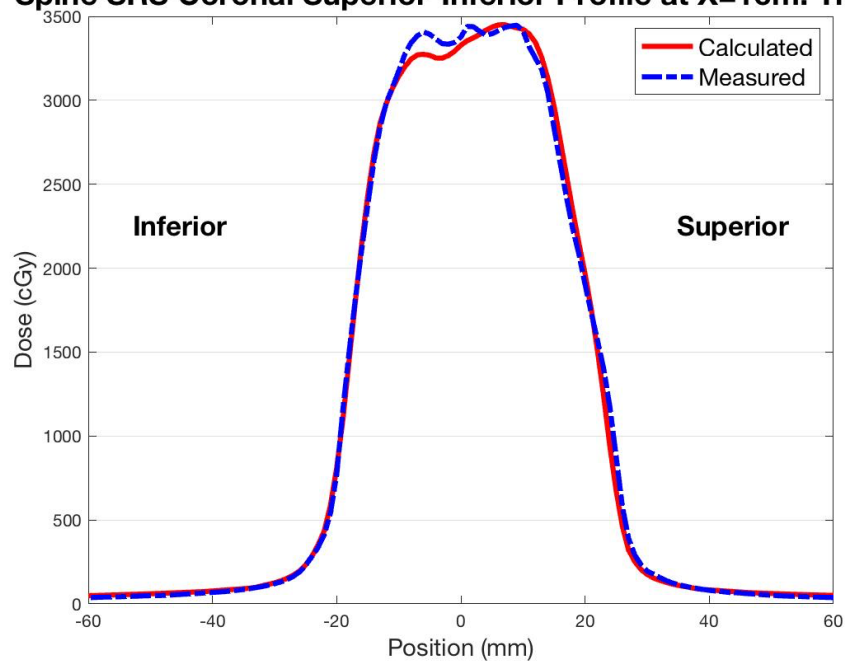


Figure A.20. Coronal left-right profile plots of Trials 1 and 2 taken through Y = -1 cm of the spine SRS treatment plan delivered on the Elekta Infinity with Agility head at the MBPCC Baton Rouge facility.



**Spine SRS Coronal Superior-Inferior Profile at X=1cm: Trial 1**



**Spine SRS Coronal Superior-Inferior Profile at X=1cm: Trial 2**

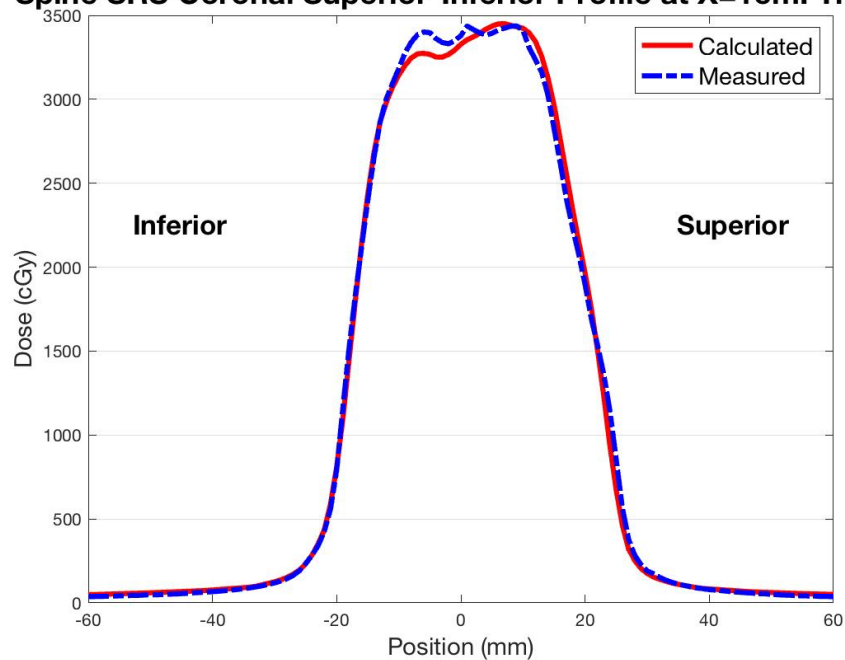
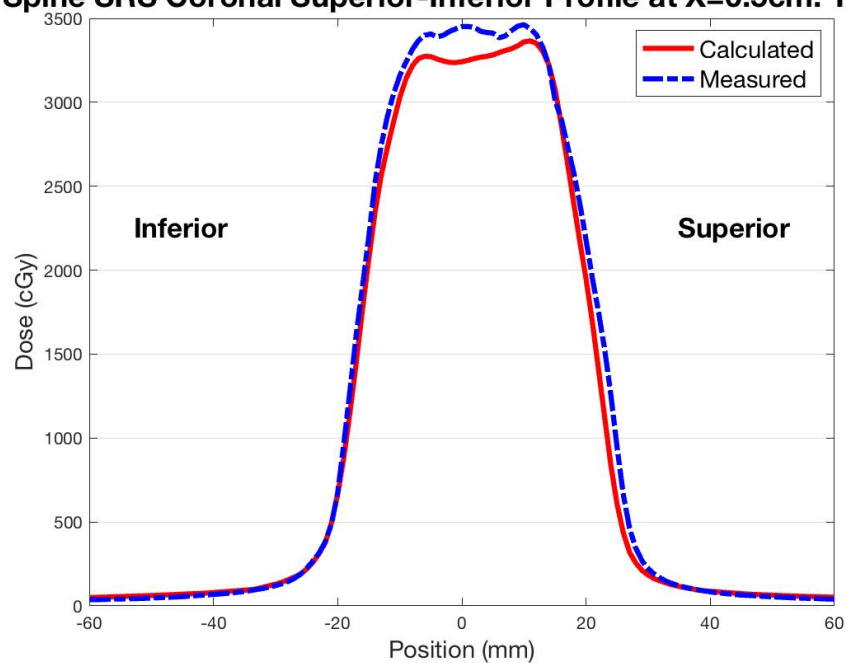


Figure A.21. Coronal superior-inferior profile plots of Trials 1 and 2 taken through X = 1 cm of the spine SRS treatment plan delivered on the Elekta Infinity with Agility head at the MBPCC Baton Rouge facility.

**Spine SRS Coronal Superior-Inferior Profile at X=0.5cm: Trial 1**



**Spine SRS Coronal Superior-Inferior Profile at X=0.5cm: Trial 2**

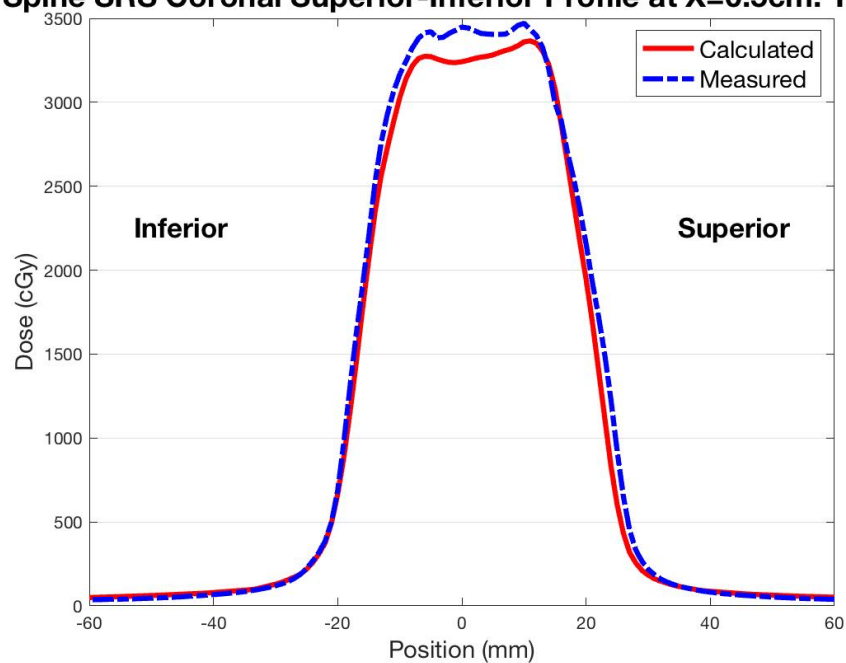
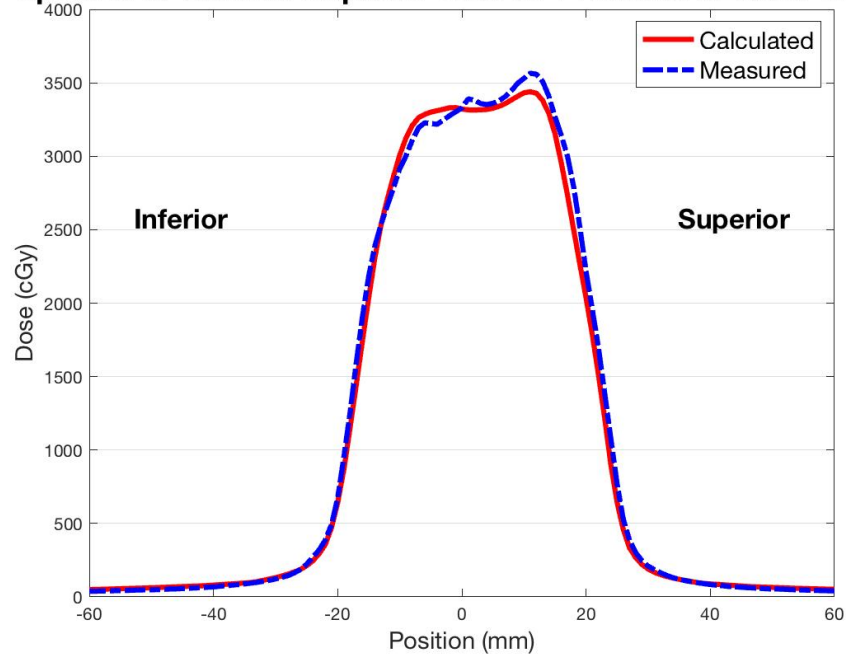


Figure A.22. Coronal superior-inferior profile plots of Trials 1 and 2 taken through X = 0.5 cm of the spine SRS treatment plan delivered on the Elekta Infinity with Agility head at the MBPCC Baton Rouge facility.

**Spine SRS Coronal Superior-Inferior Profile at X=0cm: Trial 1**



**Spine SRS Coronal Superior-Inferior Profile at X=0cm: Trial 2**

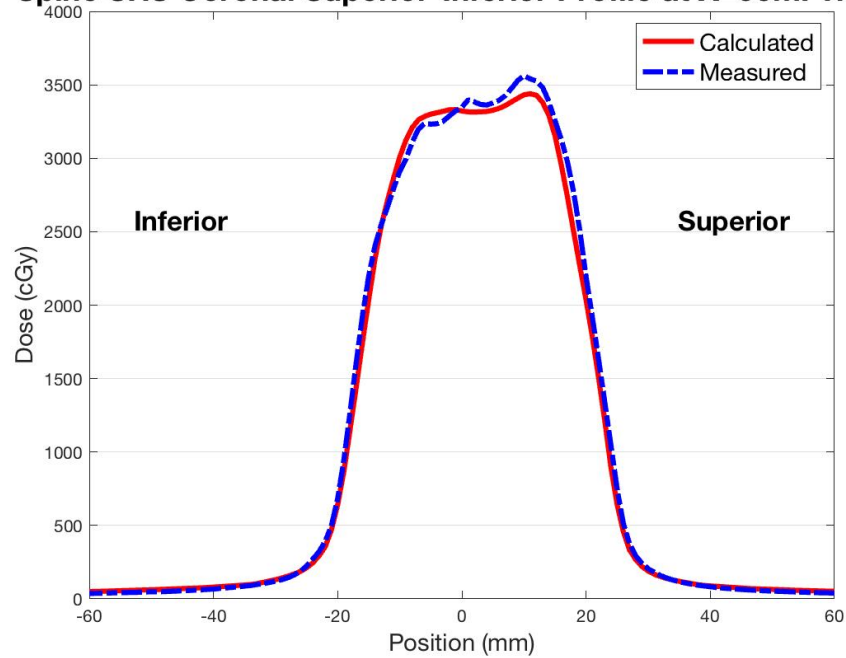
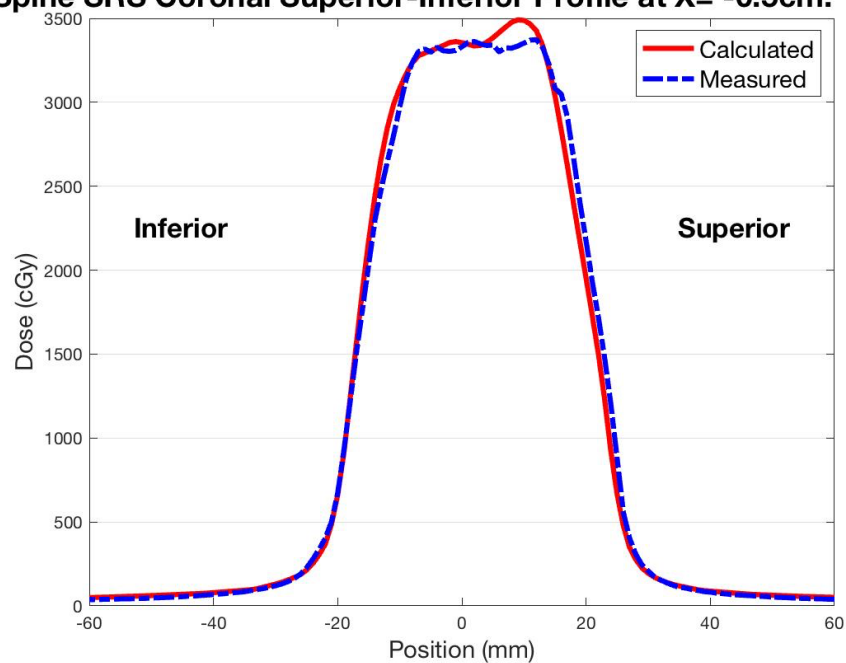


Figure A.23. Coronal superior-inferior profile plots of Trials 1 and 2 taken through X = 0 cm of the spine SRS treatment plan delivered on the Elekta Infinity with Agility head at the MBPCC Baton Rouge facility.

**Spine SRS Coronal Superior-Inferior Profile at X= -0.5cm: Trial 1**



**Spine SRS Coronal Superior-Inferior Profile at X= -0.5cm: Trial 2**

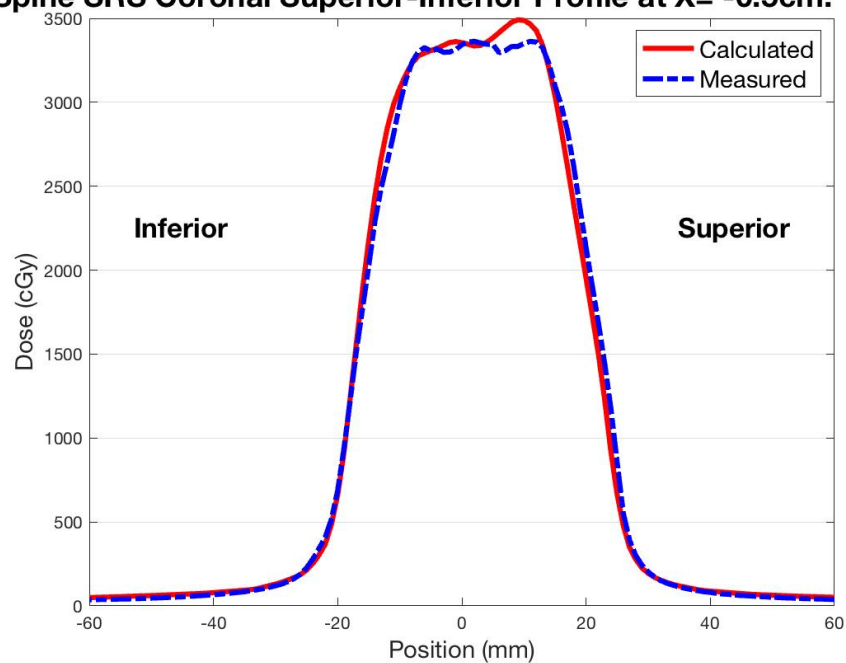
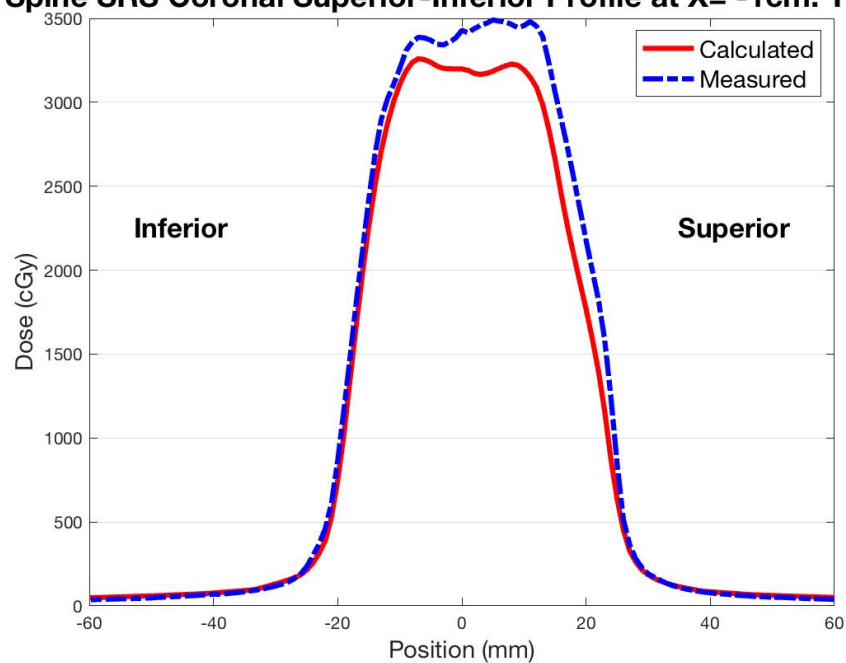


Figure A.24. Coronal superior-inferior profile plots of Trials 1 and 2 taken through X = -0.5 cm of the spine SRS treatment plan delivered on the Elekta Infinity with Agility head at the MBPCC Baton Rouge facility.

**Spine SRS Coronal Superior-Inferior Profile at X= -1cm: Trial 1**



**Spine SRS Coronal Superior-Inferior Profile at X= -1cm: Trial 2**

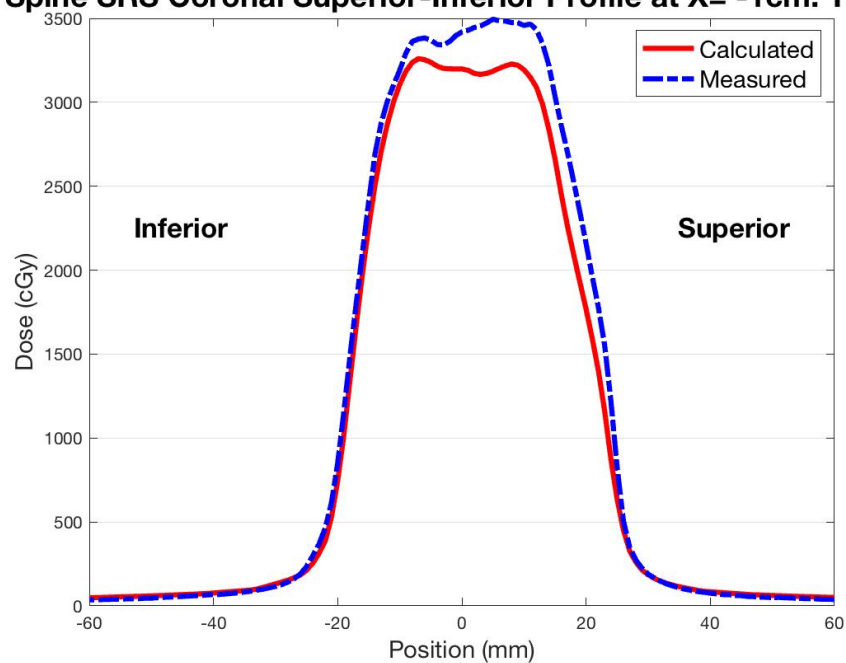


Figure A.25. Coronal superior-inferior profile plots of Trials 1 and 2 taken through X = -1 cm of the spine SRS treatment plan delivered on the Elekta Infinity with Agility head at the MBPCC Baton Rouge facility.

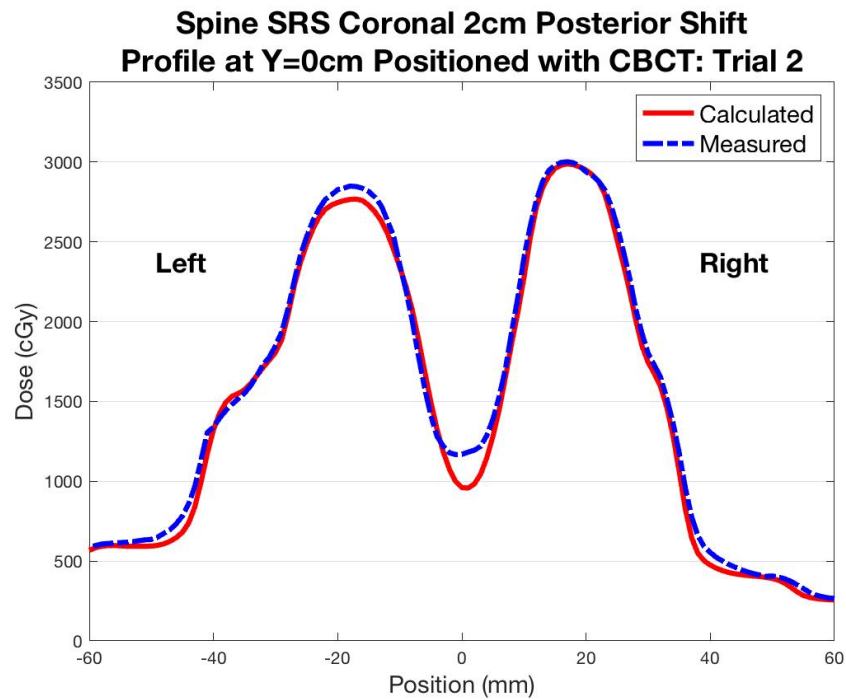
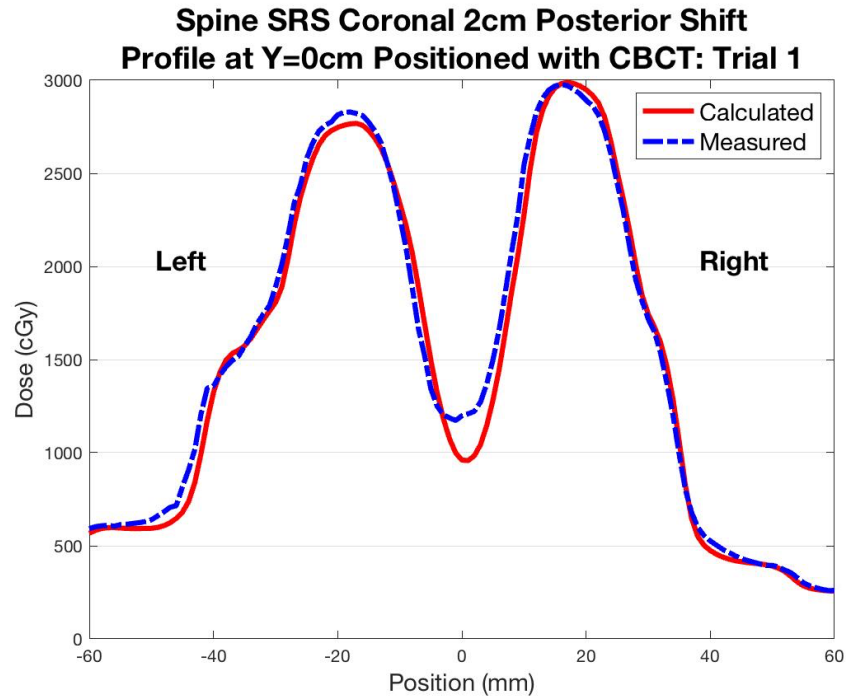


Figure A.27. Coronal left-right profile plots of Trials 1 and 2 taken through Y = 0 cm of the spine SRS treatment plan shifted posteriorly by 2 cm with kV-CBCT positioning and delivered on the Elekta Infinity with Agility head at the MBPCC Baton Rouge facility.

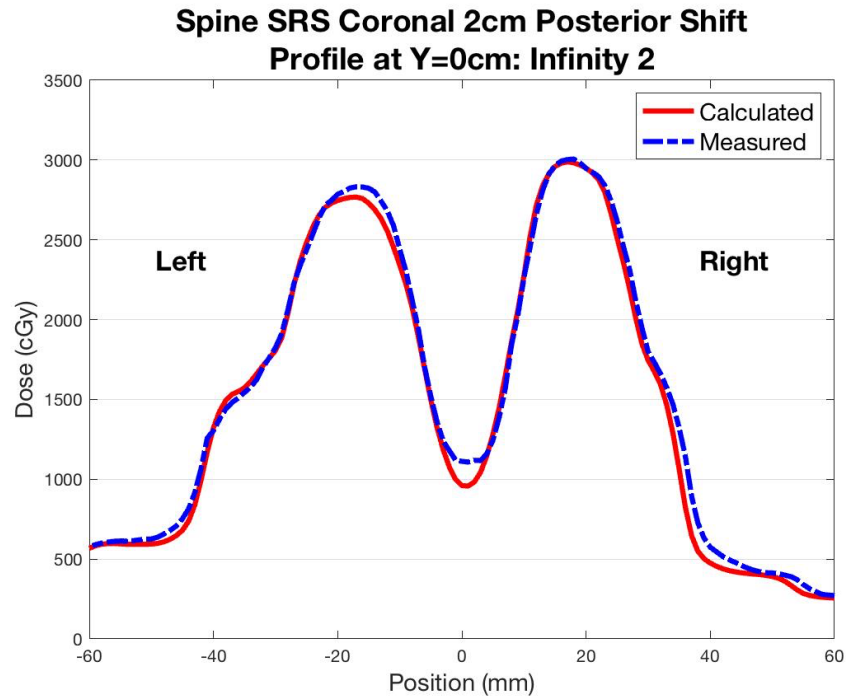
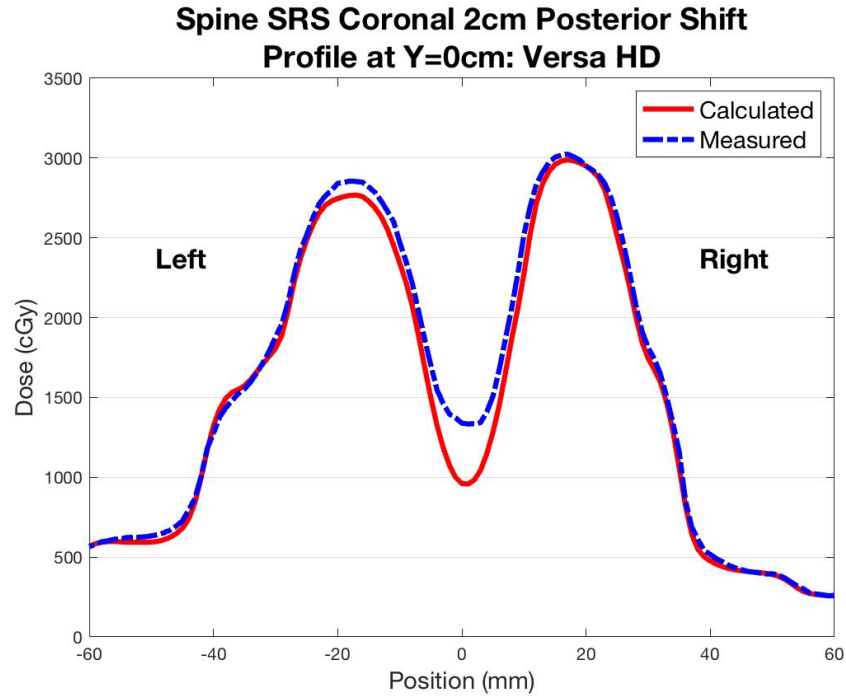


Figure A.28. Coronal left-right profile plots through Y = 0 cm of the spine SRS treatment plan shifted posteriorly by 2 cm delivered on the Elekta Versa HD at the MBPCC Baton Rouge facility and the Elekta Infinity with Agility head located at the MBPCC Gonzales facility, respectively.

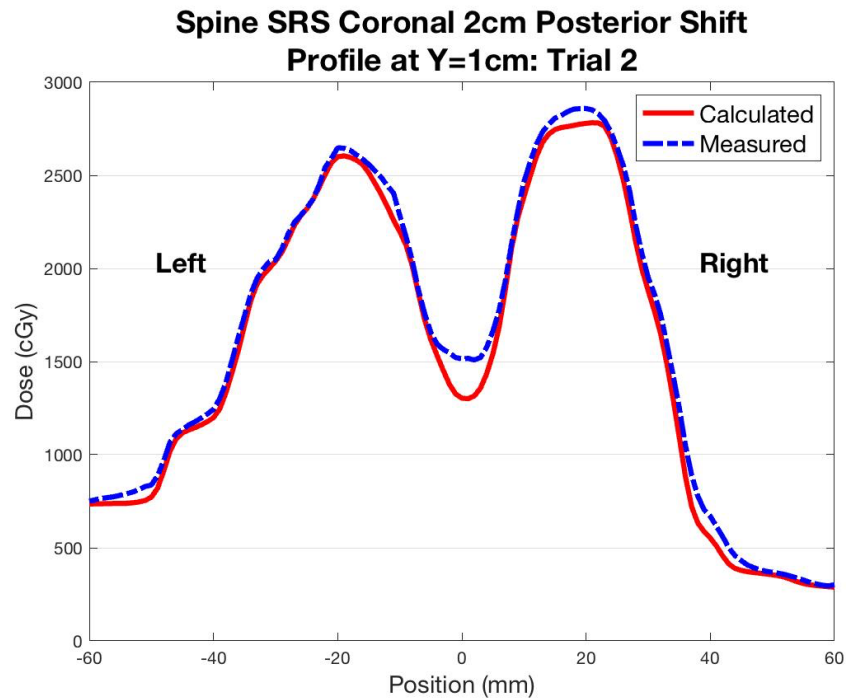
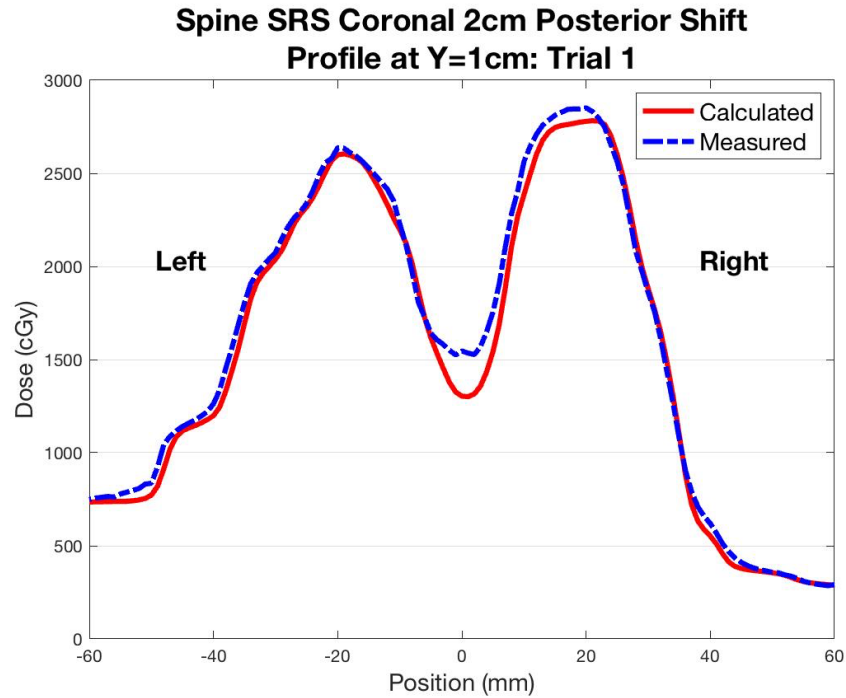


Figure A.29. Coronal left-right profile plots of Trials 1 and 2 taken through Y = 1 cm of the spine SRS treatment plan shifted posteriorly by 2 cm with kV-CBCT positioning and delivered on the Elekta Infinity with Agility head at the MBPCC Baton Rouge facility.



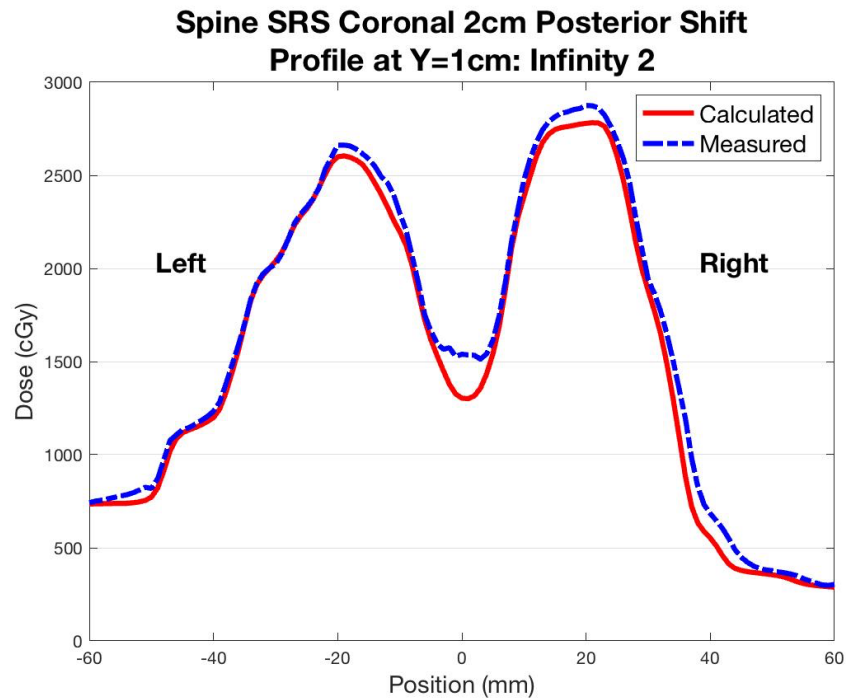
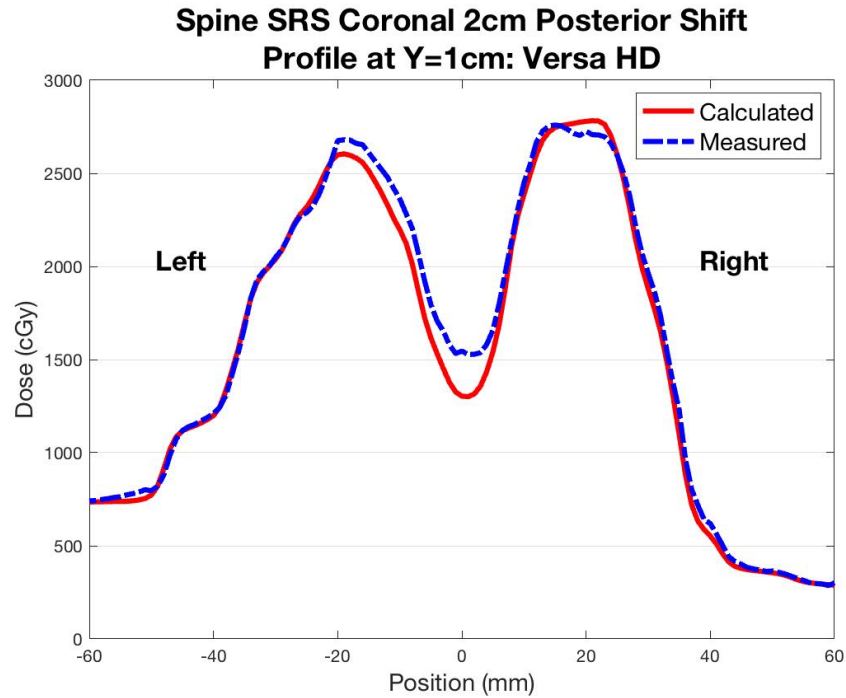


Figure A.30. Coronal left-right profile plots through Y = 1 cm of the spine SRS treatment plan shifted posteriorly by 2 cm delivered on the Elekta Versa HD at the MBPCC Baton Rouge facility and the Elekta Infinity with Agility head located at the MBPCC Gonzales facility, respectively.

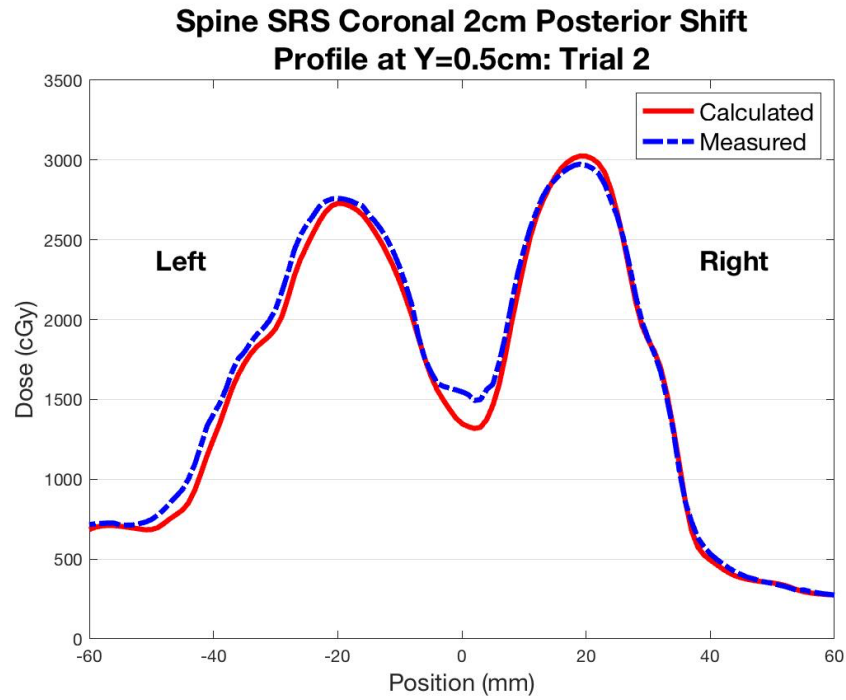
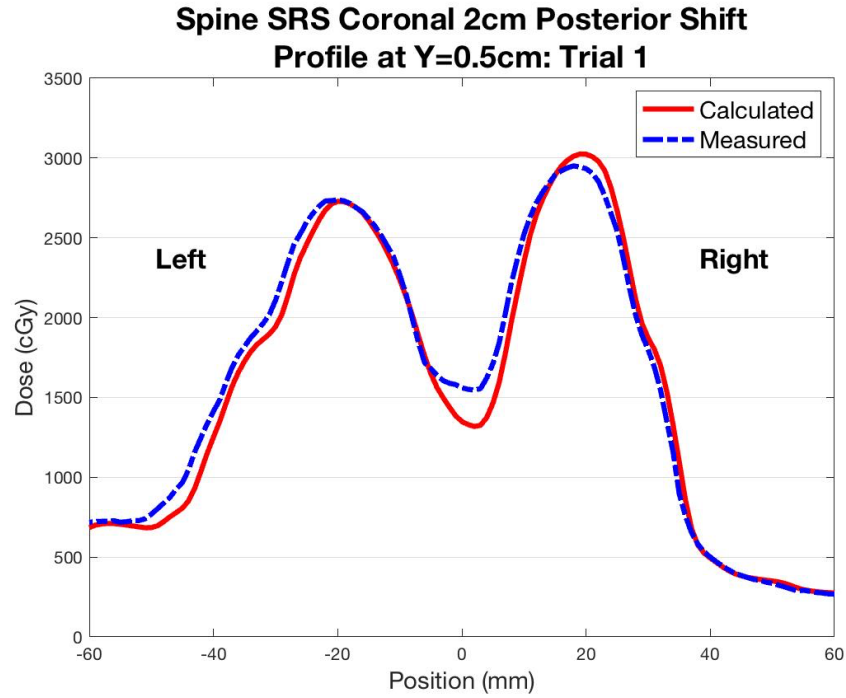


Figure A.31. Coronal left-right profile plots of Trials 1 and 2 taken through Y = 0.5 cm of the spine SRS treatment plan shifted posteriorly by 2 cm with kV-CBCT positioning and delivered on the Elekta Infinity with Agility head at the MBPCC Baton Rouge facility.

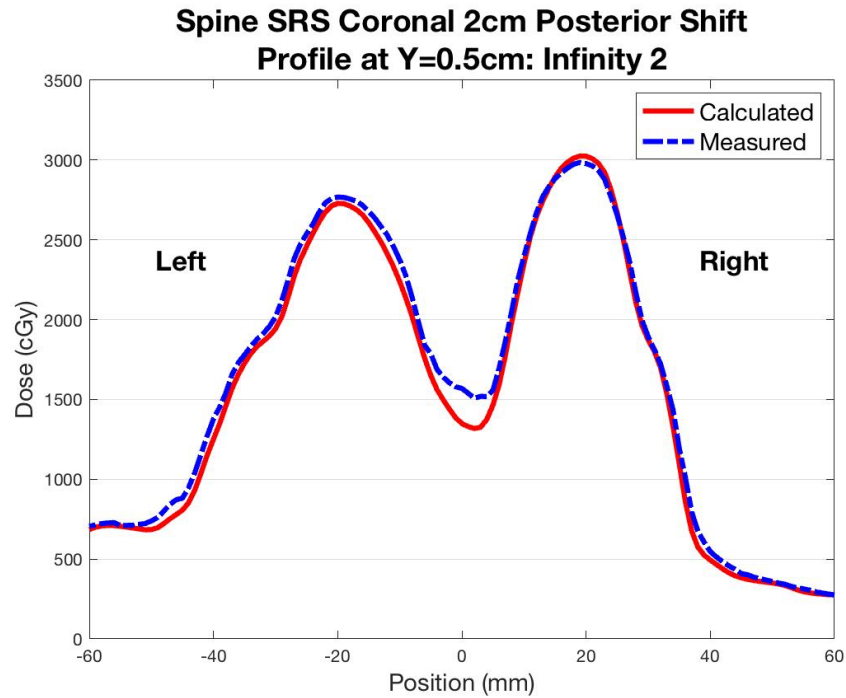
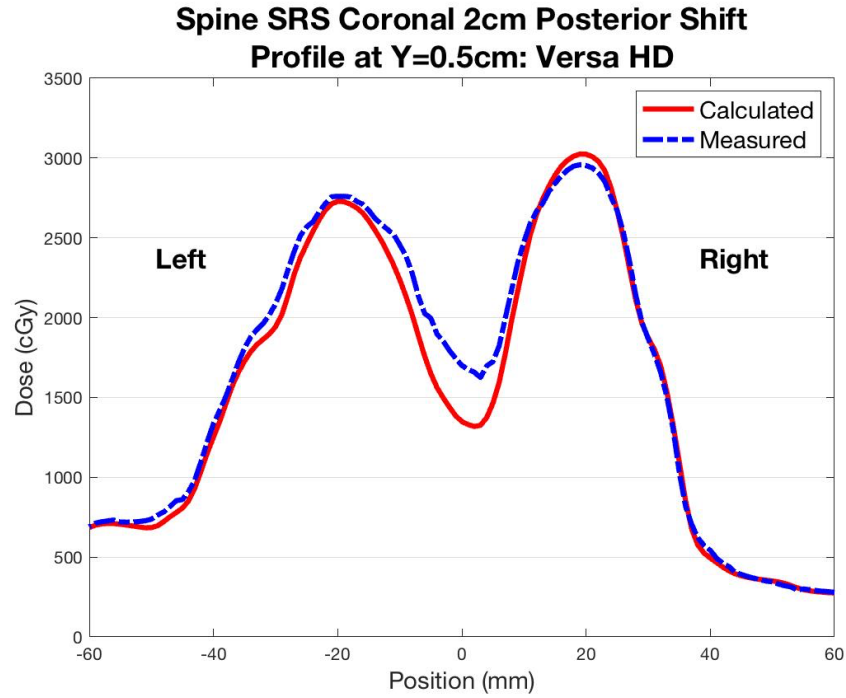


Figure A.32. Coronal left-right profile plots through Y = 0.5 cm of the spine SRS treatment plan shifted posteriorly by 2 cm delivered on the Elekta Versa HD at the MBPCC Baton Rouge facility and the Elekta Infinity with Agility head located at the MBPCC Gonzales facility, respectively.

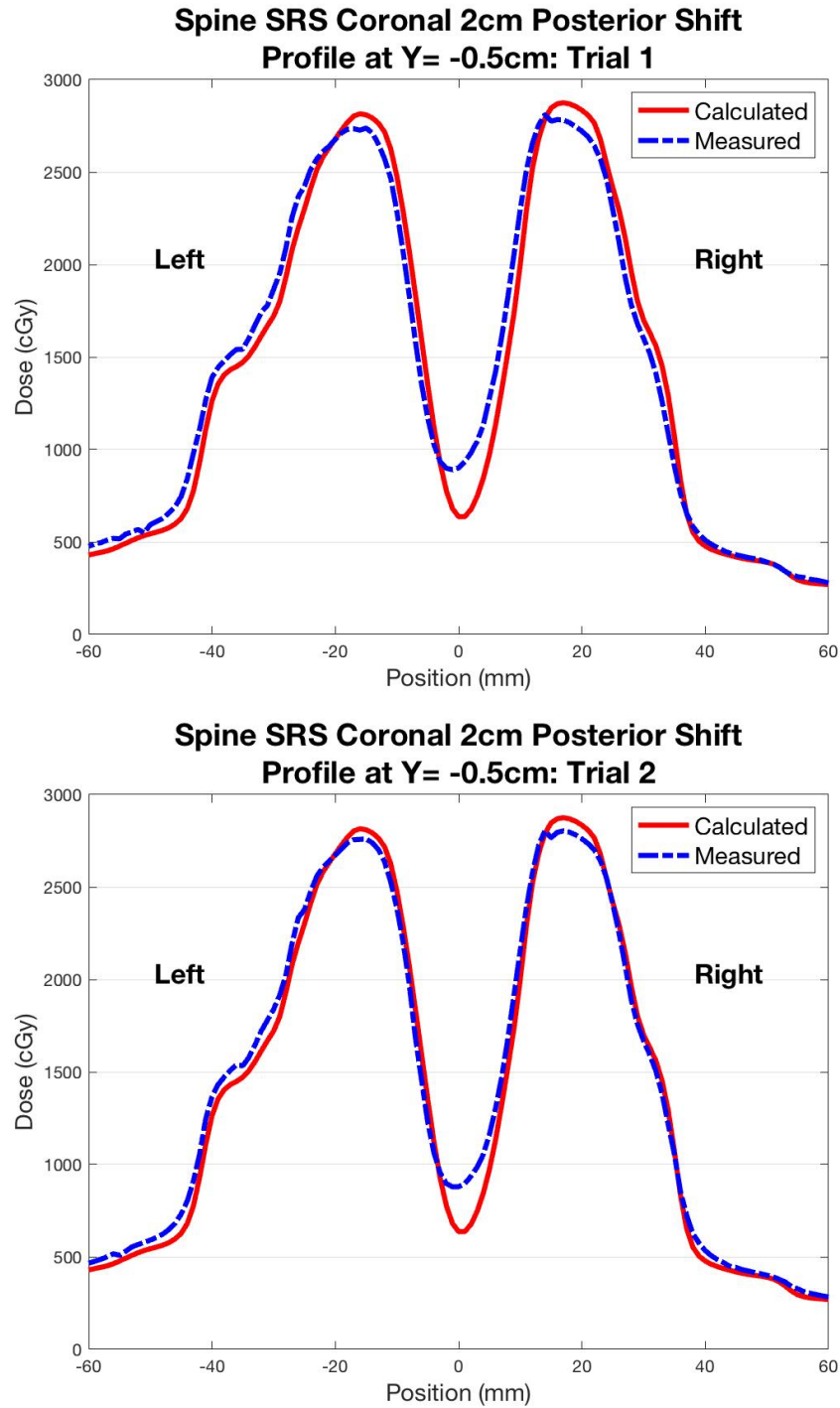


Figure A.33. Coronal left-right profile plots of Trials 1 and 2 taken through Y = -0.5 cm of the spine SRS treatment plan shifted posteriorly by 2 cm with kV-CBCT positioning and delivered on the Elekta Infinity with Agility head at the MBPCC Baton Rouge facility.

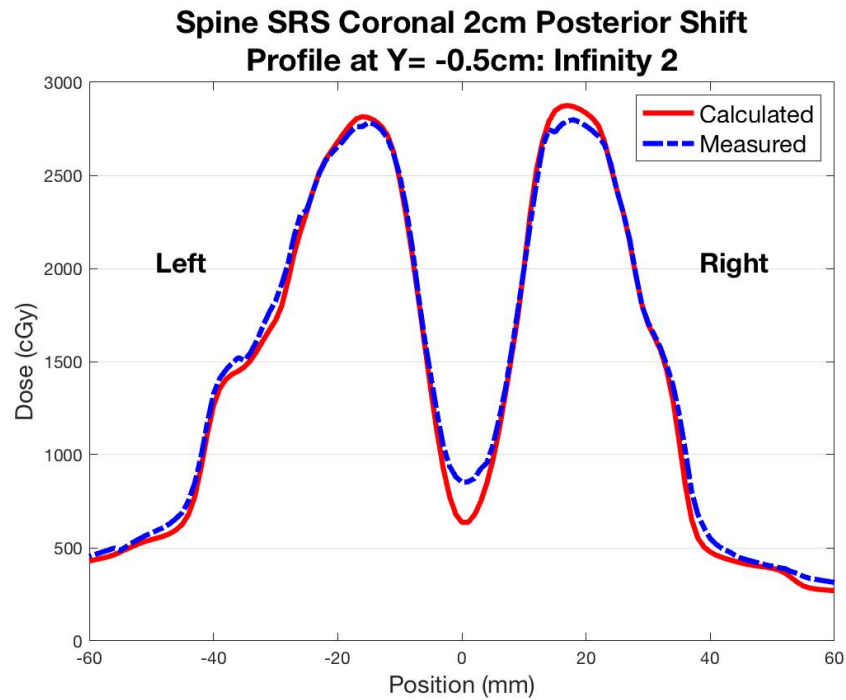
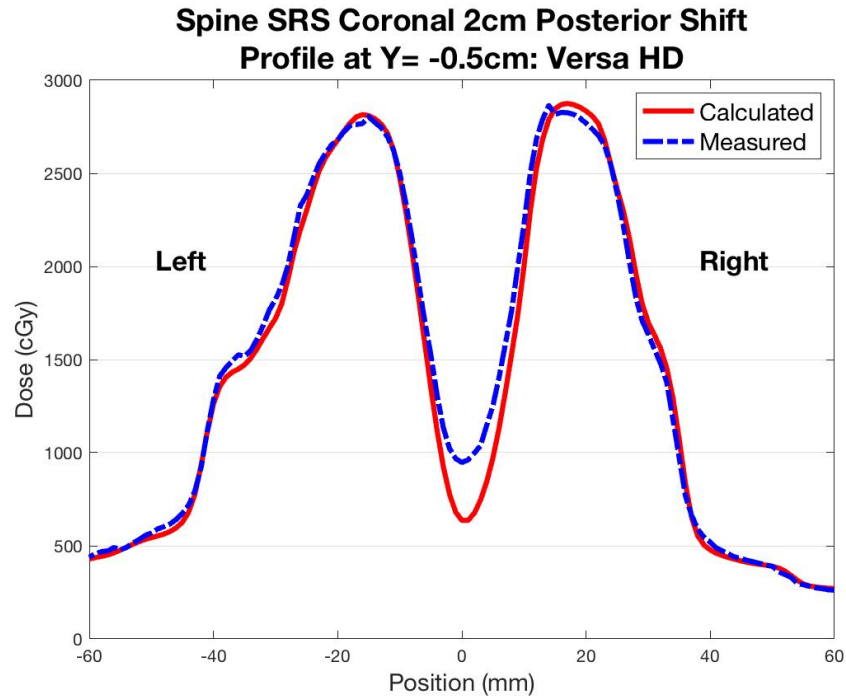


Figure A.34. Coronal left-right profile plots through Y = -0.5 cm of the spine SRS treatment plan shifted posteriorly by 2 cm delivered on the Elekta Versa HD at the MBPCC Baton Rouge facility and the Elekta Infinity with Agility head located at the MBPCC Gonzales facility, respectively.

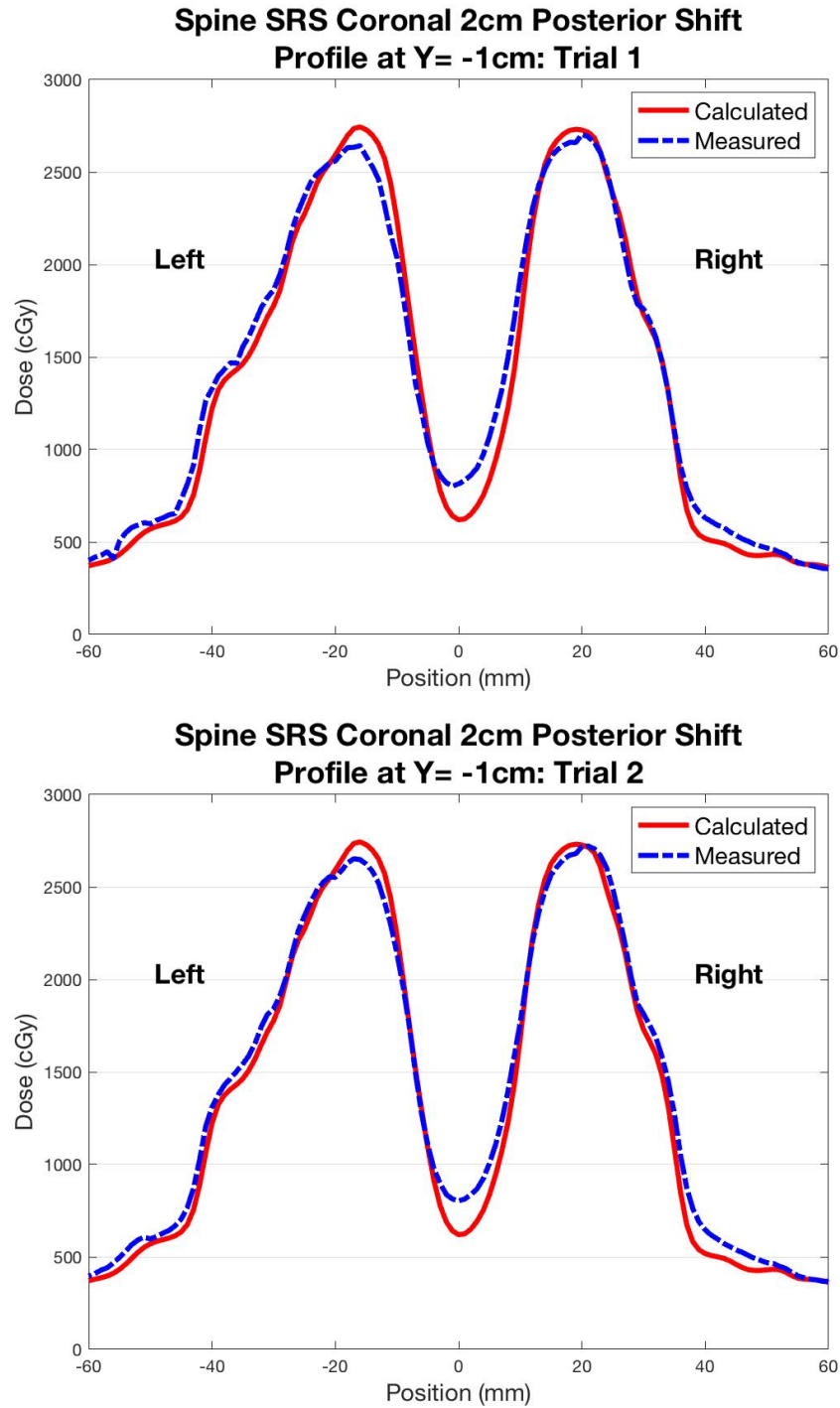


Figure A.35. Coronal left-right profile plots of Trials 1 and 2 taken through Y = -1 cm of the spine SRS treatment plan shifted posteriorly by 2 cm with kV-CBCT positioning and delivered on the Elekta Infinity with Agility head at the MBPCC Baton Rouge facility.

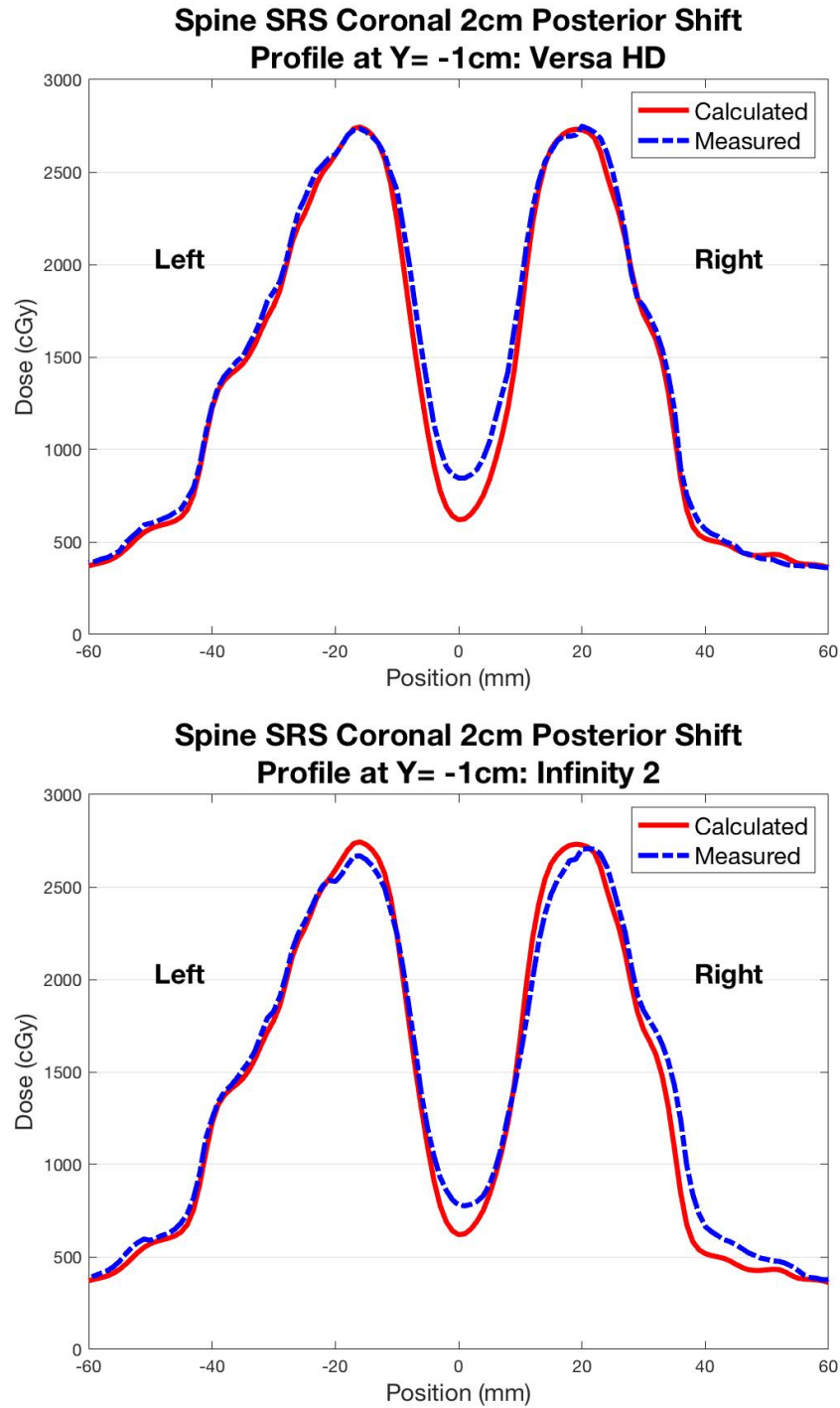


Figure A.36. Coronal left-right profile plots through Y = - 1 cm of the spine SRS treatment plan shifted posteriorly by 2 cm delivered on the Elekta Versa HD at the MBPCC Baton Rouge facility and the Elekta Infinity with Agility head located at the MBPCC Gonzales facility, respectively.

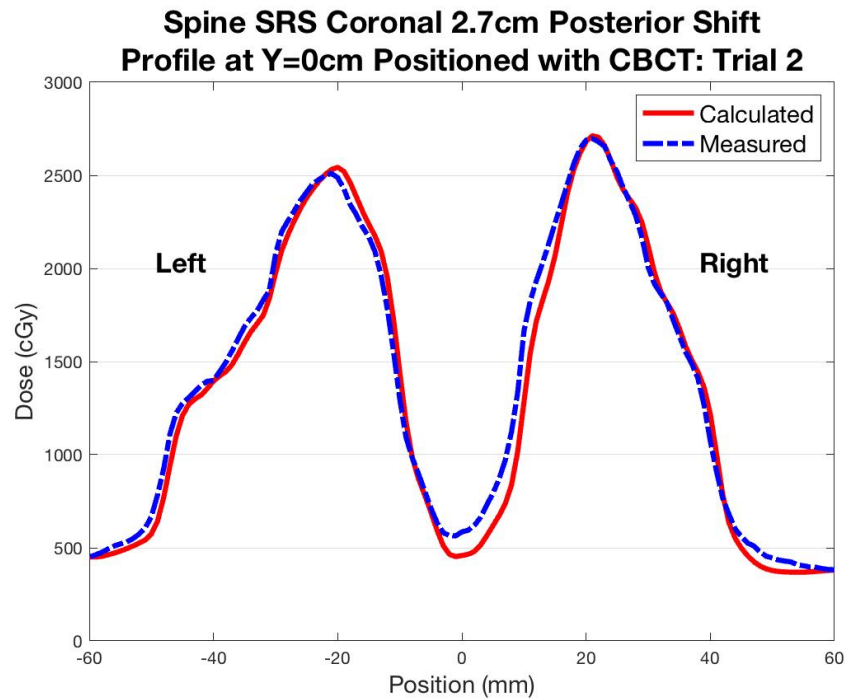
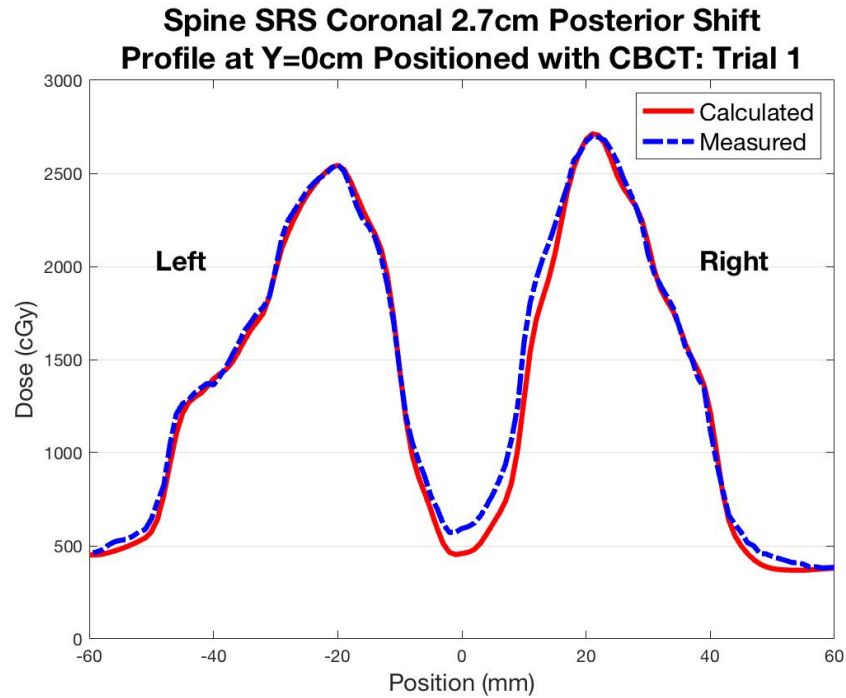


Figure A.37. Coronal left-right profile plots of Trials 1 and 2 taken through Y = 0 cm of the spine SRS treatment plan shifted posteriorly by 2.7 cm with kV-CBCT positioning and delivered on the Elekta Infinity with Agility head at the MBPCC Baton Rouge facility.



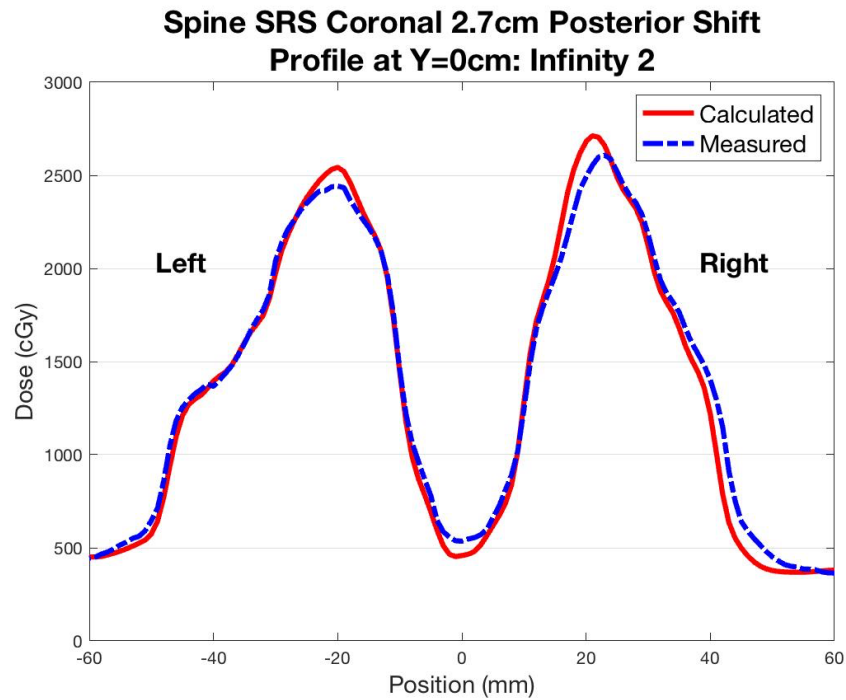
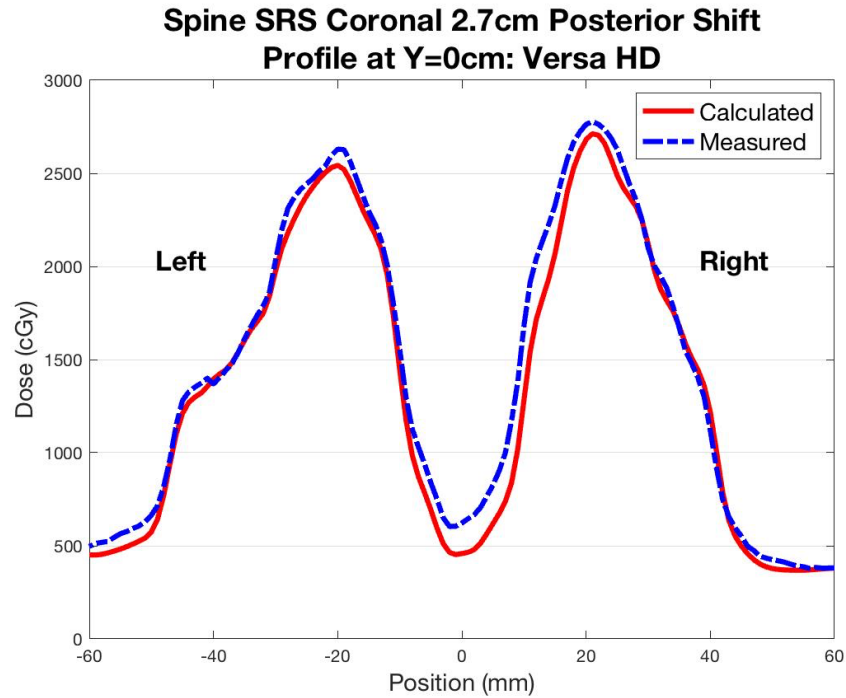


Figure A.38. Coronal left-right profile plots through Y = 0 cm of the spine SRS treatment plan shifted posteriorly by 2.7cm delivered on the Elekta Versa HD at the MBPCC Baton Rouge facility and the Elekta Infinity with Agility head located at the MBPCC Gonzales facility, respectively.

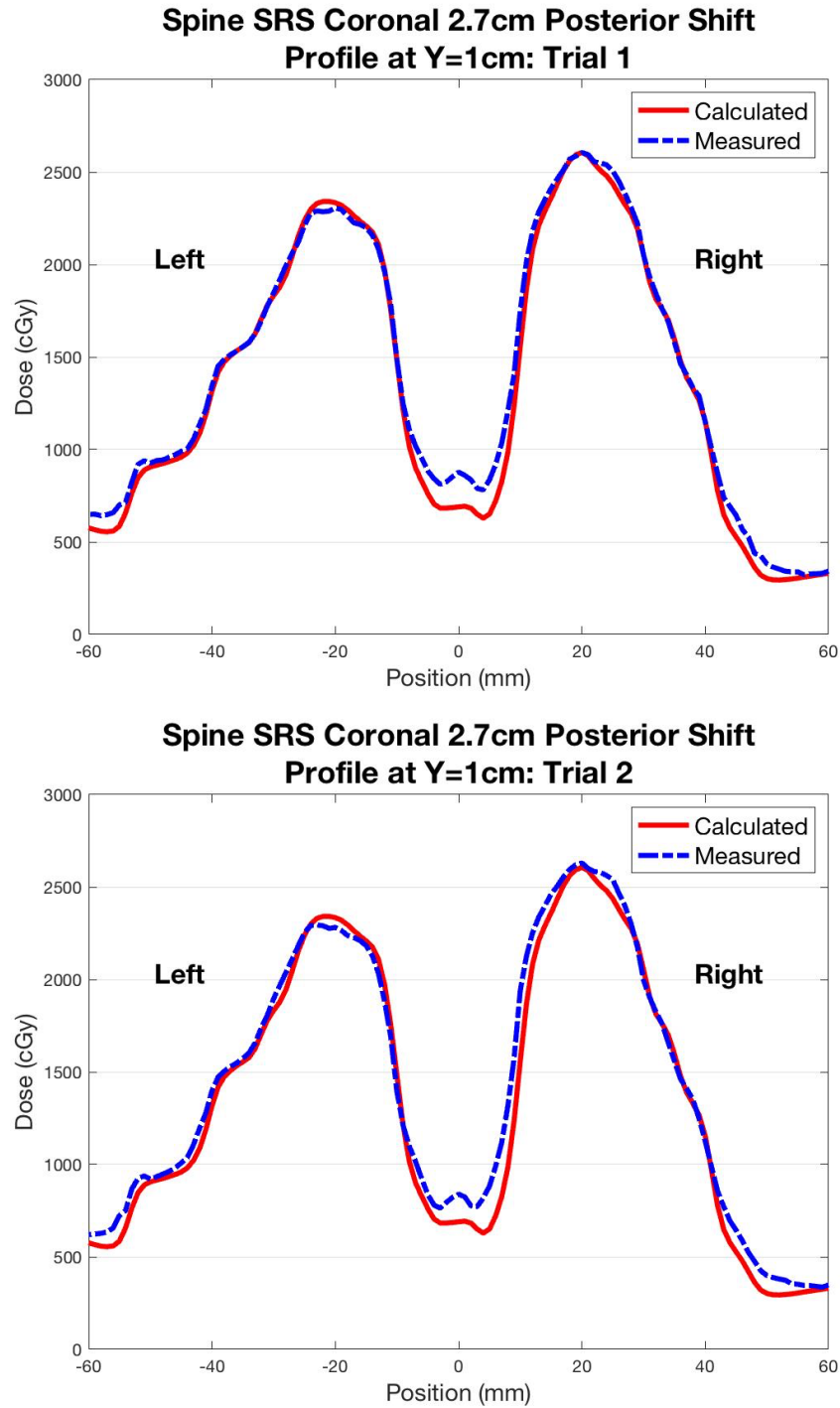


Figure A.39. Coronal left-right profile plots of Trials 1 and 2 taken through Y = 1 cm of the spine SRS treatment plan shifted posteriorly by 2.7 cm with kV-CBCT positioning and delivered on the Elekta Infinity with Agility head at the MBPCC Baton Rouge facility.

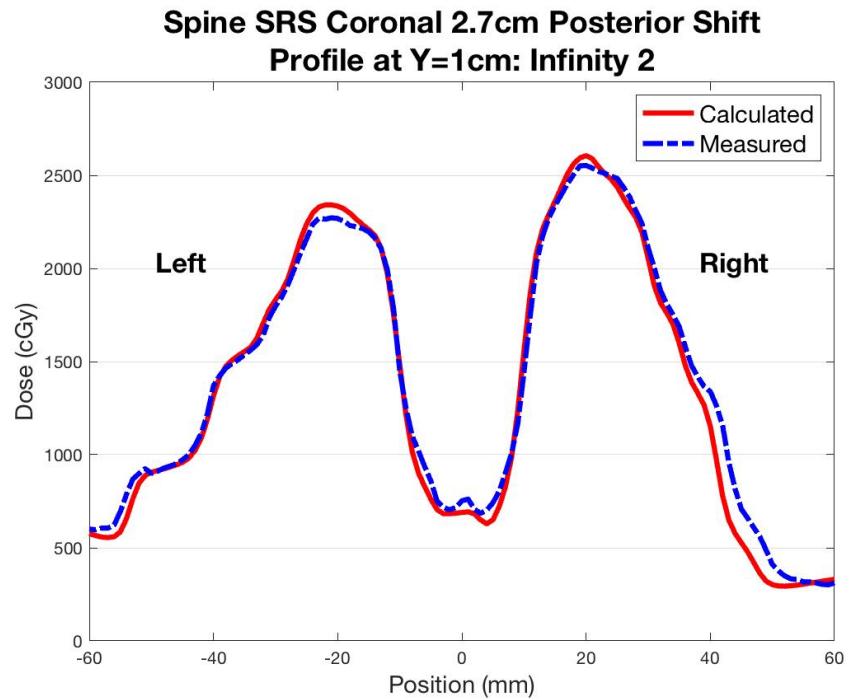
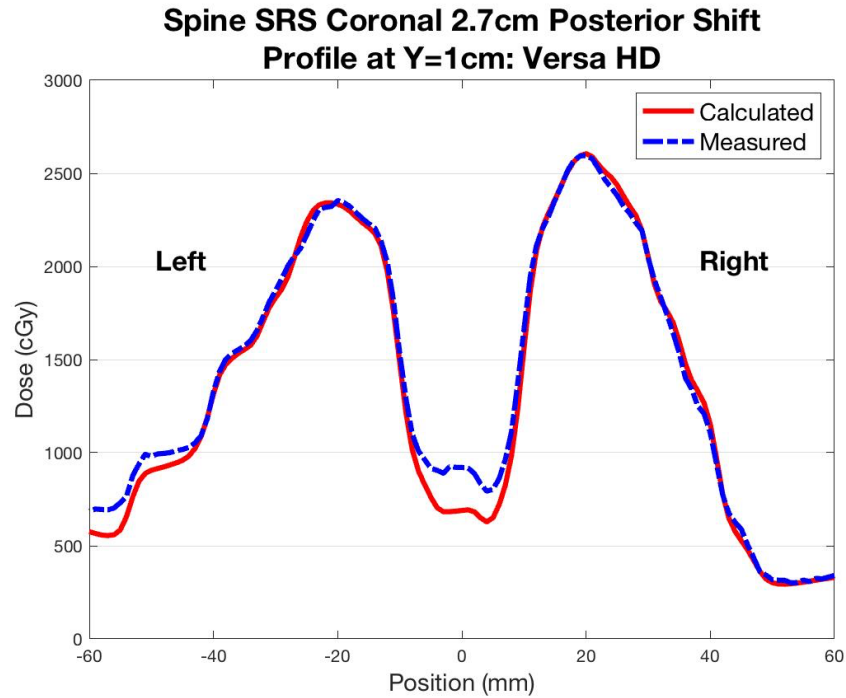


Figure A.40. Coronal left-right profile plots through Y = 1 cm of the spine SRS treatment plan shifted posteriorly by 2.7cm delivered on the Elekta Versa HD at the MBPCC Baton Rouge facility and the Elekta Infinity with Agility head located at the MBPCC Gonzales facility, respectively.

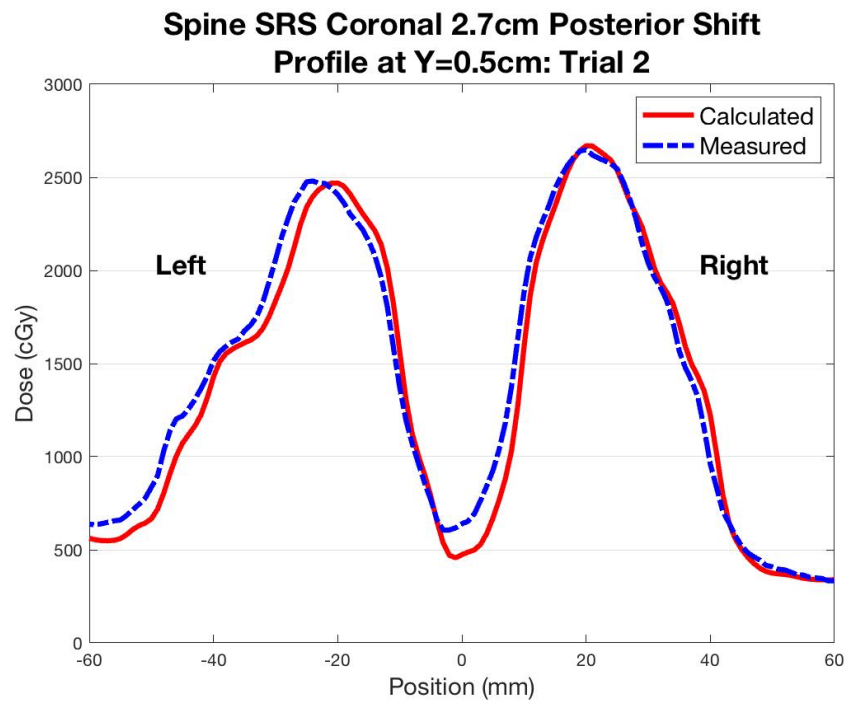
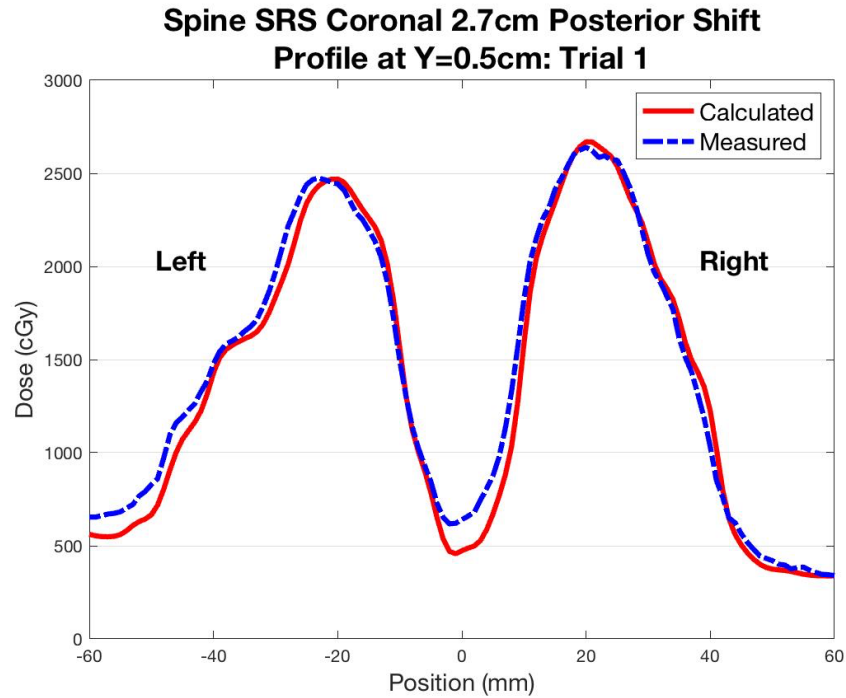


Figure A.41. Coronal left-right profile plots of Trials 1 and 2 taken through Y = 0.5 cm of the spine SRS treatment plan shifted posteriorly by 2.7 cm with kV-CBCT positioning and delivered on the Elekta Infinity with Agility head at the MBPCC Baton Rouge facility.

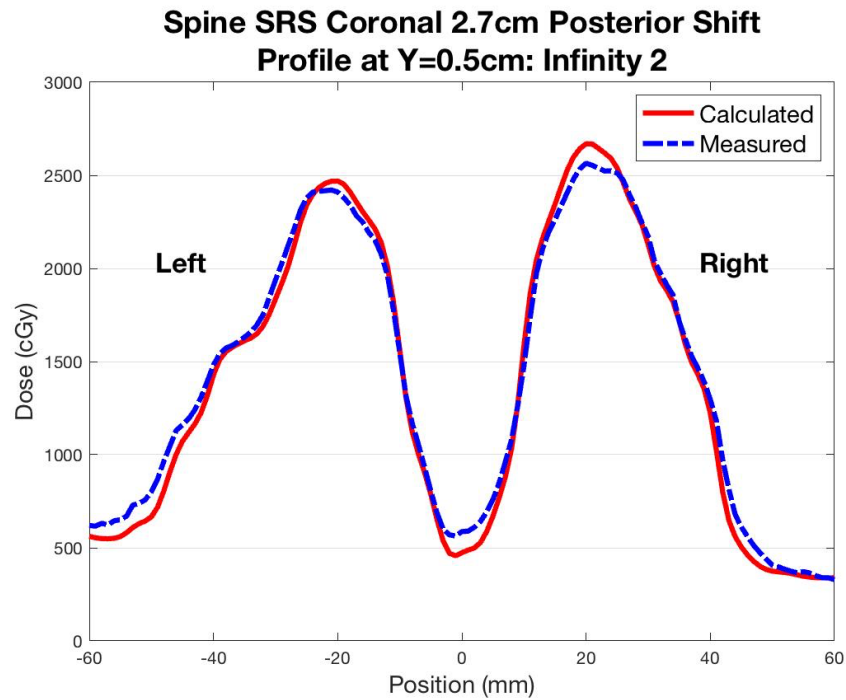
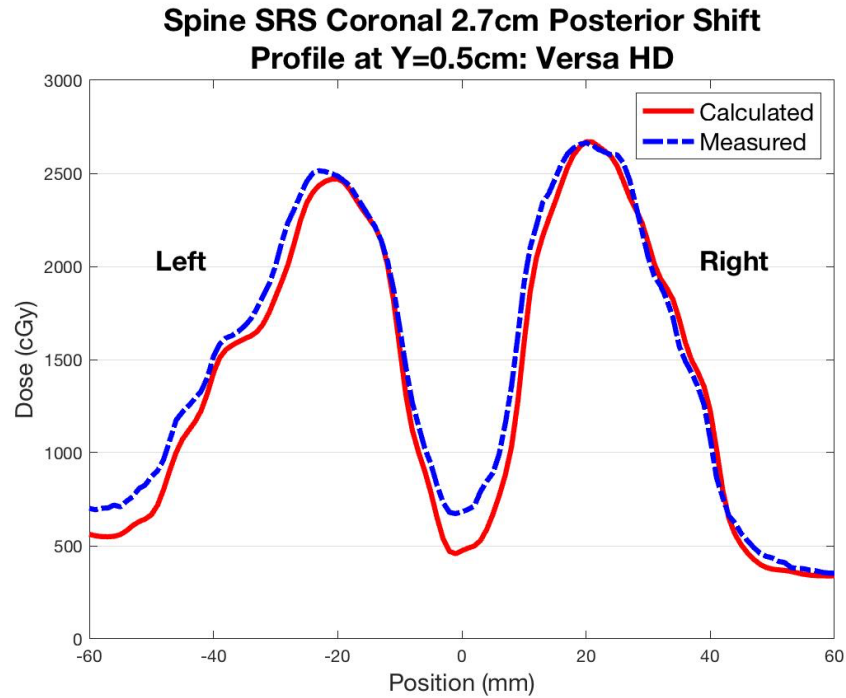


Figure A.42. Coronal left-right profile plots through Y = 0.5 cm of the spine SRS treatment plan shifted posteriorly by 2.7cm delivered on the Elekta Versa HD at the MBPCC Baton Rouge facility and the Elekta Infinity with Agility head located at the MBPCC Gonzales facility, respectively.

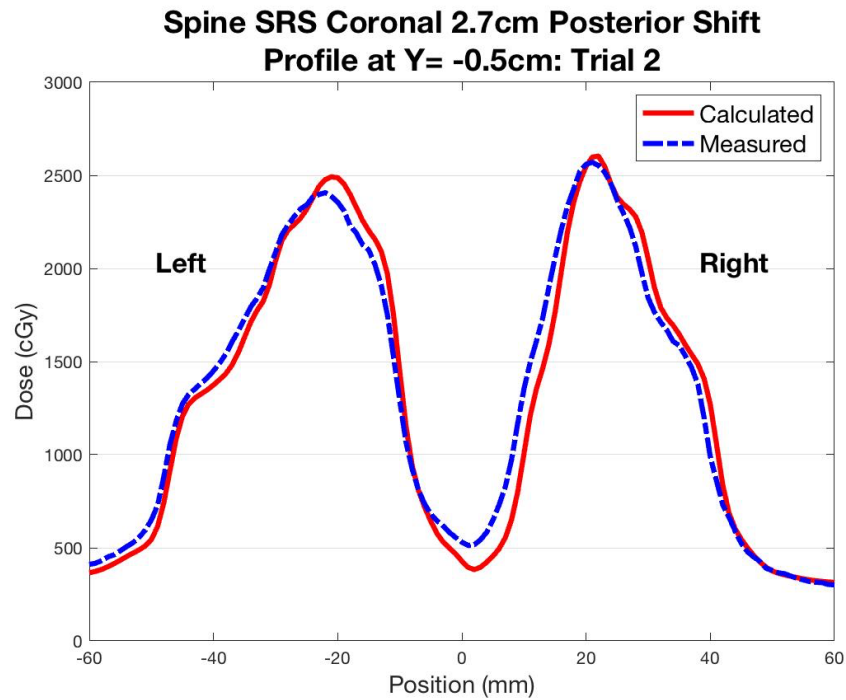
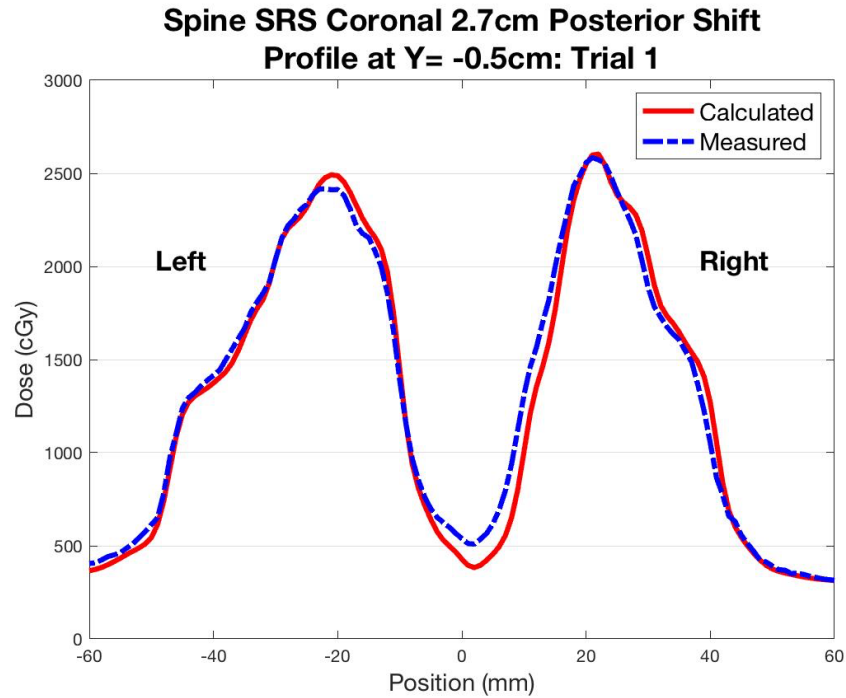


Figure A.43. Coronal left-right profile plots of Trials 1 and 2 taken through Y = -0.5 cm of the spine SRS treatment plan shifted posteriorly by 2.7 cm with kV-CBCT positioning and delivered on the Elekta Infinity with Agility head at the MBPCC Baton Rouge facility.

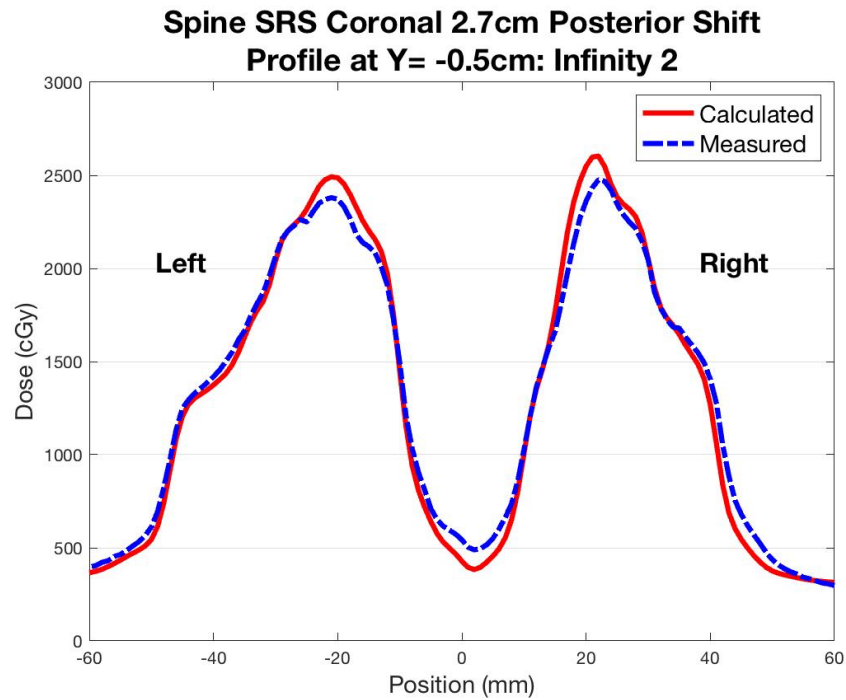
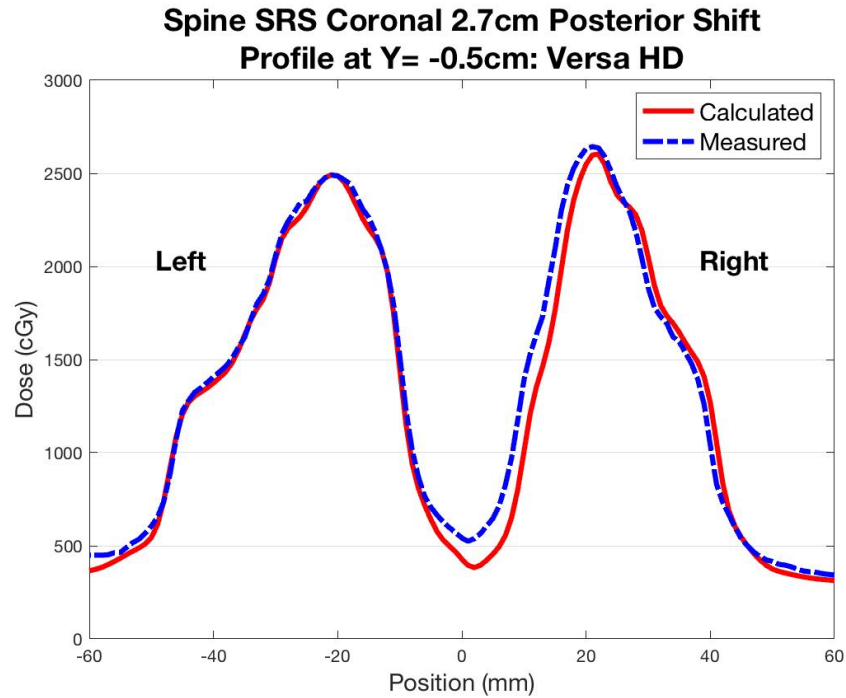


Figure A.44. Coronal left-right profile plots through Y = -0.5 cm of the spine SRS treatment plan shifted posteriorly by 2.7cm delivered on the Elekta Versa HD at the MBPCC Baton Rouge facility and the Elekta Infinity with Agility head located at the MBPCC Gonzales facility, respectively.

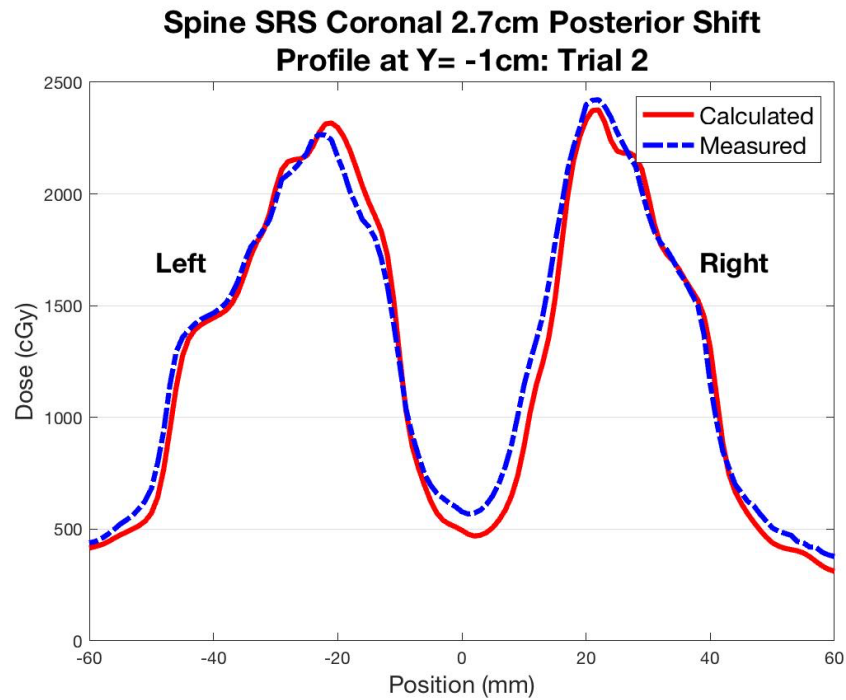
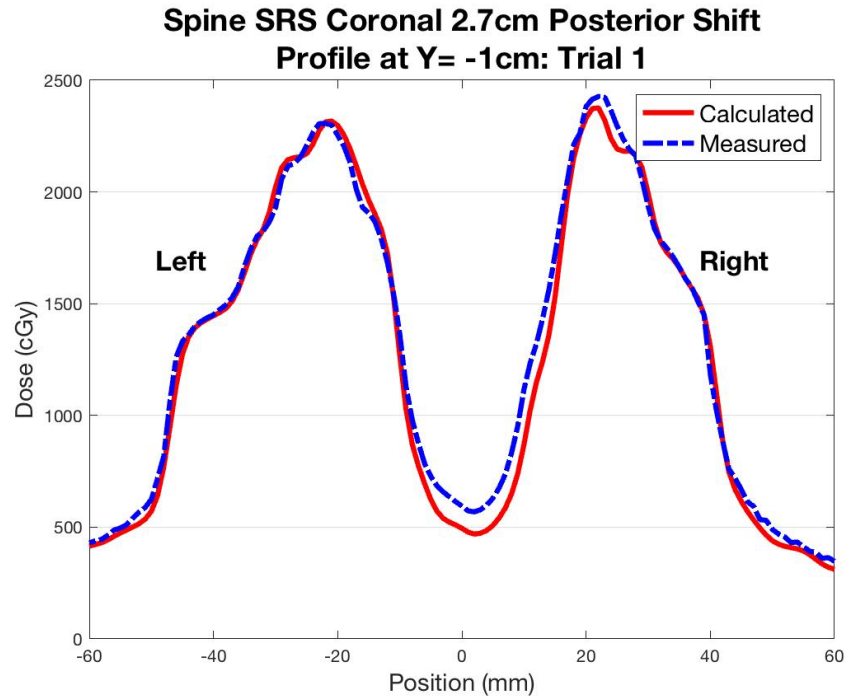


Figure A.45. Coronal left-right profile plots of Trials 1 and 2 taken through Y = -1 cm of the spine SRS treatment plan shifted posteriorly by 2.7 cm with kV-CBCT positioning and delivered on the Elekta Infinity with Agility head at the MBPCC Baton Rouge facility.



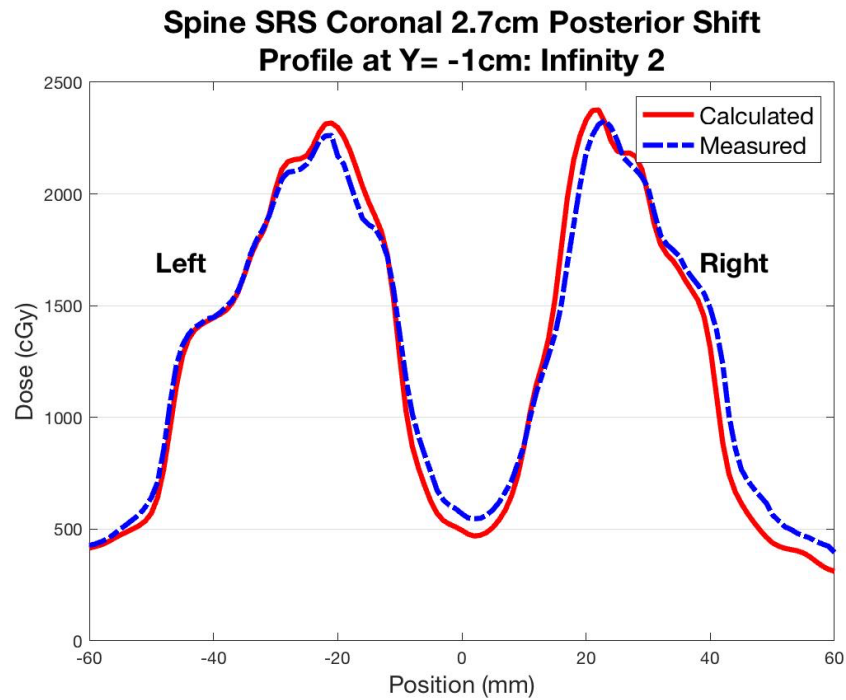
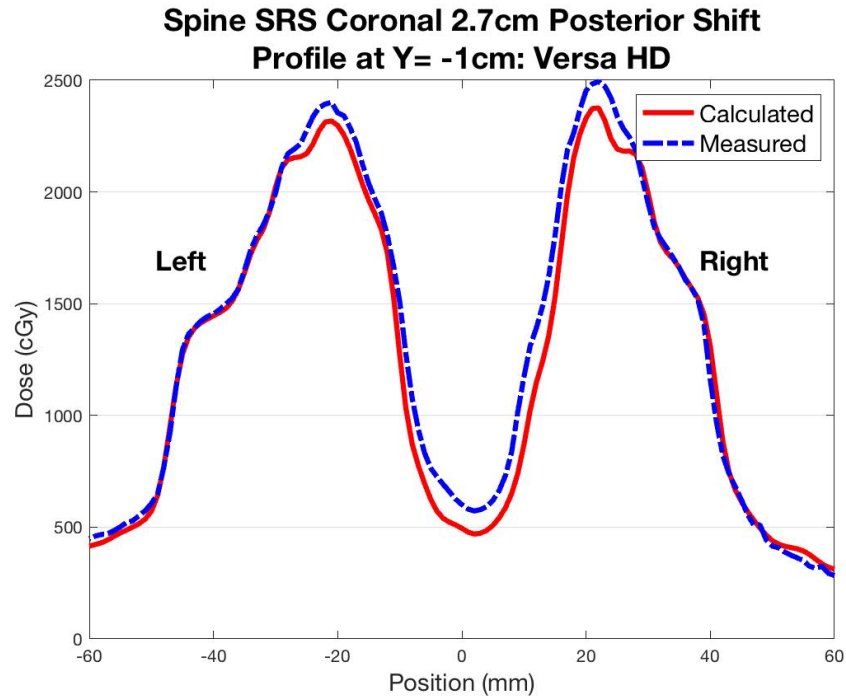


Figure A.46. Coronal left-right profile plots through Y = -1 cm of the spine SRS treatment plan shifted posteriorly by 2.7cm delivered on the Elekta Versa HD at the MBPCC Baton Rouge facility and the Elekta Infinity with Agility head located at the MBPCC Gonzales facility, respectively.

## Appendix B. MV Isocenter Accuracy Test Data

The data was analyzed with the RIT Isocenter Analysis Tool. The green circle represents the perimeter of the radiation field defined by the stereotactic cone with the green cross representing the center of the cone. Additionally, the blue circle delineates the edge of the BB with the blue cross representing the center of the BB. The maximum value of the first four numbers in the R (mm) deviation column represents the MV isocenter radius for gantry rotation. The maximum value of the eight numbers in the R (mm) column represents the radius of the MV isocenter on the gantry and the treatment table.

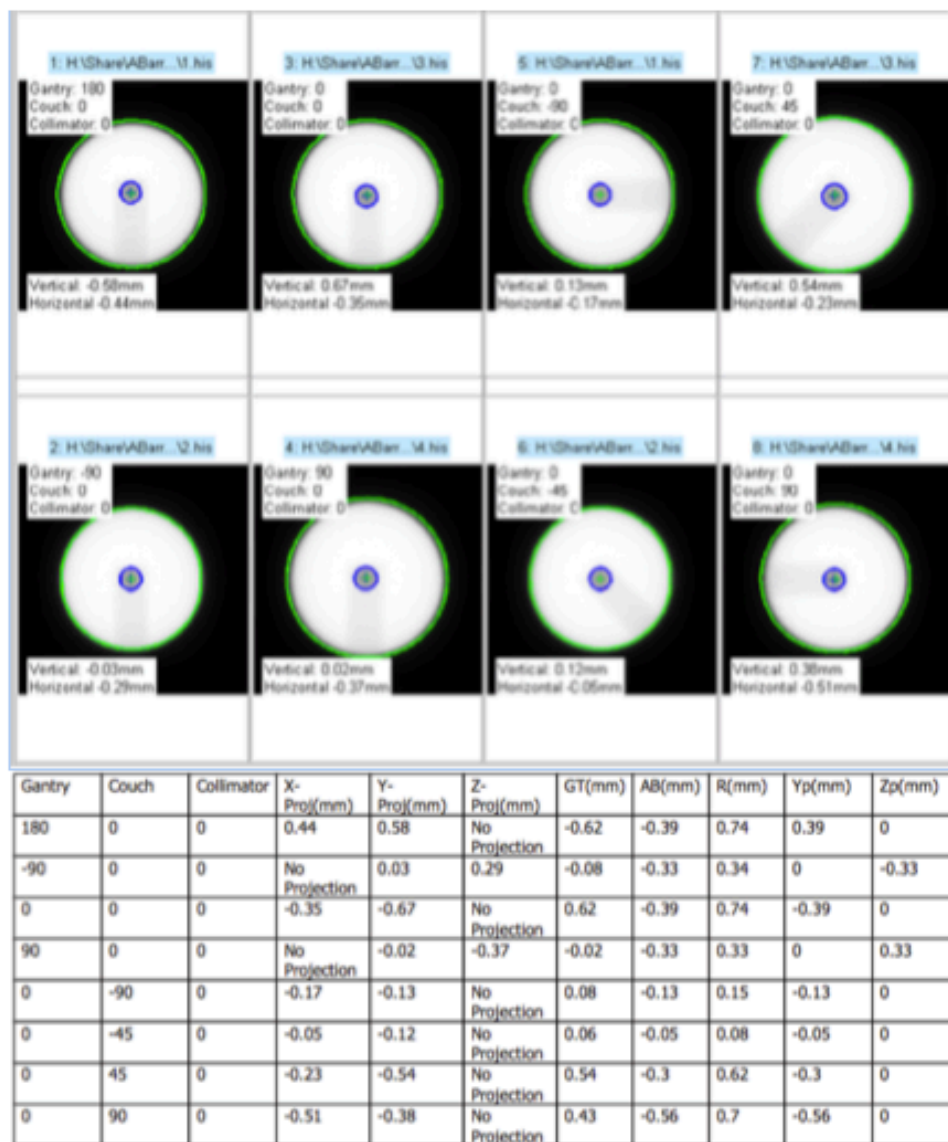


Figure B.1. MV Isocenter analysis of the Elekta Infinity platform with Agility head located at the Baton Rouge MBPCC facility (Infinity 1). EPID mages were analyzed with the RIT Isocenter Analysis Tool for the four cardinal gantry angles with couch at 0° and four couch angles with gantry at 0°.

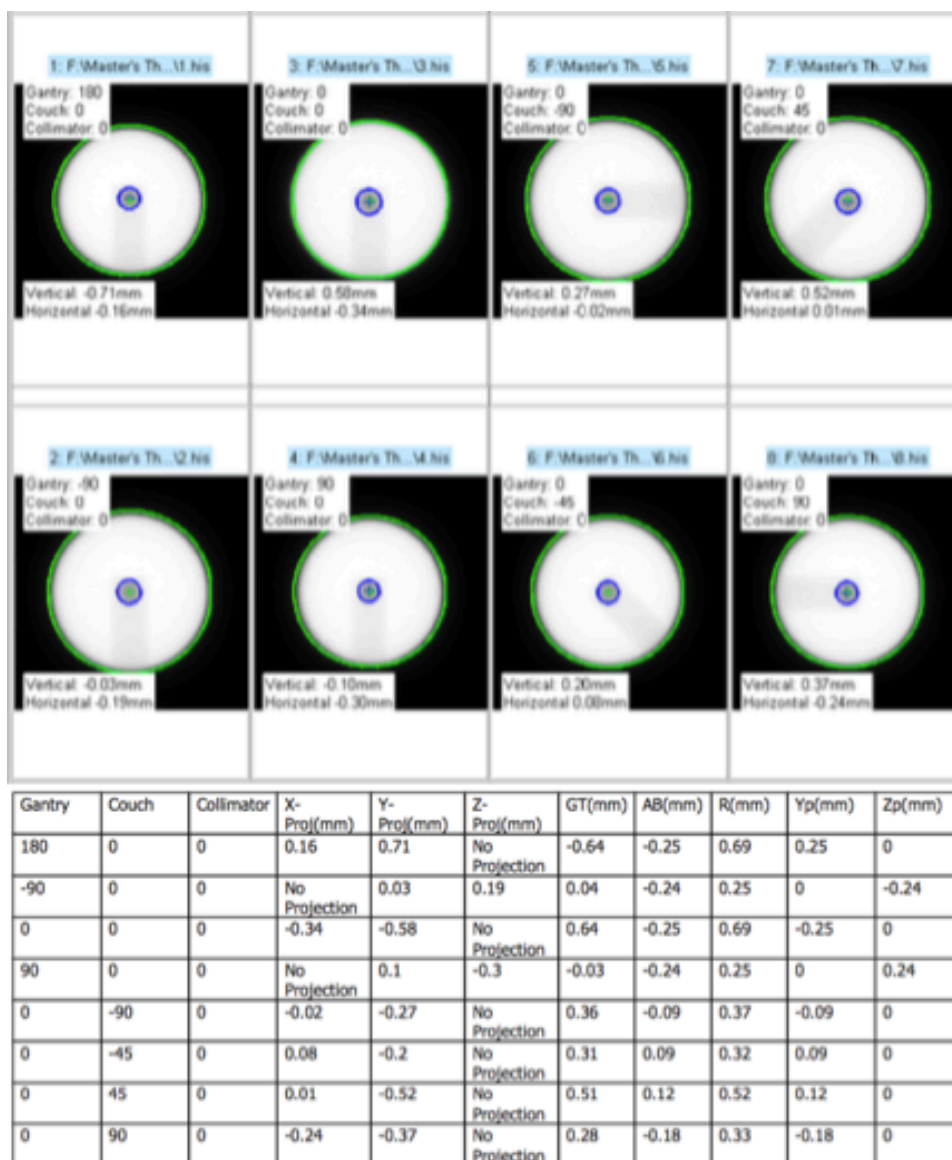


Figure B.2. MV Isocenter analysis of the Versa HD™ platform located at the Baton Rouge MBPCC facility (Infinity 1). EPID mages were analyzed with the RIT Isocenter Analysis Tool for the four cardinal gantry angles with couch at 0° and four couch angles with gantry at 0°.

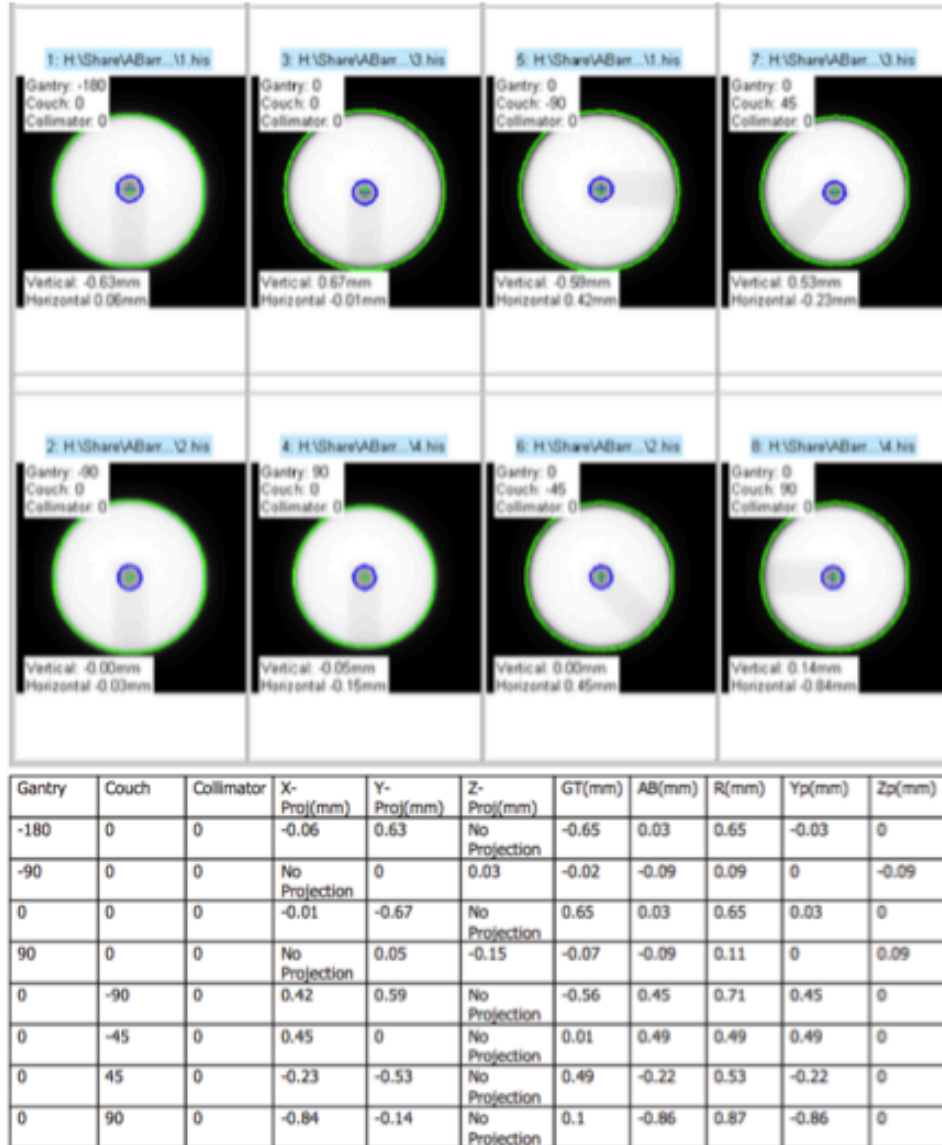


Figure B.3. MV Isocenter analysis of the Elekta Infinity platform with Agility head located at the Gonzales MBPCC facility (Infinity 2). EPID mages were analyzed with the RIT Isocenter Analysis Tool for the four cardinal gantry angles with couch at 0° and four couch angles with gantry at 0°.

## Appendix C. Data from kV-CBCT Translations

Table C.1 displays the coordinates for the initial alignment of the MapCHECK2 array to the room lasers as well as the final suggested shifts provided by XVI after translation and kV-CBCT image registration to confirm the desired position was achieved. Even though the kV-CBCT registration algorithm is capable of identifying sub-millimeter shifts, the treatment table is only capable of millimeter adjustments. Therefore, 1 mm shifts are deemed acceptable and are not required to be executed. However, a tolerance of  $\pm 0.05$  cm was set for the purpose of this study in accessing the accuracy of delivery. The data in Table 3.3 shows that the applied posterior shifts were within the acceptable range for data acquisition.

Table C.1. Data acquired from the XVI kV-CBCT image registration used for assessing the positioning of the diode array before measurement sessions.

|   | Initial Position |                     |                 | After Final kV-CBCT; Residual Shifts<br>Confirming Correct Translation |                     |                 |
|---|------------------|---------------------|-----------------|--|---------------------|-----------------|
| Measurement Session                               | X-Lateral (cm)   | Y-Longitudinal (cm) | Z-Vertical (cm) | X-Lateral (cm)   | Y-Longitudinal (cm) | Z-Vertical (cm) |
| SSRS 2cm Posterior Shift, Trial 1 on Infinity 1   | +0.03            | +0.08               | -0.04           | +0.02  | -0.03               | -2.03           |
| SSRS 2cm Posterior Shift, Trial 2 on Infinity 1   | -0.08            | -0.11               | -0.05           | +0.01  | +0.00               | -2.04           |
| SSRS 2cm Posterior Shift on Versa HD              | +0.05            | +0.12               | +0.08           | -0.02  | +0.03               | -2.05           |
| SSRS 2cm Posterior Shift on Infinity 2            | +0.02            | +0.04               | -0.05           | +0.02  | -0.05               | -2.05           |
| SSRS 2.7cm Posterior Shift, Trial 1 on Infinity 1 | -0.05            | -0.10               | +0.05           | +0.04  | 0.00                | -2.73           |
| SSRS 2.7cm Posterior Shift, Trial 2 on Infinity 1 | +0.04            | +0.09               | -0.05           | +0.03  | 0.00                | -2.74           |
| SSRS 2.7cm Posterior Shift on Versa HD            | +0.06            | +0.04               | -0.02           | +0.01  | +0.03               | -2.71           |

|   |       |       |       |       |       |       |
|---|-------|-------|-------|-------|-------|-------|
| SSRS 2.7cm<br>Posterior<br>Shift on<br>Infinity 2 | +0.02 | -0.02 | -0.09 | -0.03 | -0.01 | -2.74 |
|---|-------|-------|-------|-------|-------|-------|

## **Vita**

Addie Jane Barron was born in Ruston, Louisiana in 1993. She is the daughter of Cathey and Charles Barron. Addie grew up in Friendship, Louisiana and attended Cedar Creek High School in Ruston, Louisiana. She graduated from Cedar Creek in 2011 and enrolled at Centenary College of Louisiana, where she received her Bachelor of Science degree in Biophysics. After graduating from Centenary in the spring of 2015, she matriculated into the Medical Physics Master of Science Program at LSU. Following graduation from the medical physics program in the summer of 2018, she will begin her medical physics residency at Mary Bird Perkins Cancer Center.